Parks Victoria Technical Series

Number 116

Baseline habitat mapping and improved monitoring of reef habitats in Victoria's marine national parks and sanctuaries

March 2022

Parks VICTORIA

Healthy Parks Healthy People

VICTORIA State Government

Published by Parks Victoria

Level 10, 535 Bourke St, Melbourne Vic 3000

Author(s

Mary Young, Peter Porskamp, Sarah Murfitt, Sam Wines, Paul Tinkler, Jasmine Bursic, Blake Allan, Sasha Whitmarsh, Daniel Ierodiaconou – Deakin University

Jacqui Pocklington – Deakin University and Parks Victoria (former)

Steffan Howe – Parks Victoria (former)

National Library of Australia

Cataloguing-in-publication data

Includes bibliography

ISSN 1448-4935

Citation:

Young M, Porskamp P, Murfitt S, Wines S, Tinkler P, Bursic, J., Allan B, Howe S, Whitmarsh S, Pocklington J, Ierodiaconou D 2022. *Baseline habitat mapping and enhanced monitoring trials of subtidal and intertidal reef habitats in Victoria's marine national parks and sanctuaries*. Parks Victoria Technical Series 116.

Front cover: Basket star on gorgonian coral Photo: Museum Victoria

Executive summary

Parks Victoria has established extensive marine research and monitoring programs for its network of marine national parks and sanctuaries with the aim of addressing significant management challenges. Such challenges focus on both improving baseline knowledge of Victoria's marine protected areas (MPAs) and addressing applied management questions. Labelled as the Signs of Healthy Parks (SHP) monitoring program, we aim to ensure systematic, robust and integrated ecological monitoring across the breadth of Victoria's marine national parks and sanctuaries. Building on Parks Victoria's Conservation Action Planning process, the SHP program aims to monitor the health of protected areas using a range of environmental indicators that provide information about natural values and ecological processes occurring within the parks, and potential threats and other drivers. Data collection in the SHP is based on focused monitoring questions that address specific management needs. Parks Victoria has implemented subtidal and intertidal reef monitoring programs in a large number of its MPAs from as far back as 1998; however, they only cover a small proportion of the key habitats in the parks. Using advances in ocean technology, the SHP program can now monitor the health of the entire extent of parks, allowing the full gamut of protected features to be monitored. The SHP does this by fostering partnerships and collaborative projects to design, implement and evaluate monitoring programs. Deakin University, as part of the Research Partners Program, were approached by Parks Victoria to trial a suite of monitoring approaches with 5 objectives (which are interrelated making the projects cost-effective). The trials' objectives are to: 1) develop a full bathymetry map for the Bunurong Marine National Park (MNP) and habitats maps for both Bunurong MNP and Wilsons Promontory MNP; 2) leverage Australia's Integrated Marine Observing System (IMOS) autonomous underwater vehicle (AUV) facility to establish monitoring sites inside and outside Wilsons Promontory MNP as part of the national AUV monitoring program, the first in Victoria; 3) test, refine and implement proposed new methods for subtidal reef surveys using AUVs and other recent advances in technology, complementary to the current diver visual census method; 4) test, refine and implement new methods for intertidal reef surveys using low-cost unmanned aerial vehicles (UAVs) at Merri Marine Sanctuary (MS), Port Phillip Heads MNP, Ricketts MNP and Mushroom Reef MS; and 5) investigate species–habitat relationships present in fish and Southern Rock Lobster populations within the Wilsons Prom MNP. Unfortunately testing the portable AUV system for objective 3 was unsuccessful due to variability of terrain and inability of the platform to manoeuvre across historical diver census sites identified by the Subtidal Reef Monitoring Program (SRMP). This evaluation was moved to a lower relief site in Port Phillip Bay and is reported as part of a separate project. The results from this study provide considerable new knowledge of the distribution and functioning of intertidal, subtidal and mesophotic habitats within the Wilsons Promontory and Bunurong MNPs and provide a framework to expand monitoring across Victoria's entire MPA estate.

Contents

Index of figures

Index of tables

Section A Wilsons Promontory MNP and Bunurong MNP monitoring program

1. Introduction

Parks Victoria manages a system of 13 marine national parks and 11 marine sanctuaries, making up approximately 5.3% of Victoria's state waters. Established in 2002, the network of marine national parks and sanctuaries was designed to represent the diversity of Victoria's marine environment, its habitats, and associated flora and fauna (Victorian Environmental Assessment Council, 2014). In order to reliably manage these areas, an understanding of the natural values that occur within the parks, sanctuaries and reserves is essential (Devillers et al., 2015). Parks Victoria has established extensive marine research and monitoring programs that address significant management challenges for its marine protected areas (MPAs). Such challenges include improving baseline knowledge of the MPAs and addressing new applied management questions. Parks Victoria's research program is guided by the research themes outlined in Parks Victoria's Environmental Research Strategy 2012–2025, and their monitoring program is guided by a draft statewide marine monitoring framework based on priorities identified through the conservation planning process for the marine national parks and sanctuaries.

1.1 Previous long-term monitoring programs

Parks Victoria's long-term Subtidal Reef Monitoring Program (SRMP) was designed using best scientific practices in the early 1990s and initiated in (what is now) the system of marine national parks and sanctuaries in 1998. These surveys were historically conducted in 13 marine national parks and sanctuaries across the state (Power and Boxshall, 2007) from 1998 to 2015. This program used diver underwater visual census methods, which record descriptions of macroalgae, fish and macroinvertebrate communities at each monitoring site as well as indications of change through time. In addition, the Intertidal Reef Monitoring Program (IRMP) began in late 2002 with sampling at some sites beginning in the summer of 2002–03 (Power and Boxshall, 2007); it finished in 2013. This program involved monitoring the invertebrates and macroalgae present in the intertidal zone on reefs within 9 targeted MPAs and at 9 matched reference sites outside the MPAs (see Hart and Edmunds (2005) for full methodological details).

The results of these surveys are published in Parks Victoria Technical Series reports.

1.2 Updated monitoring framework

Parks Victoria has now adopted a new adaptive management framework and a conservation planning process that more clearly defines the goals and objectives for managing key natural assets and threats. A draft statewide monitoring plan has been developed based on conservation, management and monitoring priorities identified for each park through the conservation planning process. The monitoring plan outlines potential indicators for subtidal and intertidal reef communities and other key habitats and ecosystems, and it identifies key threats to these priority natural assets. The process for identifying monitoring priorities at

the statewide level was endorsed by Parks Victoria and involved 3 consecutive assessments, namely, identifying high-priority parks (e.g. those identified as representative or that meet the Category II criteria in the IUCN protected area categories system), their high-priority key ecological attributes and the high-priority threats to those attributes.

The new monitoring program will focus on key ecological attributes and threats in at least one of the large marine national parks within each bioregion, currently identified as Discovery Bay Marine National Park (MNP) (Otway bioregion), Point Addis MNP (Central Victoria bioregion), Port Phillip Heads MNP (Victorian Embayments bioregion), Wilsons Promontory MNP (Flinders bioregion) and Cape Howe MNP (Twofold Shelf bioregion). It will also address monitoring priorities identified for other parks using a range of delivery models as resources permit.

1.3 Objectives

This is a multifaceted project with a number of different components. The overarching objectives for the project are to:

Section A

- develop a full bathymetry map for Bunurong MNP and full habitat maps for both Bunurong and Wilsons Promontory marine national parks, using the new Combined Biotope Classification Scheme (CBiCS) developed by Australian Marine Ecology and Fathom Pacific, to provide comprehensive information on the types and distribution of habitat found within the parks and help inform management of the park
- establish monitoring sites in Wilsons Promontory MNP as part of the national IMOS autonomous underwater vehicle (AUV) program (the first in Victoria), to examine habitats not previously explored or surveyed and build a more comprehensive understanding of habitat distributions to help inform future management
- use baited remote underwater video stations (BRUVS) to continue to
  - build an inventory of fish species in Wilsons Promontory MNP
  - better understand the role of habitat in explaining the distribution of fish populations to help target future research and monitoring
  - identify populations (and areas of the park) that may be vulnerable to illegal fishing to inform future compliance efforts

- use fisheries-independent survey methods to assess rock lobster populations inside Wilsons Promontory MNP (and at suitable reference sites outside the park) in combination with various modelling approaches to
  - better understand the role of habitat in explaining rock lobster distribution
  - complement data from the Subtidal Reef Monitoring Program
  - provide important information on a key indicator of reef health

Section B

- test and refine new methods for intertidal reef surveys using low-cost UAVs so that data can be calibrated against that collected using conventional IRMP methods
- develop standard operating procedures and implement at 4 marine protected areas (Merri Marine Sanctuary (MS), Port Phillip Heads MNP, Ricketts Point MS, Mushroom Reef MS) and report on surveys in these parks.

2. Methods

Table 2.1 provides an overview of methods and data collection across the Parks estate as part of this Research Partners Program.

Table 2.1: Overview of methods applied as part of this Research Partners Program

Site	Method	Date
Bunurong MNP	Habitat mapping using multibeam sonar data and towed video with oblique and downward-facing imagery	2017–18
Wilson Promontory MNP	Habitat mapping using existing multibeam sonar and remotely operated vehicle (ROV) data with new collections with towed video with oblique and downward-facing imagery, IMOS autonomous underwater vehicles, baited remote underwater video stations (BRUVS), and commercial rock lobster surveys	2013–19
Pickering Point (MPA: −38°24′S, 142°28′E) and Shelly Beach (REF: −38°23′S, 142°27′E) Point Lonsdale (MPA: −38°17′S, 144°36′E) and Cheviot Beach (REF: −38°18′S, 144°39′E) Ricketts Point (MPA: −37°59′S, 145°01′E) and Halfmoon Bay (REF: −37°58′S, 145°05′E) Mushroom Reef (MPA: −38°29′S, 145°01′E) and West Flinders (REF: −38°28′S, 145°06′E)	Intertidal reef unmanned aerial vehicle surveys and ground truthing (quadrats)	2016

2.1 Habitat mapping and derived environmental variables

2.1.1 Multibeam echosounder mapping data

High-resolution multibeam echosounder (Coombes et al., 2013) data were collected for both the Wilsons Promontory and Bunurong marine national parks using Deakin University's 9.2-metre (m) MV *Yolla*. Mapping of the Wilsons Promontory MNP was done in April and June 2014, allowing the seafloor of the entire park to be mapped at 1 m horizontal resolution. Detailed results of this survey have since been published (Ierodiaconou et al., 2018; Kennedy et al., 2014, Schimel and Ierodiaconou, 2015). The entire extent of the Bunurong MNP was further mapped at a horizontal resolution of 1 m over 5 days in June and September 2017 using the same methods.

The multibeam echosounder (MBES) surveys were conducted using a Kongsberg Maritime EM2040C MBES integrated with an Applanix POS MV WaveMaster motion reference unit.

The MBES was operated at a constant frequency of 300 kilohertz (kHz) with a varying ping rate and pulse length (up to 50 Hz and down to 0.025 milliseconds (ms)) automatically adjusting to water depth, in high-density equidistant mode (400 soundings per ping) and with a constant sector coverage of ±65° athwartships. Sound velocity profiles were captured throughout the survey using a Valeport Monitor Sound Velocity Profiler and imported into Kongsberg Maritime's acoustic data acquisition software SIS to correct soundings for variation of sound velocity in the water column. A patch test was also completed at the end of the surveys to ensure alignment of sensors had not changed during survey operations. The POS MV WaveMaster measured the position of the vessel in differential GNSS mode using GPS/GLONASS corrections received by radio from the Fugro MarineStar satellite positioning service. The POS MV WaveMaster also measured precise vessel motion data (roll, pitch, yaw, true heave). A post-processed kinematic (PPK) solution was later obtained from these position and motion data using Applanix software POSPac Mobile Mapping Suite (MMS). This solution was then integrated with the bathymetry data in CARIS software HIPS and SIPS 8.1. The soundings were manually cleaned in HIPS and SIPS and gridded at a resolution of 1 m.

For both sites, derivatives characterising the seabed terrain were extracted using Spatial Analyst (ArcGIS 10.5.1) (ESRI Software Inc., Redland, California), Benthic Terrain Modeler tool for ArcGIS (Walbridge et al., 2018) and ENVI (Exelis Visual Information Solutions, Boulder, Colorado). Derivatives used included bathymetry, slope, aspect (northness and eastness), benthic position index, maximum curvature, rugosity, complexity, backscatter with HSI (hue, saturation and intensity) transformations and distance to reef (Table 2.2).

2.1.2 Sea-surface temperature

Sea-surface temperature (SST) data were sourced from the Integrated Marine Observing System (IMOS, 2018). IMOS is a national collaborative research infrastructure, supported by the Australian Government. These data were downloaded in NetCDF format at monthly intervals and converted into individual ArcGIS rasters for analysis. Annual and summer means in SST were computed from 1992 to 2018 from the monthly SST datasets. To assess patterns in SST within Wilsons Promontory MNP and Bunurong MNP, the mean and standard deviation of annual and summer SST were calculated for each year and plotted through time.

Table 2.2: Descriptions of bathymetry and backscatter statistics tested in this study

Derivatives	Description	Analyses used for
Bathymetry	Elevation of a plane passed through its closest grid point.	Species distribution modelling, habitat mapping
Backscatter	Strength of the acoustic return. Provides information on seafloor hardness.	Species distribution modelling, habitat mapping
Slope	Maximum change in elevation between each cell and cells in a specified surrounding neighbourhood.	Species distribution modelling, habitat mapping
Aspect (northness and eastness)	Azimuthal direction of the steepest slope through points in an analysis window. Northness relates to the sine component of the azimuthal direction and eastness relates to the cosine.	Species distribution modelling
Benthic position index	Measure of a location's elevation relative to the overall landscape. Calculated by comparing elevation of a cell with the mean elevation of surrounding cells.	Species distribution modelling
Maximum curvature	Steepest curve of convexity through a defined cell neighbourhood.	Species distribution modelling, habitat mapping
Rugosity	A measure of topographic roughness, which relates ratio of surface area to planar area.	Species distribution modelling
Complexity	Second derivative of slope (or rate of change of slope).	Species distribution modelling, habitat mapping
Vector ruggedness measure (VRM)	Incorporates the heterogeneity of both slope and aspect using 3-dimensional dispersion of vectors. See (Sappington et al., 2007) for more details.	Habitat mapping
HSI transformations (red, green and blue)	The derivatives of a backscatter image are split into high- and low-frequency information, then mapped to hue (chromatic) and intensity (achromatic) with a fixed saturation value. HSI values are then transformed to the red, green and blue colour space to produce 3 variables.	Species distribution modelling
Angular response impedance	Computed using the Jackson model, which is derived by a combination of the seabed density and sound speed characteristics (Jackson et al., 1986).	Habitat mapping
Angular response volume	Computed by multiplying the difference in height of a cell by the area if each cell. All volume calculations are relative to zero. This technique attempts to account for vegetation in the water column impacting acoustic returns.	Habitat mapping
Angular response phi	Computed grain size from the Fledermaus Geocoder Toolbox (FMGT) prosperity model.	Habitat mapping
Distance to reef	Reef position was obtained from a substrate layer classified into rock and sediment derived from the bathymetry and backscatter data. Euclidean distance tool (ArcGIS 10.1) was used to create raster of distance to reef. Sites on reef had a distance value of 0 m.	Species distribution modelling

2.2 Fisheries-independent Southern Rock Lobster survey

Catch datasets independent of the Southern Rock Lobster (SRL) (*Jasus edwardsii*) fishery were acquired to assess spatially explicit habitat use by SRL. We used standardised fishery assessment trapping methods to provide fine-scale SRL population information in Wilsons Promontory MNP. Lobster pots were baited with 1 kilogram (kg) of locally available bait, and escape gaps were wired shut (Woods and Edmunds, 2013). Sampling occurred in February 2016 over 4 nights: 150 pots were sampled within the bounds of the park and 75 pots sampled outside. The sampling design allowed comparisons between inside and outside the MPA over 3 distinct areas: shallow waters in the East sites, deep waters in the West sites, and shallow waters in the West sites. Each area had 25 pots inside and 25 pots outside the MPA (Figure 2.1). The remaining 75 pots only provided information from inside the MPA so were not used in the inside versus outside analyses. All SRL captured in the pots were counted and sexed, females were assessed for reproductive condition, and all lobsters were measured for carapace length (CL). To calculate SRL biomass, we used the length–weight relationship provided in Punt (2003) and used by Woods and Edmunds (2013): $W = aCL^b$, where W is the weight in kilograms, CL is carapace length and a and b are coefficients related to sex and size class (females: a = 0.000271, b = 3.135; males: a = 0.000285, b = 3.114).

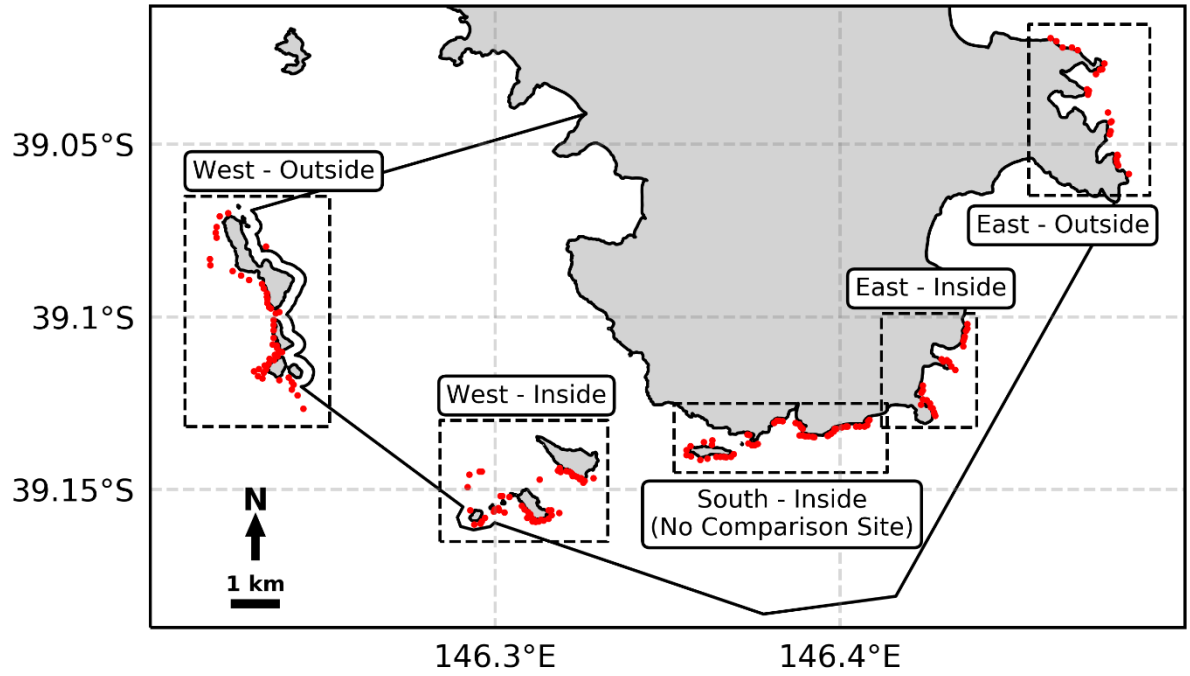

Figure 2.1: Wilsons Promontory Southern Rock Lobster study site in south-eastern Australia, February 2016. The red circles represent sample locations inside and outside the Wilsons Promontory MPA (outlined in black)

2.3 Baited remote underwater video stations

Baited remote underwater video stations (BRUVS) surveys took place from 24 to 28 February 2016. Sample sites were selected using an image segmentation of MBES seafloor maps in order to cluster areas of like habitat across bathymetry, backscatter, benthic position index and complexity. This approach ensured sites could capture the variability across the MPA. In total, 78 BRUVS deployments were made of which 52 were successful due to challenging current conditions. Two high-definition video cameras (Sony Legria HF G10 or M300 cameras) were fitted on each of 6 BRUVS frames deployed during this study. The pairs of cameras were mounted 0.7 m apart and angled in at 8° to allow for stereo imaging. This stereo imaging allows the lengths and distance from the camera of fish to be determined (Langlois et al., 2018). A synchronising diode was placed in the field of view so the camera frames could be synced for size measurements. Each BRUVS frame was calibrated in a pool prior to fieldwork being undertaken. As bait for each of these frames, 1 kg of Pilchards *(Sardinops sagax*) was suspended 1.2 m in front of the cameras. The BRUVS were located at least 300 m apart to minimise movement of fish between sites. Sixty minutes of footage on the seafloor was analysed for each drop location. Lights were attached to BRUVS frames for deeper deployments. Each light contained a bank of 7 Cree XLamps XP-E LEDs delivering a radiant flux of 350 to 425 milliwatt (mW) and royal blue colour at wavelengths ranging from 450 to 465 nanometres (nm).

Post-processing of BRUVS footage was completed using the program EventMeasure (SeaGIS). For each video, the *MaxN* (maximum number of individuals of a particular species in the frame at any given time) was recorded. Species richness was then evaluated for each drop location. The use of stereo cameras also allowed measurement of fish lengths using EventMeasure. Fish were measured for total length with a minimum precision of 5 millimetres (mm). Length–weight relationships were obtained for each species from the FishBase database and were used to calculate biomass for each individual measured fish. Biomass measurements were summed to provide a relative biomass measure for each drop location. To account for fish unable to be measured, a mean length for the corresponding species was assigned to each unmeasured individual to derive relative biomass measures for each drop location (Barley et al., 2017).

Derivatives of the seabed terrain were extracted using the Spatial Analyst module in ArcGIS 10.5.1 (ESRI) and the ‘benthic terrain modeller’ tool for ArcGIS (Walbridge et al., 2018). Derivatives used included bathymetry (depth), vector ruggedness measure (VRM), slope, rugosity, aspect (northness and eastness), bathymetric position index (BPI), curvature and distance to reef (Table 2.2). We calculated the mean of all variables at circular radius scales of 5, 10, 25, 50, 100, 150 and 300 m using the ‘focal statistics’ geoprocessing function in ArcGIS’s Spatial Analyst toolbox. This tool calculates the mean of each cell in an input raster using a roving window that varies in size depending on the scale being tested. The ‘extract multi values to points’ tool in ArcGIS was then used to extract the underlying seafloor

variables of all spatial scales at each BRUVS deployment location. The 'findCorrelation' function from the R package 'caret' (Kuhn, 2008) was used to remove highly correlated variables (>0.7) (Dormann et al., 2013). Variance inflation factors were calculated following analysis, but values were all below 2.5, indicating no multicollinearity was present (James et al., 2013).

Generalised additive models (GAMs) were used to investigate and model the effect of environmental variables on various subsets of the fish assemblages captured using BRUVS. GAMs were selected for use in this study because of their ability to allow for nonlinear relationships (Austin, 1998; Yee and Mitchell, 1991), as well as being a conventional and well-developed method for modelling fish–habitat relationships (Galaiduk et al., 2017; Valavanis et al., 2008). Before running GAMs, spatial autocorrelation of the response variables were tested using a spline correlogram generated in the R package 'ncf' (Bjørnstad, 2009). The R package 'mgcv' (Wood, 2015) was then used to run GAMs, using species richness, family richness, total abundance, Shannon–Wiener diversity index and total biomass as response variables for multi-species analyses, and abundance for single-species analyses. In GAMs, the number of predictor variables able to be included is limited by the ability of the sample size to capture the variability across the study region. Bolker et al. (2009) recommends using a rule of thumb of more than 10 to 20 samples per predictor variable.

Of the 52 successful BRUVS deployments, 39 (75%) were used for training the models while the remaining 13 (25%) were used for evaluating the model performance. Therefore, a maximum of 3 predictor variables could be used per model. All combinations of the 10 predictor variables selected (n = 175 combinations) were modelled to obtain the highest possible model performance. Model selection was conducted using the 'MuMIn' package in R (Barton, 2018), in which a confidence set of models was made. Because the ratio of Akaike weights for 2 candidate models can be used to assess the preference for one model over another (Anderson et al., 2000), the confidence set of models included only those candidate models with Akaike weights within 5% of the largest weight (Thompson and Lee, 2000). These were selected after passing the general rule of thumb (i.e. 1/8 or 12%) suggested by Royall (1997), for evaluating whether strength of evidence was met. To be included in the confidence set, models also had to have a difference in Akaike information criterion (AIC) value from the best model (ΔAIC) of less than 5. From the confidence set, the model with the lowest second-order AIC (AIC_C) was deemed the best model.

To account for variations in the scale of habitat relationships between different groups of demersal fish, modelling in this study was completed using environmental derivatives extracted at multiple spatial scales (5, 10, 25, 50, 75, 100, 150, 200, 250, 300, 400 and 500 m) around the BRUVS deployment location. This allowed models to consider the individual spatial ecology of species interactions with the surrounding environment. Pearson's correlations were used to assess the accuracy of the predicted data compared

with observed data. To assess individual variable importance, models with the best performance for each subset of the assemblage were run with and without each variable included to single out the contribution of the variable in question. Individual contributions were then summed and a percentage of relative importance in the model was derived. The R package 'raster' (Hijmans and van Etten, 2014) was used to create predictive maps extrapolating model predictions over the entire study area.

2.4 Autonomous underwater vehicle

Since 2006, the Integrated Marine Observing System (IMOS) has been routinely operating a wide range of observing equipment throughout Australia's coastal and open oceans, making all of its data accessible to the marine and climate science community, other stakeholders and users, and international collaborators. IMOS observations are guided by science planning undertaken collaboratively across the nodes of the Australian marine and climate science community with input from government, industry and other stakeholders. Five major research themes unify IMOS science plans and related observations: multi-decadal ocean change; climate variability and weather extremes; major boundary currents and interbasin flows; continental shelf and coastal processes; and ecosystem responses.

As part of the IMOS national autonomous underwater vehicle (AUV) monitoring program, this study established AUV monitoring sites within Wilsons Promontory MNP and collected a baseline dataset for this area. The AUV *Sirius* (operated by the Australian Centre for Field Robotics, University of Sydney) is capable of collecting high-resolution, georeferenced imagery at depths to 700 m (Bewley et al., 2015; Williams et al., 2016; Williams et al., 2012). *Sirius* has been designed for low-speed, high-resolution benthic imaging and has high pitch and roll stability. It is further equipped with a suite of sensors including a high-resolution stereo camera pair with strobe lighting, a multi-beam sonar, a depth sensor, Doppler velocity log (DVL), a compass with integrated roll and pitch sensors, ultra-short baseline (USBL) acoustic positioning system, forward-looking obstacle-avoidance sonar and an array of oceanographic sensors.

Prior to deployment, the AUV is instructed to transit to a specific site on the surface before diving and following a pre-programmed route. It aims to maintain a camera height of approximately 2 m above the seafloor and collects stereo images every second. The suite of navigation instruments, including a depth sensor, Doppler velocity log, compass and pressure sensor, are used while the vehicle is underway to estimate its position relative to the local navigation frame. Post-survey, a stereo-based simultaneous localisation and mapping (SLAM) technique (Barkby et al., 2009; Palomer et al., 2013) is used to further refine the estimated vehicle trajectory based on common seafloor features identified in the imagery. For more technical information and standard procedures for operation of the IMOS *Sirius* AUV, see Williams et al. (2012) and Monk et al. (2018).

Post-processing of downward-facing imagery from the AUV was conducted using the program TransectMeasure (SeaGIS). Images were subsampled using the criteria of a minimum of 20 seconds and 5 m distance separation between any 2 images to decrease effects of spatial autocorrelation. Twenty-five randomly spaced points were classified for each image using the CATAMI classification scheme (Althaus et al., 2015), with an additional classification made at the highest possible taxonomic resolution. From this, differences in contribution of each biotic component at the lowest taxonomic resolution possible were identified for each site.

For the purpose of establishing long-term monitoring within the Wilsons Promontory MNP, and to compare AUV survey ability with diver surveys, a total of 8 sites were selected across the MNP, of which 7 were successfully completed. As this was the first study completed using an AUV in this MNP, a range of survey configurations were conducted.

2.5 Towed video and downward-facing imagery

Towed video was used to obtain transect data on benthic habitats extending beyond diving depths within the marine national park. A single towed video survey was conducted on 16 June 2016 using a VideoRay remotely operated vehicle (ROV) modified to function as a drift camera by inserting it into a stainless steel frame and adding a micro-wing attachment to assist in drifting across the seafloor. Forward-facing, high-definition, stereo video footage was obtained from 2 GoPro Hero 3+ cameras fastened to the top of the frame in a custom-built stereo housing with a 40 centimetre (cm) base bar positioned at a 45° angle to the seabed. To reduce the distorting effect of the fish-eye lens in the cameras, footage was recorded with medium field of view, at a resolution of 1,920 × 1,080 pixels and 60 frames per second. A Ricoh Caplio GX100 downward-facing stills camera with an attached strobe light was additionally used to create photo quadrats every 10 seconds. These detailed images make it possible to obtain high-resolution taxonomic identification.

The position of the unit in the water column was tracked at 1-second intervals using a Tracklink 1500MA ultra-short baseline (USBL) acoustic tracking system. The unit was flown approximately 1 m above the seafloor using a winch system while observing a live feed obtained via an umbilical cable from the ROV unit. Boat speed was kept between 0.5 and 1.0 knots (0.26 to 0.5 metres per second (m/s)) for the majority of transects. Time synchronisation between the live towed video, stereo GoPro HD footage, downward-facing still images and the USBL system enabled measurement of the geographical location of benthic habitat observations along transects. Pictures are then synchronised with time stamps from the GPS feed and positioned using the USBL system.

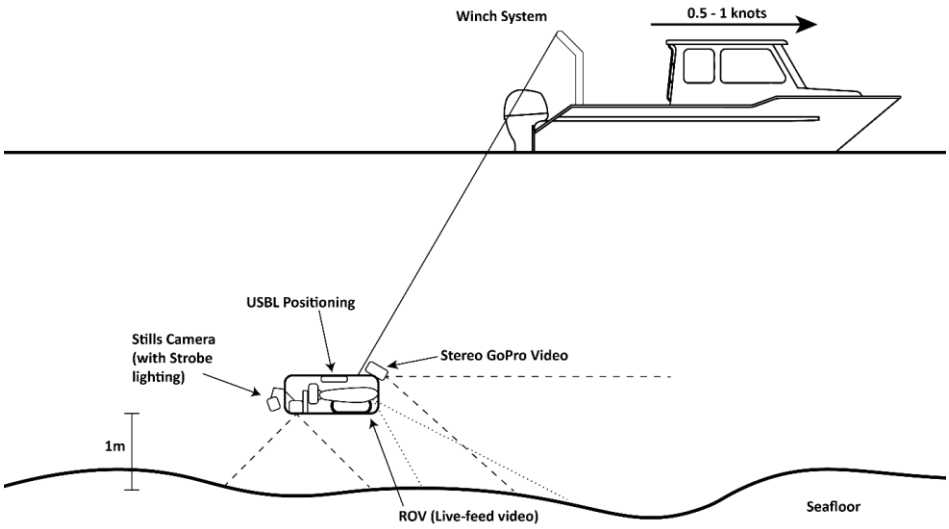

Figure 2.2: Typical arrangement of equipment in a towed video survey

Post-processing of towed video observations was conducted using the program TransectMeasure (SeaGIS). Georeferenced downward-facing stills were overlaid on previously mentioned environmental variables (Section 2.1), allowing depth to be extracted for each image. Images were subsequently grouped into 5 m depth strata, where 40 images were randomly chosen per depth category. Twenty-five randomly spaced points were classified for each image using the CATAMI classification scheme (Althaus et al., 2015), with an additional classification made at the highest possible taxonomic resolution. From this, differences in contribution of each biotic component at the lowest taxonomic resolution possible were identified for each depth stratum, allowing observation of depth-related patterns.

2.6 Habitat mapping

Full habitat maps for both Bunurong and Wilsons Promontory marine national parks were developed using classes derived from the new Combined Biotope Classification Scheme (CBiCS) developed by Australian Marine Ecology and Fathom Pacific. Habitat maps were developed using derivatives from high-resolution multibeam sonar as environmental variables, and ground truthing from a range of sources including ROV, AUV, towed video and drop cameras. This mapping also developed new techniques for integrating angular response derivatives from multibeam backscatter in the habitat mapping workflow (both sites) and water column characteristics in the habitat mapping process.

2.6.1 Angular response analysis variables and analytical scales

Angular response analysis was undertaken from the backscatter mosaic FMGT v7.9.2 (Quality Positing Services, SAAB group) to compute the derivative impedance, phi and volume heterogeneity. Impedance is the ratio between acoustic pressure and velocity,

resulting in a measurement for the 'hardness' of the seafloor (Hou et al., 2018; Fonseca et al., 2009). Sediment grain sizes are represented in a scale known as phi (Fahrulian et al., 2016). FMGT has a proprietary model that predicts phi from the results of the angular response analysis. Volume heterogeneity is a measure of the fluctuations and sound speed within sediments. Sediment density and porosity are described from volume heterogeneity (Jackson and Briggs, 1992). Angular response curve surfaces, mean, slope and kurtosis were produced in MATLAB (v2018b) through a package published by Che Hasan (2014).

Derivative values were extracted in ArcPro v2.1.1 (ESRI). To test the influence of analytical scale on model results, each derivative was created at multiple analytical scale sizes. These scale sizes ranged from 3 × 3 pixels to 201 × 201 pixels, resulting in products at the following scales for each seafloor derivative at Wilsons Promontory MNP: 3, 5, 7, 9, 11, 21, 51, 101 and 201 pixels. Bunurong MNP is a much smaller study site so an additional analytical scale of 501 pixels was used.

2.6.2 Ground truthing and classification

In addition to towed video surveys of Wilsons Promontory MNP (detailed in Section 2.5), observations from separate drop-camera and remotely operated vehicle (ROV) surveys were obtained for use in training models. Drop-camera surveys took place between 1996 and 2016. For this, a Delta vision HD camera was used on a drop-camera system to collect video footage of the seafloor. A total of 85 drops were completed with a maximum survey depth of 22 m (Figure 2.3). Drop positions were determined using vessel DPGS (differential global position system). The towed video, drop video and ROV video surveys were combined and used as a single ground truth dataset. Additionally, Parks Victoria collected video data via ROV at 41 sites in 2013. Ground truthing for Bunurong MNP was entirely obtained from the towed video survey detailed in Section 2.5.

Ground truthing for Bunurong MNP was completed in 2018 using a modified towed video system with 2 oblique-facing GoPro Hero 3+ cameras. Positioning, unit flight speed and unit flight height were the same as at the Wilsons Promontory MNP. Transect locations were chosen using a modified National Environmental Science Programme (NESP) spatially balanced sampling design (Foster et al., 2018). Bunurong MNP was split into 5 classes by an unsupervised ISO clustering in ArcPro, with depth, backscatter, slope, eastness, northness and curvature as predictors. These 5 classes were used as the stratification for the NESP sample design. For best site coverage, a total of 80 transects (250 m each) were completed.

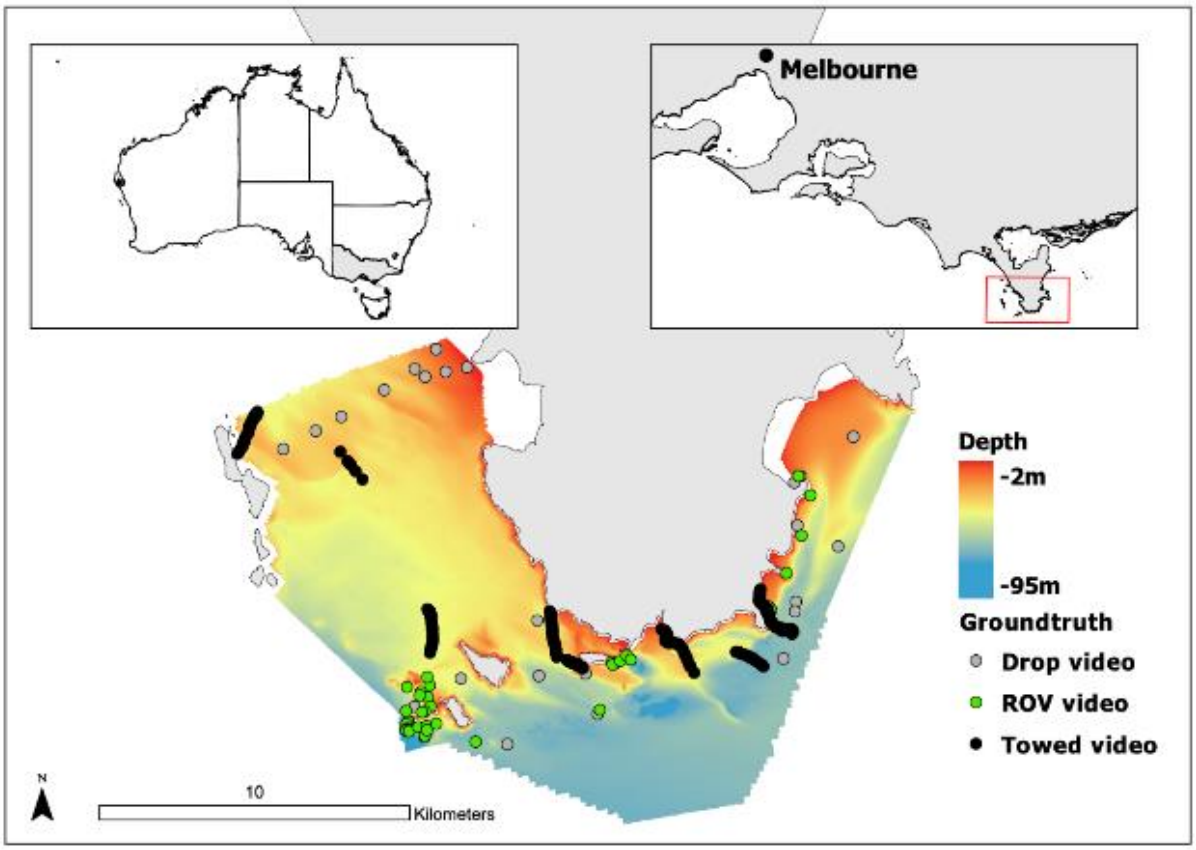

Figure 2.3: Bathymetric coverage of Wilsons Promontory MNP. Ground truth locations in grey (drop video), green (ROV video) and black (towed video)

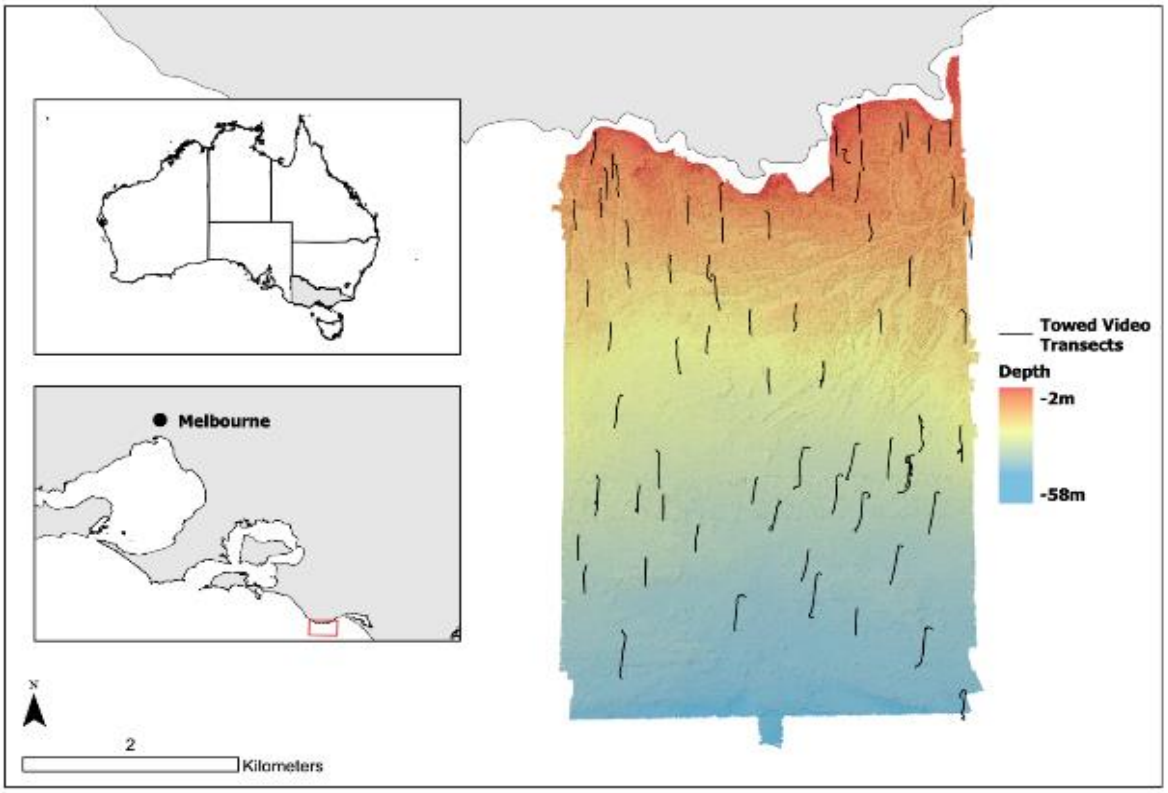

Figure 2.4: Bathymetric coverage for Bunurong MNP. Towed video transects in black

The Combined Biotope Classification Scheme (CBiCS), which has been adopted by the Department of Environment, Land, Water and Planning (DELWP) (Victorian Government, Australia) (Edmunds and Flynn, 2015) was used to classify video observations. CBiCS delineates habitat classes, based on observations of biota from the video data, into multiple categories for each of the CBiCS hierarchies (Edmunds and Flynn, 2015). There are 6 hierarchical levels within CBiCS (Eigenraam et al., 2016). Due to the large number of rare classes, 2 levels of the scheme were used for both the Wilsons Promontory MNP and Bunurong MNP: habitat complexes (BC3) and biotope complexes (BC4). Habitat complexes are defined by the broad substrate class (e.g. infralittoral or circalittoral reef and sediment) while the biotope complexes include information on the predominant biological structural characteristics and morphotypes. The biological groups delineating the different biotope complexes include bare rock, sediments, barnacles, gastropods, mussel beds, oyster beds, turf algae and macroalgal beds.

To assess spatial autocorrelation within the ground truth data, R was used to create a semi-variogram for each CBiCS class across Wilsons Promontory MNP and Bunurong MNP. To limit spatial autocorrelation, the minimum distance between points was 35 m for Wilsons Promontory MNP and 15 m for Bunurong MNP. The observations were then stratified by class and randomly assigned to subsets with a minimum distance between points of 35 m and 15 m for Wilsons Promontory MNP and Bunurong MNP, respectively.

2.6.3 Object-based image analysis

In an attempt to reduce artefacts introduced from the backscatter mosaic, object-based image analysis (OBIA) was used to partition the surface into small continuous regions that share the same or similar attributes (Blaschke, 2010). OBIA was carried out using the ENVI 5.3.1 EX toolbox on the backscatter mosaic from FMGT. OBIA in ENVI uses an edge-detection algorithm to partition the backscatter mosaic. In the FX toolbox, the ‘segment only feature extraction workflow’ tool was used with the following settings: edge-detection scale level 5 and merge full Lambda schedule level 98. To reduce processing time, the segmented surface was filtered in ArcPro; any segment with fewer than 50 pixels was merged with the closest larger segment.

2.6.4 Statistical approaches

To derive rule-based relationships between geophysical derivatives and corresponding observational data, random forest models were used from the ‘randomForest’ (RF) package in R (Liaw and Wiener, 2002), which has often been used in habitat mapping studies and has often generated the most accurate result. By including the results of multiple trees from bootstrap samples, the RF classification approach reduces the chances of overfitting the model (Cutler et al., 2007). RF randomly chooses predictors for each selection, which keeps predictor bias low. Tree-based methods, which include RF, better predicted sediment classes from acoustic and ground truth data sets compared to other machine learning

techniques in previous studies (Diesing et al., 2016). To assess correlation of predictor variables, Pearson product-moment correlation was used. Any predictors with a value greater than 0.7 were removed from the model, retaining the predictors with the highest variable importance.

Variable importance was calculated by assessing out-of-bag (OOB) errors and percentage increase in misclassification. OOB errors and percentage increase in misclassification were calculated by randomly removing each predictor variable and measuring their respective changes. From both OOB errors and percentage increase in misclassification, mean decrease accuracy was computed and used as a representation of variable importance. The lower the mean decrease accuracy value, the smaller the impact of the variable on model accuracy.

The classified habitat maps for both Wilsons Promontory MNP and Bunurong MNP were created using the R package ModelMap (Freeman et al., 2018). Model accuracies were determined following the methods of Lyons et al. (2018), which randomly splits ground truth data into training and validation samples. Typically, 70% of the observation data is used as the training sample to train the model and predict habitat classes, while the remaining 30% is used as a validation dataset to compare predicted classes with known validation points. Rather than using individual model accuracy to represent model performance, Lyons et al. (2018) repeated the 70/30 split 500 times, then calculated the mean and variance of the error metrics and used them as an indication of map confidence. Here we assess class accuracies using user (error of inclusion) and producer (error of exclusion) class accuracies. Map confidence was used for both Wilsons Promontory MNP and Bunurong MNP.

3. Results

3.1 Seabed of Wilsons Promontory MNP and Bunurong MNP

For use in this study, high-resolution (1 m horizontal resolution) bathymetric grids were obtained for the Wilsons Promontory MNP (Figure 3.1) and Bunurong MNP (Figure 3.2), a combined area of approximately 190 square kilometres (km^2). From this, 19 derivatives of bathymetry and backscatter were calculated to further our understanding of seafloor features. Derivatives created included bathymetry, bathymetry standard deviation, backscatter, bathymetric position index (BPI), slope, aspect (northness and eastness), rugosity, maximum curvature, HSI Red, HSI Green, HSI Blue, complexity, impedance, volume, standard deviation of volume, phi, standard deviation of phi, angular response slope and angular response skewness.

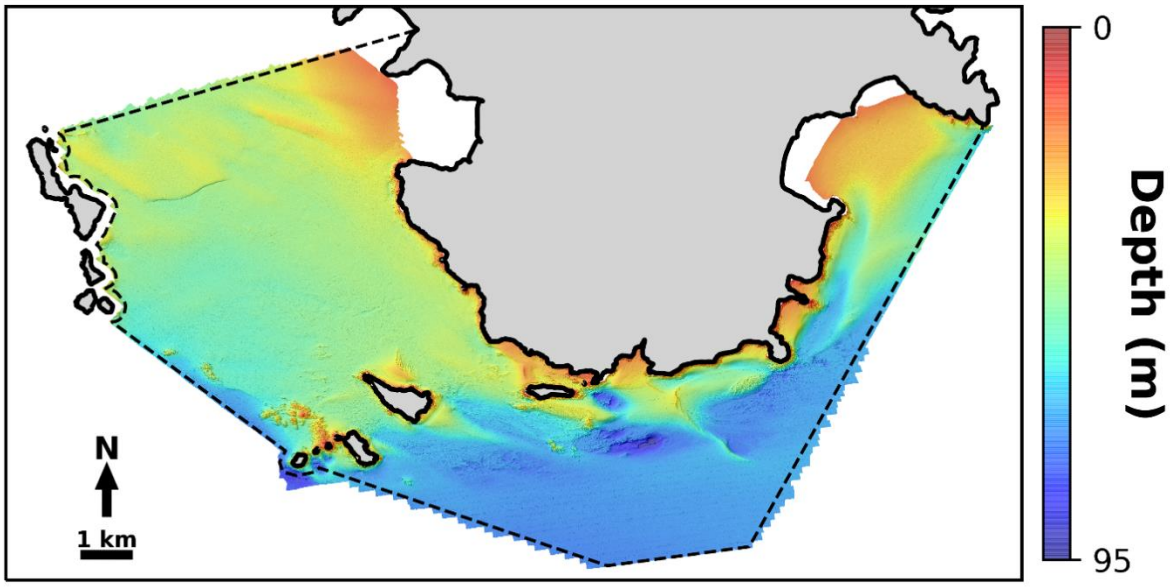

Figure 3.1: Hillshaded (shading to show 3D relief) bathymetric coverage of the Wilsons Promontory MNP. Dashed line indicates the boundary of the marine national park

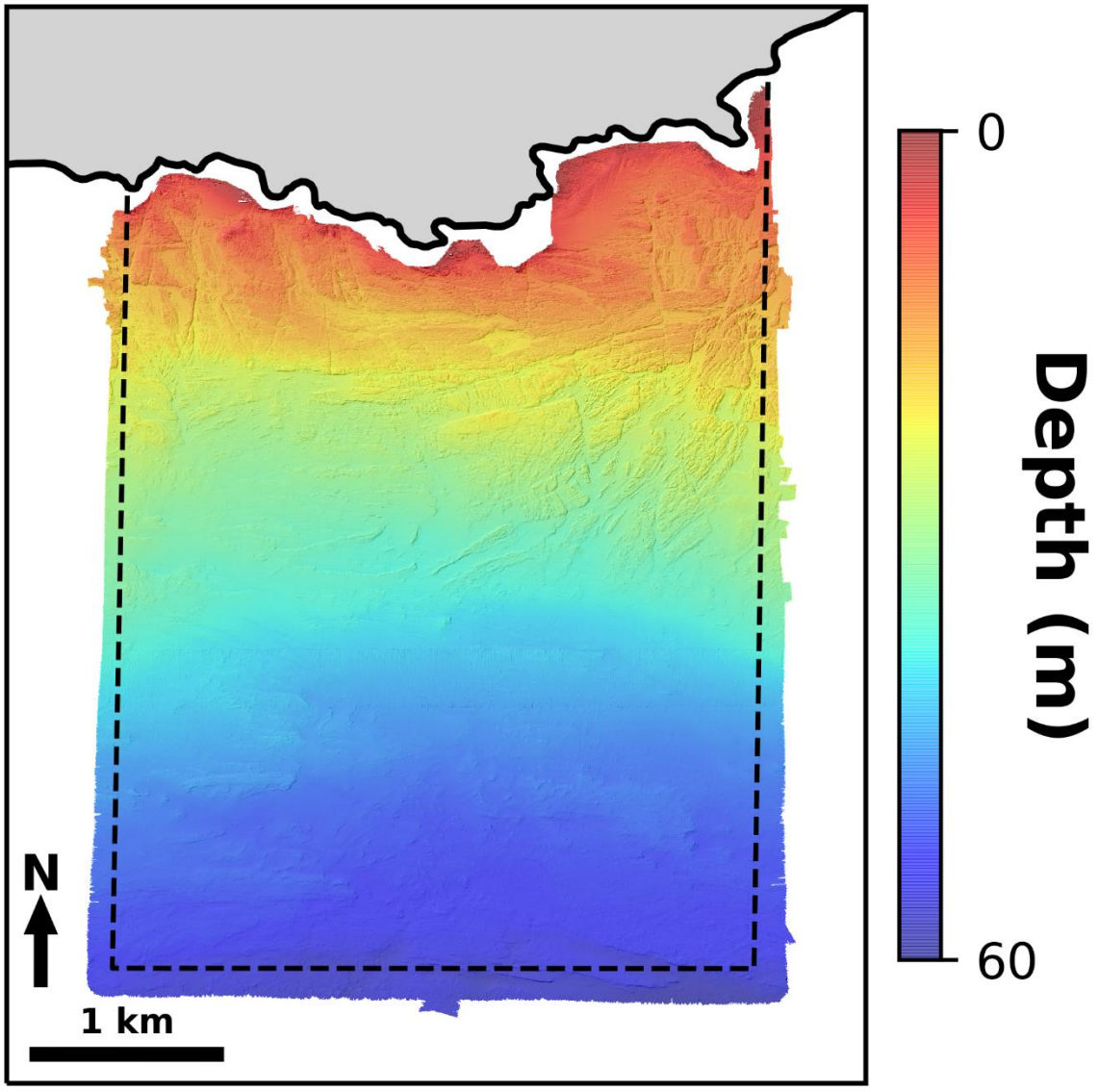

Figure 3.2: Hillshaded multibeam sonar bathymetric coverage of the Bunurong MNP. Dashed line indicates the boundary of the marine national park

3.2 Patterns of sea-surface temperature within marine national parks

Mean sea-surface temperature (SST) varies seasonally and temporally in the Bunurong MNP and Wilsons Promontory MNP with higher mean temperatures during summer. The SST has experienced an overall mean increase since 1992 in both annual and summer time series for both parks; however, this trend is not linear and temperatures oscillate through time. The larger increases in SST occurred during the summer months in both parks. These trends also show that SST does not vary much throughout the parks: standard deviations were very low except in 2006 when both parks experienced large variations in annual mean SST.

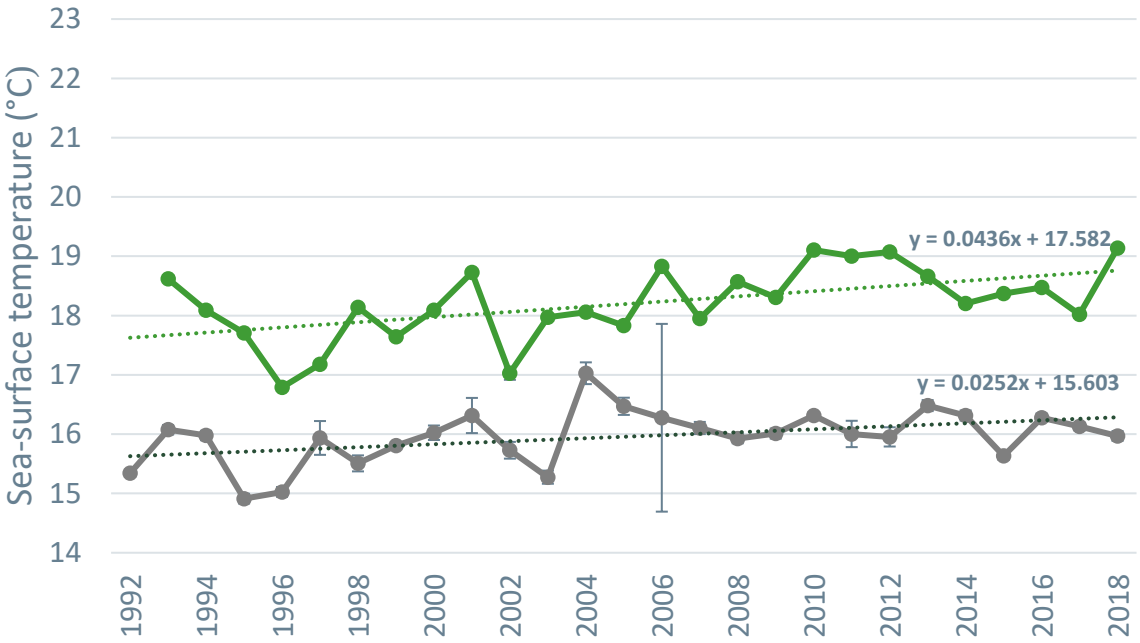

Figure 3.3: Sea-surface temperature (SST) trends through time for annual (grey line) and summer (green line) means in the Wilsons Promontory MNP. Error bars show the standard deviations of the means across the park

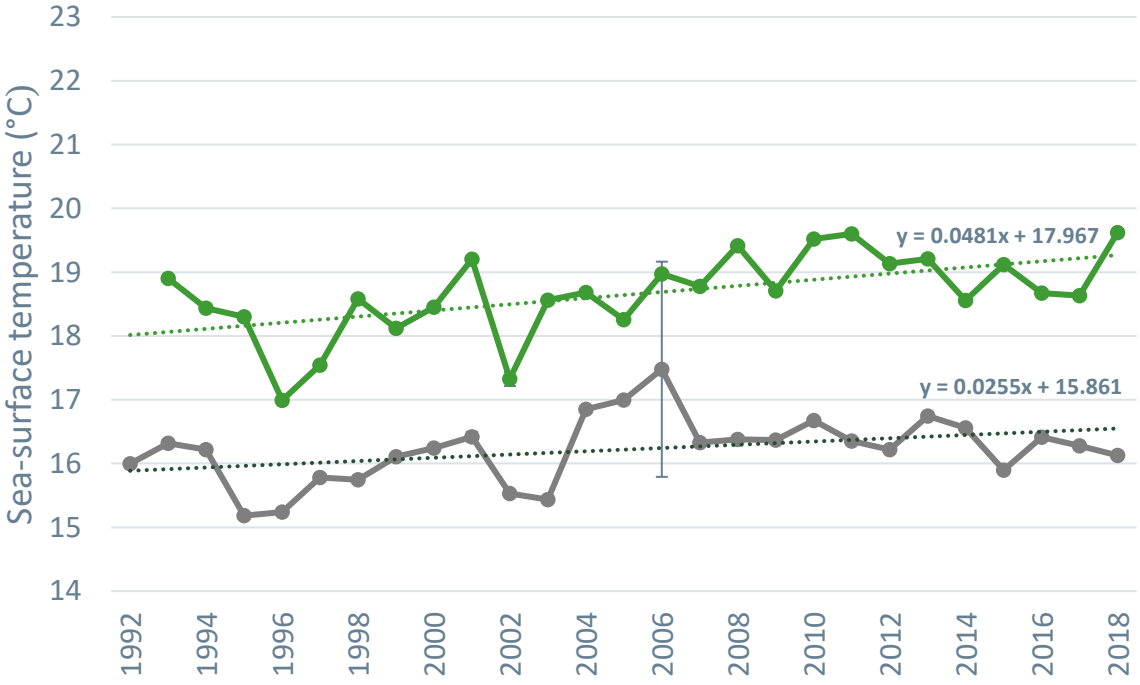

Figure 3.4: Sea-surface temperature (SST) trends through time for annual (grey line) and summer (green line) means in the Bunurong MNP. Error bars show the standard deviations of the means across the park

3.3 Fisheries-independent Southern Rock Lobster survey, Wilsons Promontory

We used spatially explicit, standardised fishery sampling methods to compare Southern Rock Lobster (SRL) populations inside and outside Wilsons Promontory MNP. All but 2 individuals from 162 caught over the duration of this study were of legal size, and the overall average weight was just over 2 kg per individual. Results from t-tests comparing population characteristics inside and outside Wilsons Promontory MNP showed that there were no significant differences in length or biomass between any of the sampling regions (Bonferroni $P = 0.01$). Table 3.1 summarises the measurements obtained. In the West (deep) region, larger individuals and greater biomass were captured inside the MPA than outside, but these differences were not significant (length: mean (inside) = 172, mean (outside) = 148, $P = 0.05$; biomass: mean (inside) = 2.72, mean (outside) = 1.68, $P = 0.05$; Table 3.2). The West (shallow) region also experienced greater size and biomass inside the MPA but, again, these differences were not significant (length: mean (inside) = 163.6, mean (outside) = 153.0, $P = 0.07$; biomass: mean (inside) = 2.25, mean (outside) = 1.82, $P = 0.06$). The East (shallow) region experienced a similar pattern as the other sites with the differences being significant for both length and biomass (length: mean (inside) = 169, mean (outside) = 140, $P = 0.00$; biomass: mean (inside) = 2.51, mean (outside) = 1.51, $P = 0.00$).

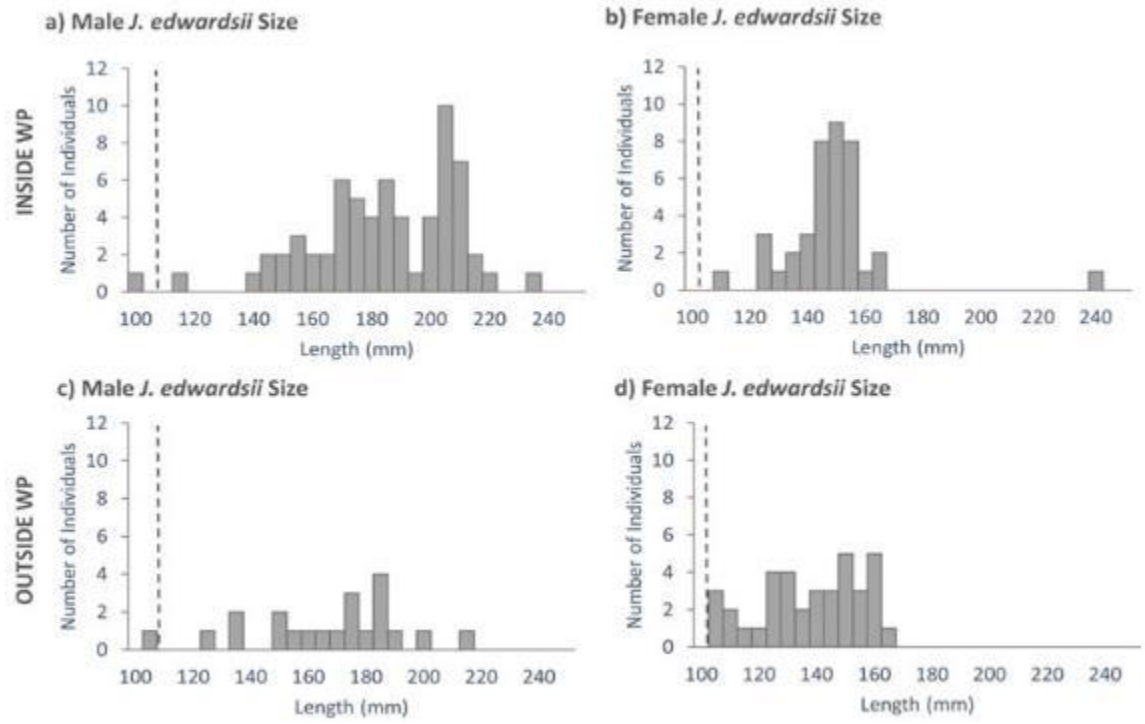

Figure 3.5: Southern Rock Lobster (*Jasus edwardsii*) male and female size (carapace length) distributions inside and outside Wilsons Promontory MNP (WP): (a) males inside the WP, (b) females inside the WP, (c) males outside the WP and (d) females outside the WP. The length of legal size for males and females is displayed as a dashed black line in each distribution plot

The zero-inflated generalised linear models (GLMs) used to associate SRL length and weight with habitat characteristics were unsuccessful in understanding habitat associations. The habitat variables used in the models were non-significant and less than 5% of the deviance was explained (not shown).

Table 3.1: Southern Rock Lobster (*Jasus edwardsii*) statistics inside (*n* = 125) and outside (*n* = 75) Wilsons Promontory MNP

Location	Sex	No. of individuals	No. of legal size individuals	Average carapace length (mm)	SD of average carapace length (mm)	Biomass (kg)	Average biomass per pot lift (kg)	Average weight (kg)	SD of average weight (kg)
Inside park	Male	65	64	182	25	197.123	1.049	3.033	1.112
	Female	39	39	146	19	61.102	0.361	1.567	0.761
	Total	104	103	164		258.225	1.41	2.3	
Outside park	Male	21	21	165	27	48.488	0.674	2.309	0.996
	Female	37	37	135	18	46.98	0.686	1.27	0.438
	Total	58	58	150		95.468	1.36	1.79	

Table 3.2: Southern Rock Lobster (*Jasus edwardsii*) statistics for each of the comparable zones from the sampling design inside and outside Wilsons Promontory MNP

Comparison zone	Inside/outside marine park	No. of individuals	No. of legal size individuals	Average carapace length (mm)	SD of average carapace length (mm)	Average biomass (kg)	SD of average biomass (kg)
West Deep	Inside	9	9	172	38	2.724	1.563
	Outside	18	17	148	23	1.677	0.723
West Shallow	Inside	29	29	164	25	2.251	1.022
	Outside	16	16	153	21	1.818	0.761
East Shallow	Inside	28	28	169	27	2.513	1.109
	Outside	24	24	140	28	1.508	0.950

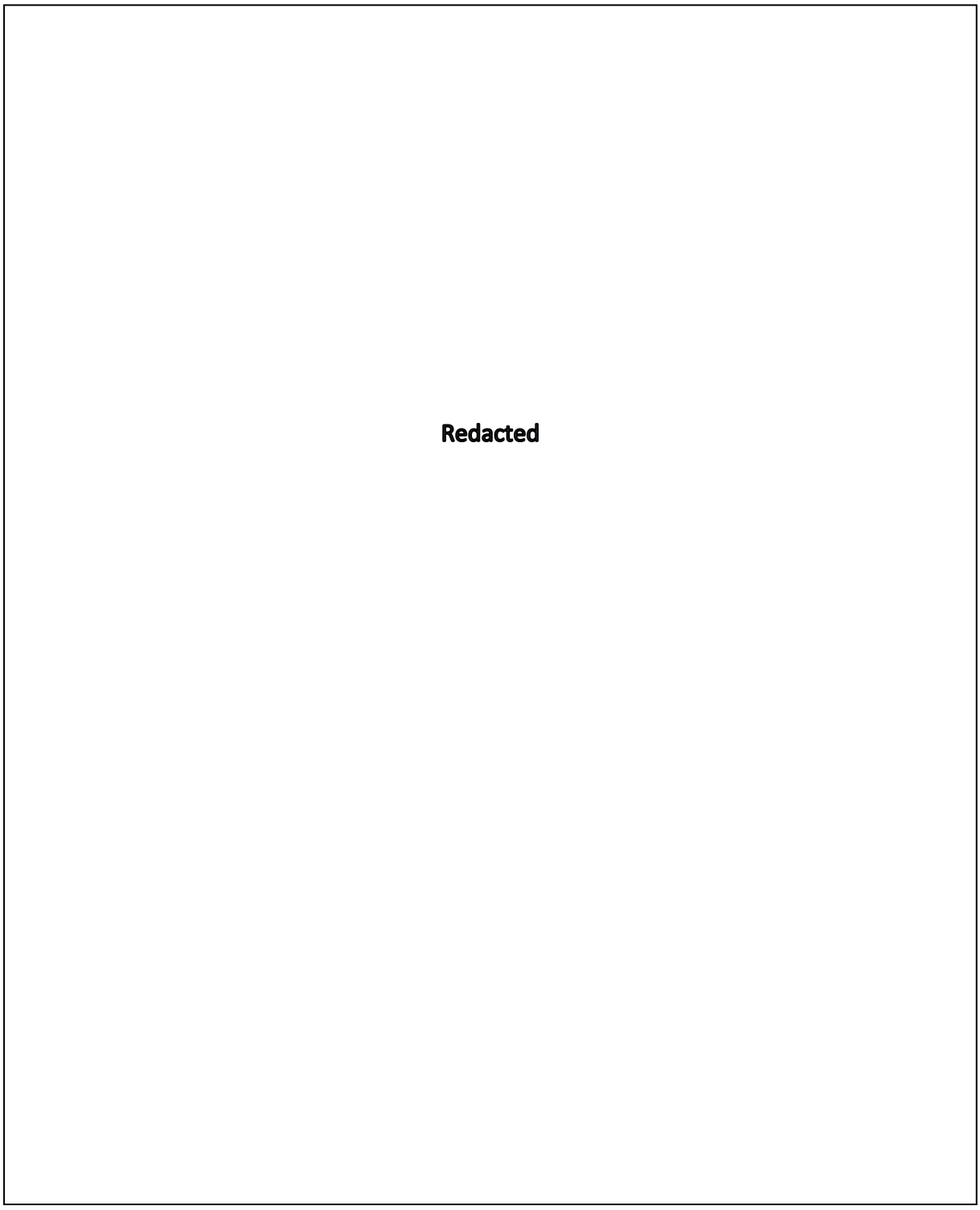

Figure 3.6: Total abundance of *Jasus edwardsii* for all lobster pot deployment sites. The size of each site marker corresponds to the total abundance of *J. edwardsii* observed at that site. These sites are overlaid on hillshaded bathymetry of the study area, coloured by depth. Black boxes denote Wilsons Promontory MNP boundaries

Table 3.3: Bycatch observed from lobster potting using research pots with no escape gaps, in the Wilsons Promontory MNP and adjacent fished reference locations. All bycatch observed was identified, measured and promptly returned to the water

Bycatch species	Inside park	Outside park
Cephaloscyllium laticeps (Draughtboard Shark)	195	50
Diogenidae spp. (hermit crabs)	56	45
Notolabrus tetricus (Blue-Throat Wrasse)	15	6
Heterodontus portusjacksoni (Port Jackson Shark)	11	6
Nectocarcinus tuberculosus (Velvet Crab)	9	5
Meuschenia freycineti (Six-Spine Leatherjacket)	3	4
Octopodidae spp. (octopus)	3	1
Nemadactylus macropterus (Jackass Morwong)	1	1
Echinodermata spp. (starfish)	1	1
Arctocephalus pusillus (Australian Fur Seal)	1	0
Caesioperca spp. (Barber Perch and Butterfly Perch)	1	0
Scorpis spp. (sweep)	1	0
Moridae spp. (morid cods)	0	3

Overall, an average of 2 organisms were caught as bycatch per pot (mean bycatch per pot = 2.095). Draughtboard sharks (*Cephaloscyllium laticeps*) (58.4%) and hermit crabs (24.1%) made up the vast majority of all bycatch (Table 3.3). More bycatch was caught inside (*n* = 297) than outside (*n* = 122) the MPA.

3.4 Baited remote underwater video stations

A total of 3,501 observations across 76 taxa belonging to 42 families were recorded from 52 stereo-BRUVS deployments (Table 3.4). Depths of sample sites ranged from 16 to 91 m. Twenty-three of these locations sampled sediment habitat and 29 sampled reef substratum. Mean species richness was consistent (15 ± 1 species). The largest differences in species richness across habitats occurred between reef and sediment. On sediment, an average of only 7 taxa were observed per drop (Table 3.4). High species richness and biomass were associated predominantly with reef habitat, with 36 species found exclusively at reef sites (Table 3.4, Figures 3.8 and 3.9). Eight species were found exclusively in sediment environments (Table 3.4).

The families with the greatest abundance of individuals were Serranidae (41.8%), Labridae (11.4%) and Monacanthidae (10.4%) (Figure 3.8). The most abundant species in this study were perch (*Caesioperca* spp., 45.9%), Rosy Wrasse (*Pseudolabrus rubicundus*, 6.3%), Degen's Leatherjacket (*Thamnaconus degeni*, 5.4%), Blue-Throat Wrasse (*Notolabrus tetricus*, 5.4%) and Longfin Pike (*Dinolestes lewini*, 4.1%) (Table 3.5,Figure 3.8). Shark species such as Gummy Shark (*Mustelus antarcticus*, 30.4% of total biomass),

Cephaloscyllium laticeps (25.9%) and Port Jackson Shark (*Heterodontus portusjacksoni*, 8.8%) were the highest contributors to biomass (Figure 3.9). The large number of individuals observed from the *Caesioperca* genus also contributed to the biomass observed (3.98% of relative biomass within the park).

Table 3.4: Summary of stereo baited remote underwater video stations (BRUVS) observations

	Reef	Sediment	Total
Total no. of deployments	29	23	52
Total no. of individuals	2,704	797	3,501
Mean no. of taxa	15	7	13
Total no. of taxa	68	40	76
Total no. of taxa exclusive to habitat	36	8	-

Figure 3.7: Screen grabs from high-definition BRUVS video exhibiting the diversity of habitat and species that can be sampled by this method

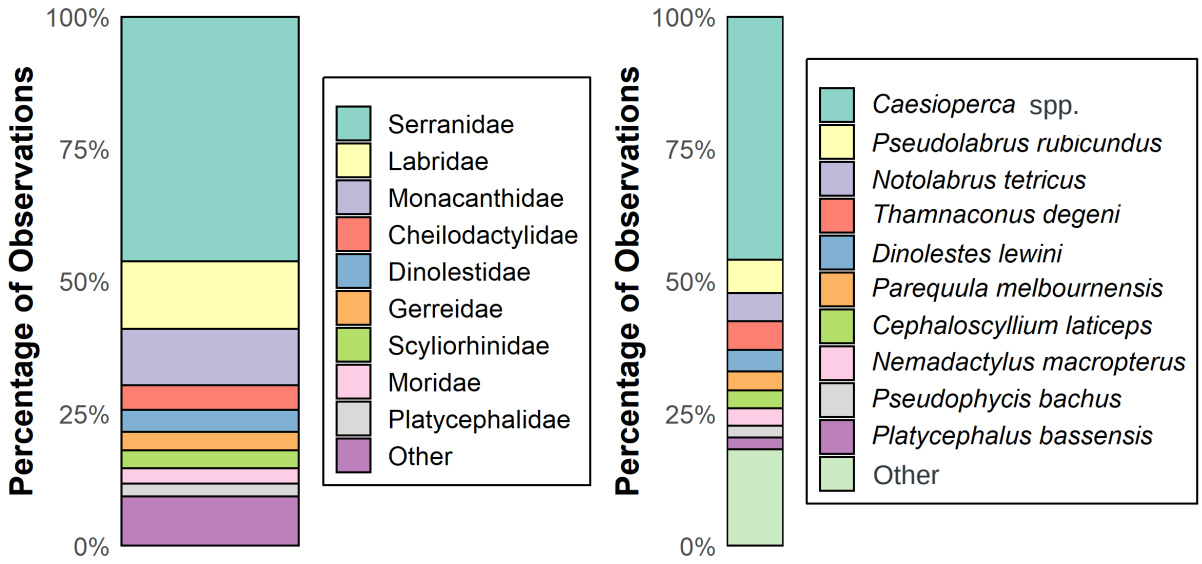

Figure 3.8: Proportions (as percentages) of the complete fish assemblage from BRUVS sampling based on family (left) and species (right). Other represents families or species with total observation of less than 2%

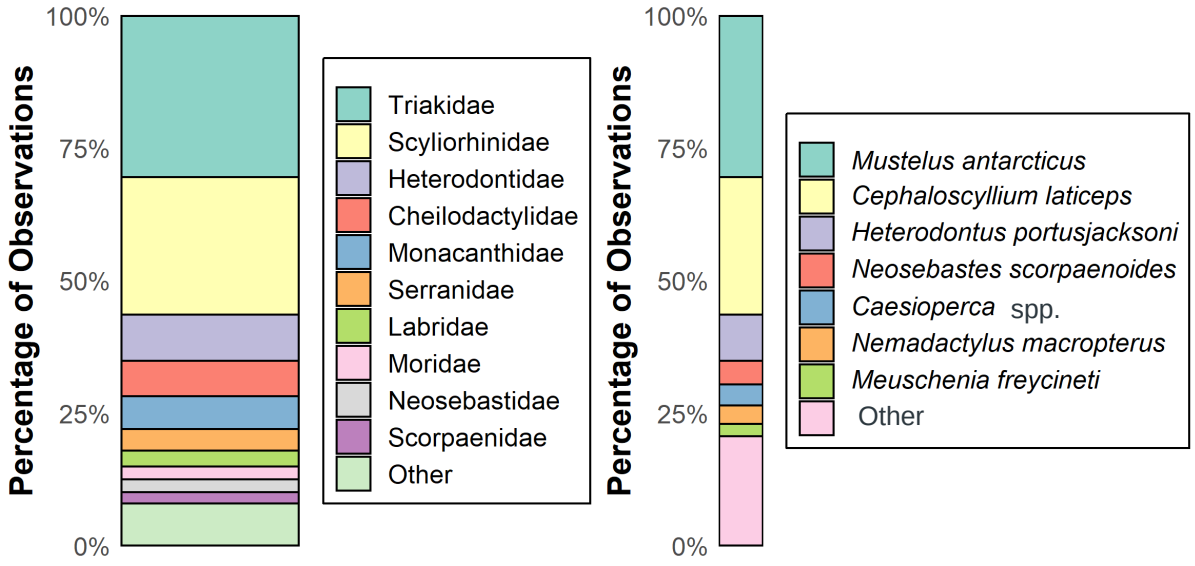

Figure 3.9: Proportions (as percentages) of the complete fish biomass from BRUVS sampling based on family (left) and species (right). Other represents families or species with total observation of less than 2%

Table 3.5: Proportions (as percentages) of the total abundance and total biomass of fish observed in BRUVS surveys. Note that this is not a complete species list. This list only contains top contributors (greater than 1% of total)

Species	Total abundance (%)
Caesioperca spp.	45.92
Pseudolabrus rubicundus	6.29
Notolabrus tetricus	5.38
Thamnaconus degeni	5.38
Dinolestes lewini	4.11
Parequula melbournensis	3.51
Cephaloscyllium laticeps	3.43
Nemadactylus macropterus	3.26
Pseudophycis bachus	2.29
Platycephalus bassensis	2.21
Meuschenia scaber	1.90
Meuschenia freycineti	1.73
Upeneichthys vlamingii	1.33
Neosebastes scorpaenoides	1.19
Mustelus antarcticus	1.16
Heterodontus portusjacksoni	0.91
Pseudogoniistius nigripes	0.82
Scorpis lineolata	0.54
Nemadactylus valenciennesi	0.51
Pseudophycis barbata	0.51
Trygonorrhina dumerilii	0.51
Pictilabrus laticlavius	0.48
Ophthalmolepis lineolata	0.45
Helicolenus percoides	0.42
Latropiscis purpurissatus	0.40
Chrysophrys auratus	0.40
Eubalichthys gunnii	0.37
Enoplosus armatus	0.34
Monacanthidae spp.	0.34
Acanthaluteres vittiger	0.28
Hypoplectrodes nigroruber	0.28
Meuschenia venusta	0.28
Platycephalus spp.	0.25
Parma microlepis	0.23
Eubalichthys mosaicus	0.17
Meuschenia spp.	0.17
Notolabrus fucicola	0.14
Aplodactylus arctidens	0.11
Cyttus australis	0.11
Parma victoriae	0.11

Species	Total biomass (%)
Mustelus antarcticus	30.43
Cephaloscyllium laticeps	25.92
Heterodontus portusjacksoni	8.75
Neosebastes scorpaenoides	4.49
Caesioperca spp.	3.97
Nemadactylus macropterus	3.48
Meuschenia freycineti	2.33
Pseudophycis bachus	1.92
Meuschenia scaber	1.89
Nemadactylus valenciennesi	1.76
Notolabrus tetricus	1.26
Thamnaconus degeni	1.19
Platycephalus bassensis	1.18
Pseudogoniistius nigripes	1.16
Pseudolabrus rubicundus	0.93
Dinolestes lewini	0.73
Achoerodus viridis	0.68
Chrysophrys auratus	0.65
Latris lineata	0.65
Trygonoptera imitata	0.55
Helicolenus percoides	0.54
Latridopsis forsteri	0.43
Parequula melbournensis	0.42
Pseudophycis barbata	0.42
Parascyllium ferrugineum	0.39
Pentaceropsis recurvirostris	0.29
Girella zebra	0.27
Eubalichthys gunnii	0.26
Aplodactylus arctidens	0.25
Upeneichthys vlamingii	0.25
Nemadactylus douglasii	0.23
Scorpis lineolata	0.20
Pictilabrus laticlavius	0.20
Chelidonichthys kumu	0.19
Platycephalus spp.	0.18
Eubalichthys mosaicus	0.17
Notolabrus fucicola	0.13
Meuschenia spp.	0.13
Cyttus australis	0.12
Meuschenia venusta	0.12
Parma microlepis	0.12
Acanthaluteres vittiger	0.11

3.4.1 Performance of species distribution models using BRUVS data

Overall, when species richness was modelled for the entire assemblage using BRUVS data, the best performing models were found using environmental variables at a spatial scale of 25 m. In this model, 55.11% of the deviance in species richness was explained and a Pearson's correlation of 0.51 (P = 0.128) was present between test data (which were set aside and not used in training the models) and predictions (Table 3.6). However, when family richness was modelled for the entire assemblage using BRUVS data, the best performing models were found using environmental variables at a spatial scale of 300 m. In this model, 41.09% of the deviance is explained and a correlation of 0.61 (P = 0.062) was found with test data. Models for relative total biomass, relative total abundance and Shannon– Wiener diversity index had low performance.

When relative abundances of key species within the MNP were modelled, models for *Notolabrus tetricus* showed a strong ability to be explained by environmental variables with 78.18% of deviance explained and a 0.9 (P < 0.001) correlation with the data reserved to test the predictive accuracy of the models. *N. tetricus* is a common predator along the coast of Victoria that helps to shape the distribution and abundance of invertebrates (Shepherd and Clarkson, 2001). It has even been linked to the recruitment of abalone (Shepherd and Cannon, 1988). As it is also a commercially targeted species, understanding the distribution of *N. tetricus* can provide insights into the performance of MPAs.

Other strongly performing models were for *Pseudolabrus rubicundus*, *Cephaloscyllium laticeps* and *Thamnaconus degeni*. Like *N. tetricus*, these 3 species prey on invertebrates and help shape the structure of marine communities. Models for *Dinolestes lewini*, *Mustelus antarcticus* and Silverbelly (*Parequula melbournensis*) were deemed poor performing as they had low correlation with the reserved test data (<0.4 correlation, P > 0.171). These species were likely more difficult to model as they are either more mobile schooling fish (*D. lewini*) or are associated with lower relief habitats, such as muddy or sandy substrates, which are harder to distinguish across seafloor variables (*M. antarcticus* and *P. melbournensis*) (Sarre et al., 1997; Walker, 2007). Despite the lower performance of the models, these species shape coastal food webs as predators of invertebrates and fishes. Additionally, *M. antarcticus* is a very important fishery species along the coast, and understanding its distribution could help to better manage the fishery (Walker 2007).

Table 3.6: Summary statistics of best performing generalised additive models (GAMs) completed at spatial scales of 5, 10, 25, 50, 75, 100, 150, 200 and 300 m, and whether models were deemed to perform well enough to be useful spatially. Best descriptor variables are identified by +

Subset	Optimal radius scale (m)	Bathymetry	Rugosity	Fine BPI[1]	Broad BPI[1]	Northness	Eastness	Reef/sediment	Degrees of freedom	AICc [2]	Deviance explained[3] (%)	Test data correlation [4]	Test data correlation (*P* value)	Spatial predictions made
Cephaloscyllium laticeps	300	+	+			+			10	171.26	57.47	0.72	0.018	Yes
Dinolestes lewini	300				+		+		10	356.04	58.58	0.14	0.690	No
Mustelus antarcticus	150		+		+				9	122.46	43.64	0	0.171	No
Notolabrus tetricus	300		+				+		8	223.56	78.18	0.90	0.000	Yes
Parequula melbournensis	50	+		+	+				6	244.22	32.83	0.37	0.286	No
Pseudolabrus rubicundus	25	+	+					+	13	264.70	75.56	0.84	0.002	Yes
Thamnaconus degeni	100	+		+			+		11	353.84	45.67	0.38	0.283	Yes
Species richness	25		+					+	7	298.17	55.11	0.51	0.128	Yes
Family richness	300		+		+		+		7	249.44	41.09	0.61	0.062	Yes
Total abundance	150				+		+		9	523.23	68.66	0	0.791	No
Total biomass	25				+		+		17	1,113.22	83.14	0	0.539	No

Notes: **1 BPI = bathymetric position index**
2 AICc = AICc = Akaike information criterion (AIC) with correction for small sample sizes
3 Deviance explained is an indication of the model's goodness-of-fit
4 Pearson's correlation between test data and corresponding predictions

The BRUVS deployments within Wilsons Promontory MNP show that there is a lot of variability in richness across the site with higher richness occurring closer to areas of reef (Figure 3.10). These patterns are also apparent in the distribution model of richness (Figure 3.11) where richness is predicted to be much higher on the shallow reef areas (warmer colours in the predictive map). These patterns are expected as higher topographic complexity is often associated with greater fish diversity (Friedlander and Parrish, 1998; Kuffner et al., 2007; Roberts and Ormond, 1987). Similar patterns are also observed with family richness (Figures 3.12 and 3.13) but with a slightly broader scale.

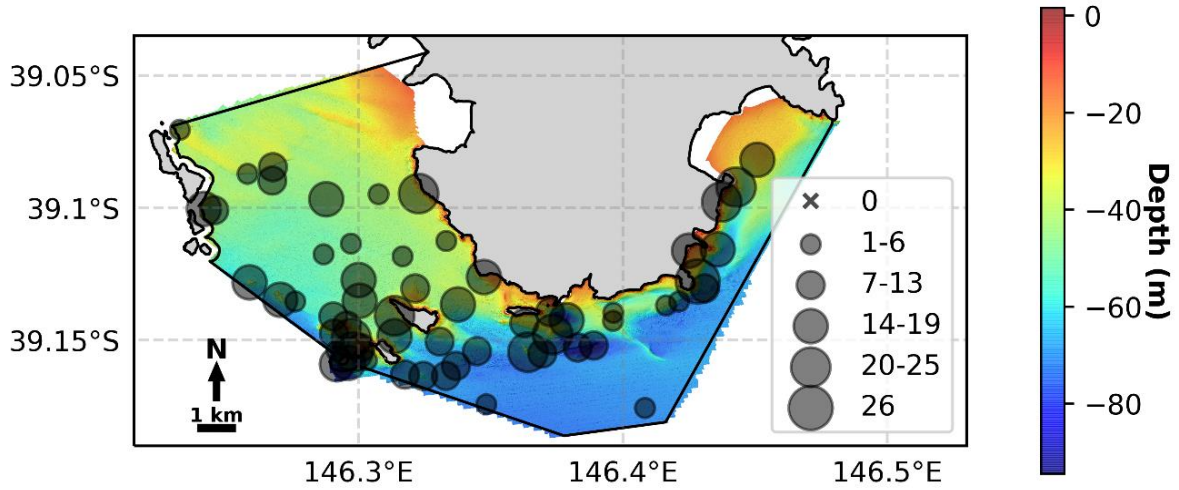

Figure 3.10: Relative species richness of fish for all BRUVS deployments. The size of each site marker corresponds to the relative species richness of fish observed at that site. These sites are overlaid on hillshaded bathymetry of the study area, coloured by depth. The black box denotes the boundary of Wilsons Promontory MNP

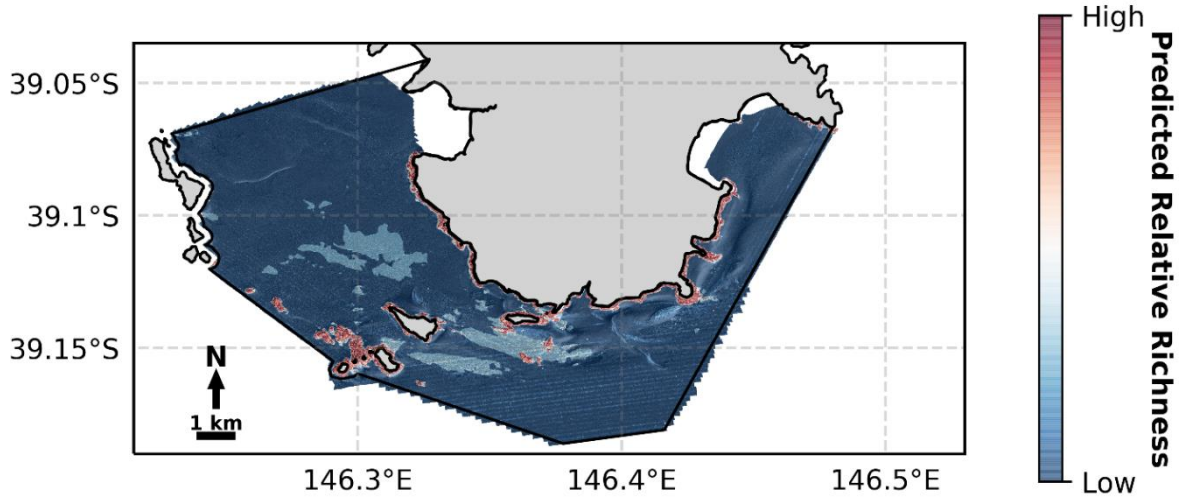

Figure 3.11: Species richness from BRUVS sampling across the whole study site

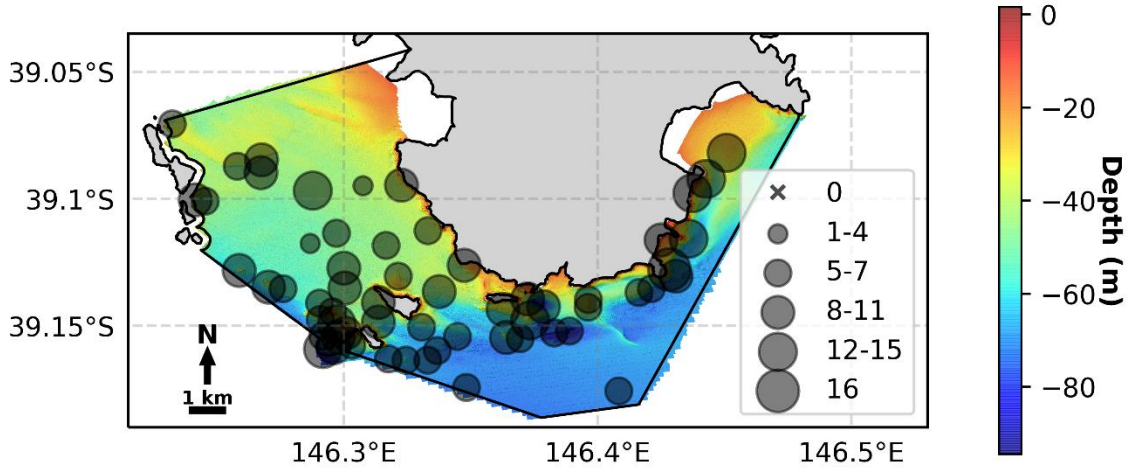

Figure 3.12: Relative family richness of fish for all BRUVS deployments. The size of each site marker corresponds to the relative family richness of fish observed at that site. These sites are overlaid on hillshaded bathymetry of the study area, coloured by depth. The black box denotes the boundary of Wilsons Promontory MNP

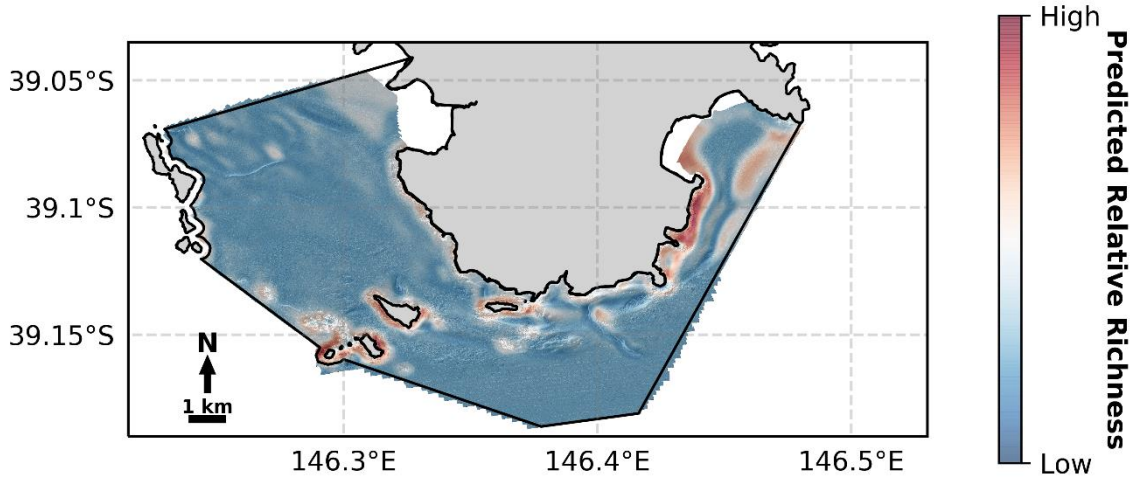

Figure 3.13: Predicted family richness from BRUVS sampling across the whole study site

The BRUVS sampling shows that *C. laticeps* is found in varying abundances throughout Wilsons Promontory MNP in areas of both sediment and reef (Figure 3.14). These patterns are consistent with the more general habitat associations of *C. laticeps*, which is found on sediment and rocky reefs in depths up to 60 m (Daley et al., 2003). A movement study by Awruch et al. (2009) showed that, although it prefers inhabiting reef areas, *C. laticeps* can travel large distances for prey and may move out of its preferred habitat for the bait on the BRUVS.

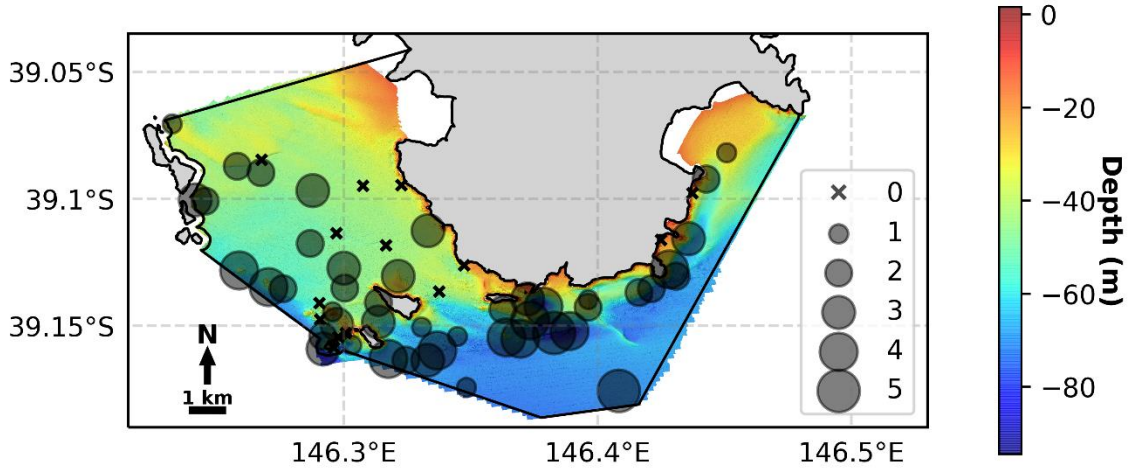

Figure 3.14: Relative abundance of *Cephaloscyllium laticeps* for all BRUVS deployments. The size of each site marker corresponds to the relative abundance of *C. laticeps* observed at that site. These sites are overlaid on hillshaded bathymetry of the study area, coloured by depth. The black box denotes the boundary of Wilsons Promontory MNP

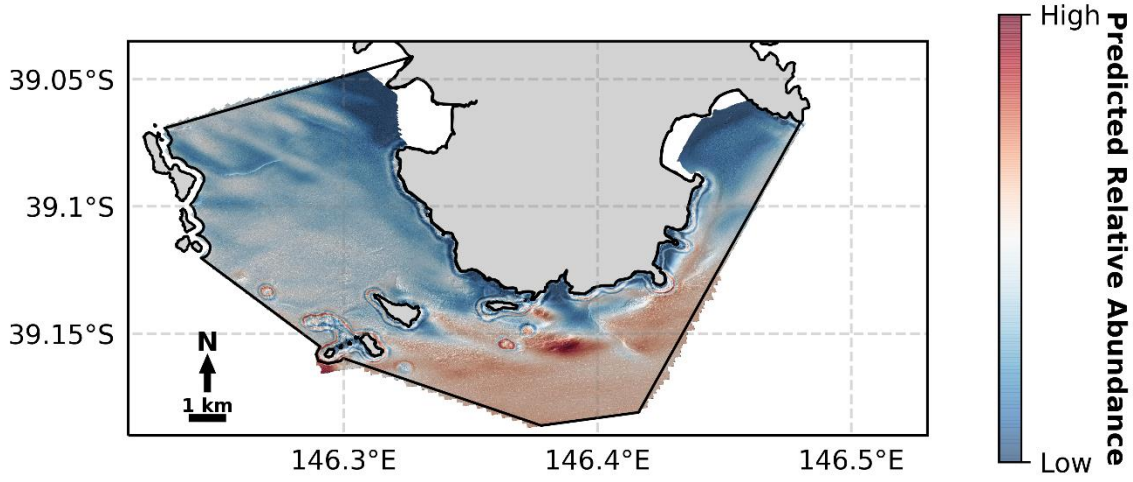

Figure 3.15: Predicted relative abundance of *Cephaloscyllium laticeps* from BRUVS sampling across the whole study site

The distribution of *N. tetricus* observed with the BRUVS deployments shows that it is mostly found in close proximity to shallow reefs (Figure 3.16). This pattern is expected due to its dependence on reef-associated invertebrates as a food source (Shepherd and Cannon, 1988). The predictive map also shows that its relative abundance is greatest in areas of reef near the coast and surrounding the offshore islands (Figure 3.17).

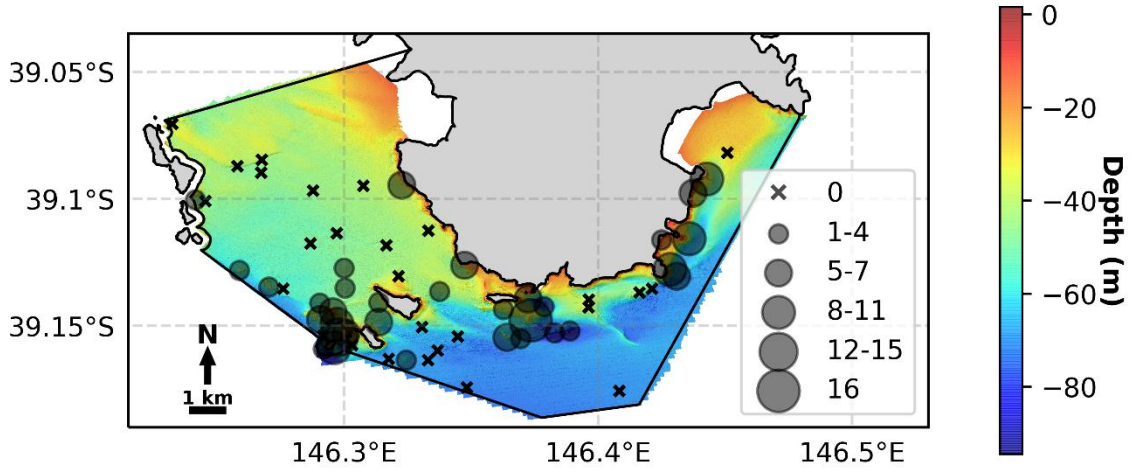

Figure 3.16: Relative abundance of *Notolabrus tetricus* for all BRUVS deployments. The size of each site marker corresponds to the relative abundance of *N. tetricus* observed at that site. These sites are overlaid on hillshaded bathymetry of the study area, coloured by depth. The black box denotes the boundary of Wilsons Promontory MNP

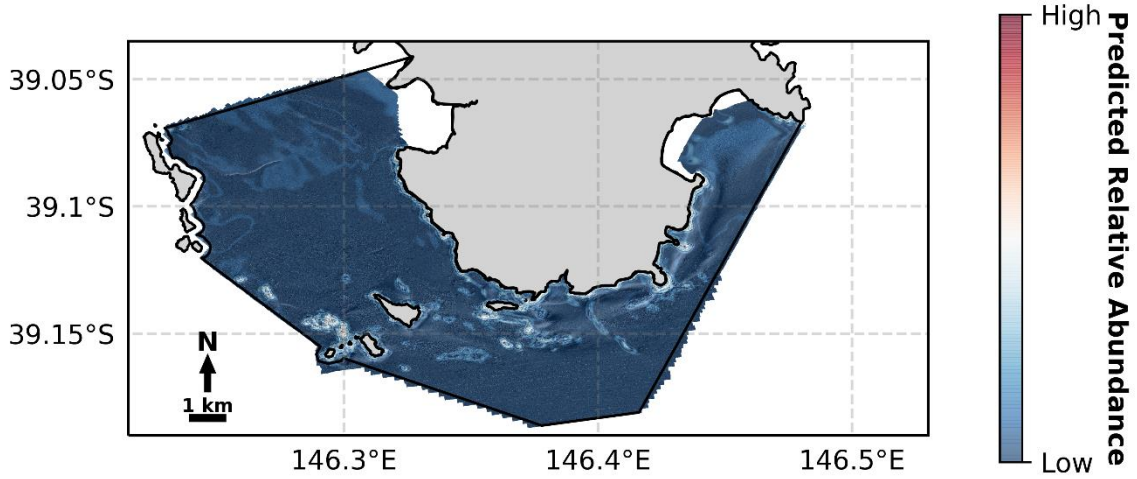

Figure 3.17: Predicted relative abundance of *Notolabrus tetricus* from BRUVS sampling across the whole study site

Pseudolabrus rubicundus also feeds on benthic invertebrates (Russell, 1988), resulting in its distribution with close proximity to reef areas, similar to *N. tetricus* (Figure 3.18). The predictive distribution map also picks up this pattern with the areas of highest predicted abundance being over areas of more complex reef (Figure 3.19).

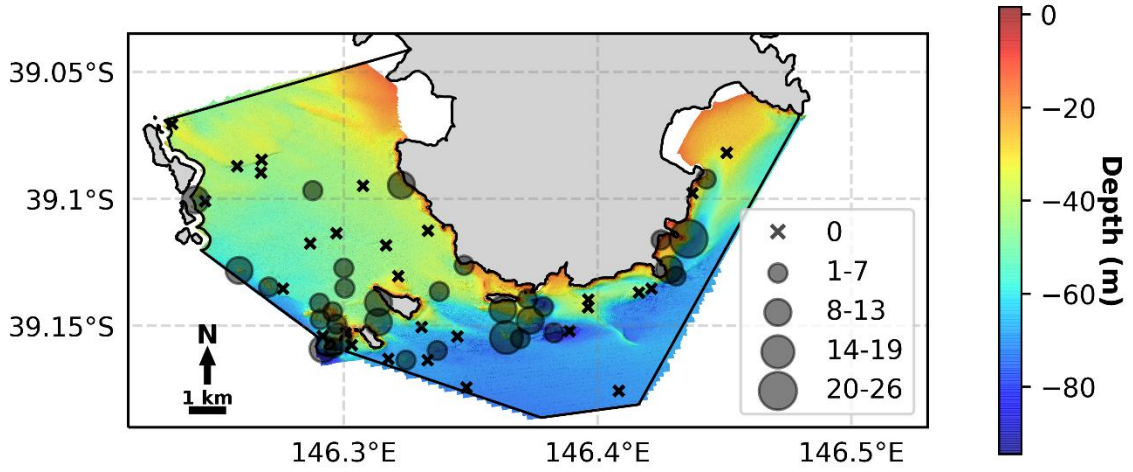

Figure 3.18: Relative abundance of *Pseudolabrus rubicundus* for all BRUVS deployments. The size of each site marker corresponds to the relative abundance of *P. rubicundus* observed at that site. These sites are overlaid on hillshaded bathymetry of the study area, coloured by depth. The black box denotes the boundary of Wilsons Promontory MNP

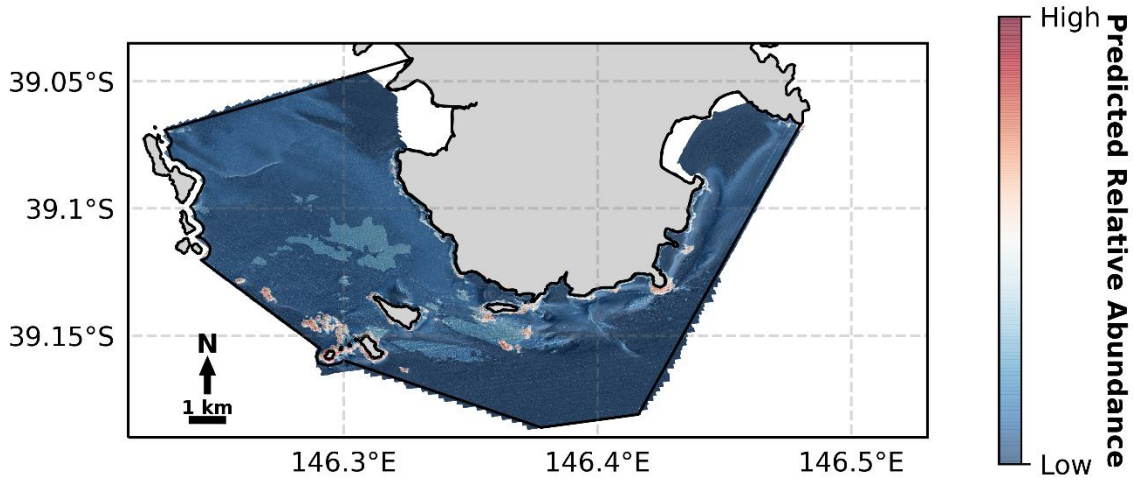

Figure 3.19: Predicted relative abundance of *Pseudolabrus rubicundus* from BRUVS sampling across the whole study site

The pattern of relative abundance for *T. degeni* from the BRUVS deployments shows that this species is found across a variety of bottom types (Figure 3.20), which is similar to findings in other studies (e.g. Arachchige Weerarathne et al., 2021). The predictive map picks up the variability in habitats by predicting higher relative abundances both across reef areas and in areas of mixed substrates (Figure 3.21).

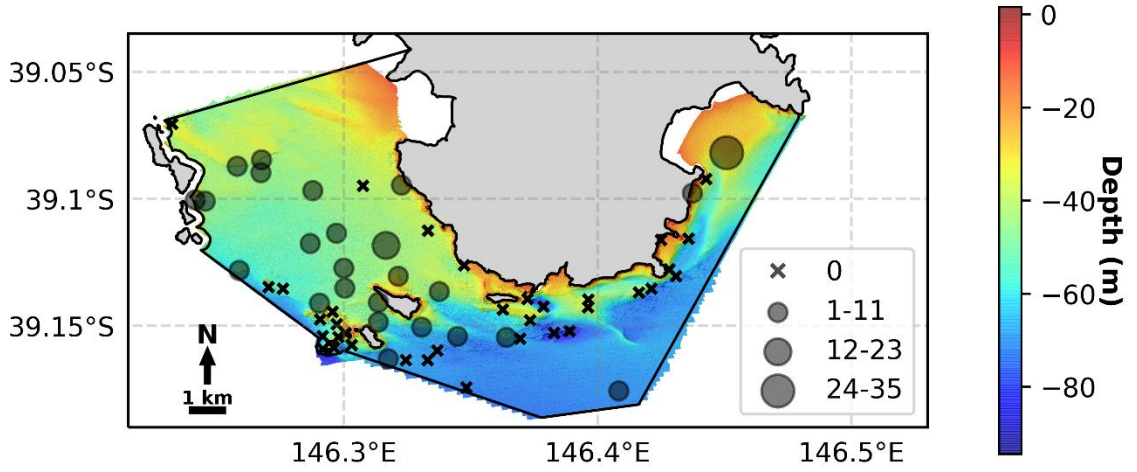

Figure 3.20: Relative abundance of *Thamnaconus degeni* for all BRUVS deployments. The size of each site marker corresponds to the relative abundance of *T. degeni* observed at that site. These sites are overlaid on hillshaded bathymetry of the study area, coloured by depth. The black box denotes the boundary of the Wilsons Promontory MNP

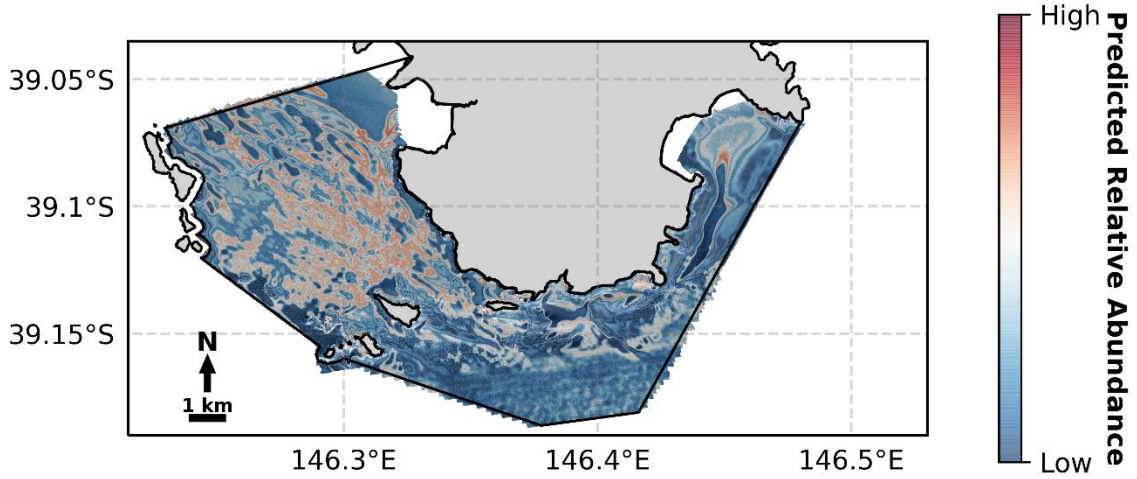

Figure 3.21: Predicted relative abundance of *Thamnaconus degeni* from BRUVS sampling across the whole study site

The patterns of total relative abundance across the site show that higher abundances are found in areas in close proximity to reef habitat (Figure 3.22). These patterns are consistent with other studies showing that temperate reef complexity often increases fish abundance (Trebilco et al., 2015; Tuya et al., 2009; Young and Carr, 2015). However, biomass is more even across the site (Figure 3.23). This pattern may be due to the observed lower abundances but higher biomass of mobile carnivorous species, which may travel longer distances over sediment due to attraction to the bait of BRUVS.

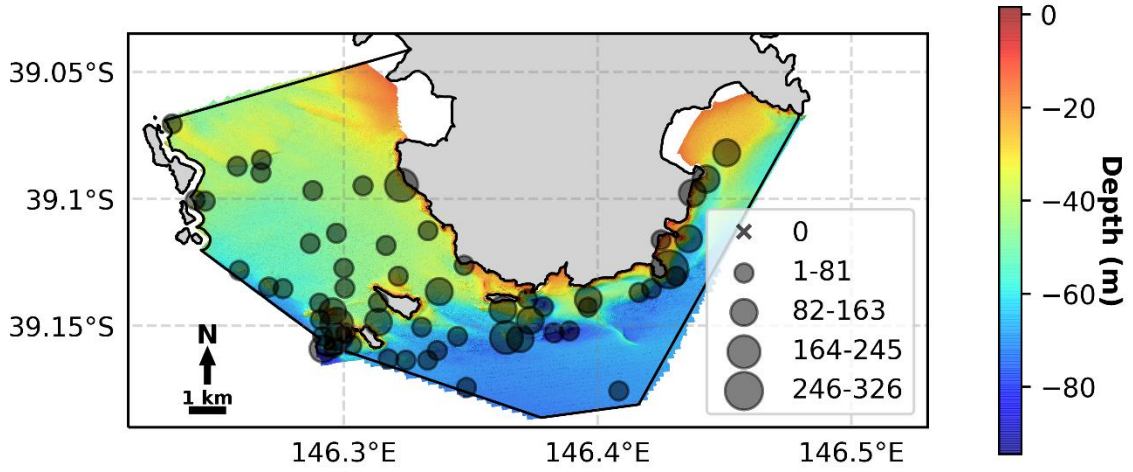

Figure 3.22: Total relative abundance of fish for all BRUVS deployments. The size of each site marker corresponds to the total relative abundance of fish observed at that site. These sites are overlaid on hillshaded bathymetry of the study area, coloured by depth. The black box denotes the boundary of Wilsons Promontory MNP

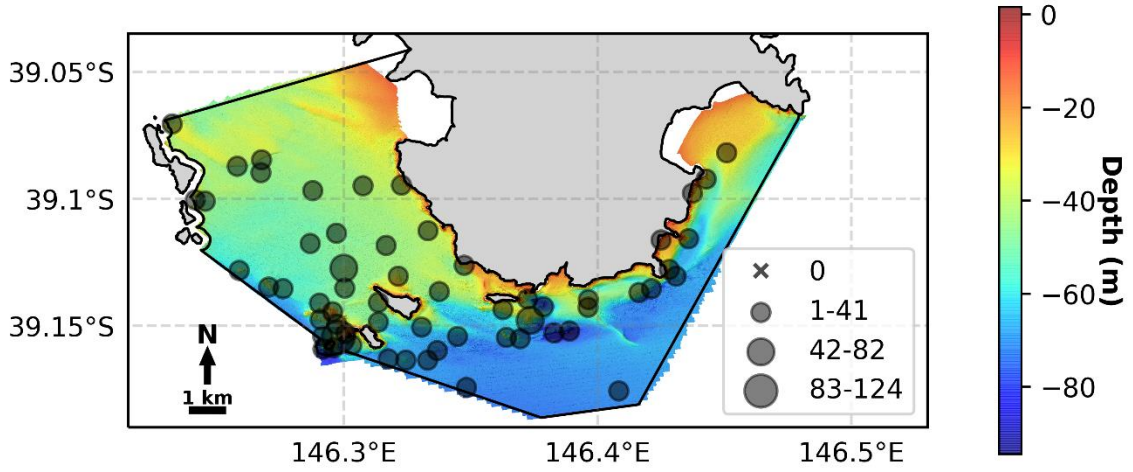

Figure 3.23: Total biomass of fish for all BRUVS deployments. The size of each site marker corresponds to the total biomass (kg) of fish observed at that site. These sites are overlaid on hillshaded bathymetry of the study area, coloured by depth. The black box denotes the boundary of Wilsons Promontory MNP

Dinolestes lewini is a pelagic schooling species found over a variety of habitats in both sheltered and open water (Miskiewicz et al., 1999). The BRUVS deployments show that it is found in highest relative abundance in shallow coastal areas near higher relief reefs (Figure 3.24). As it feeds mostly on other fishes and squid, it is likely to be found in those areas of higher species richness.

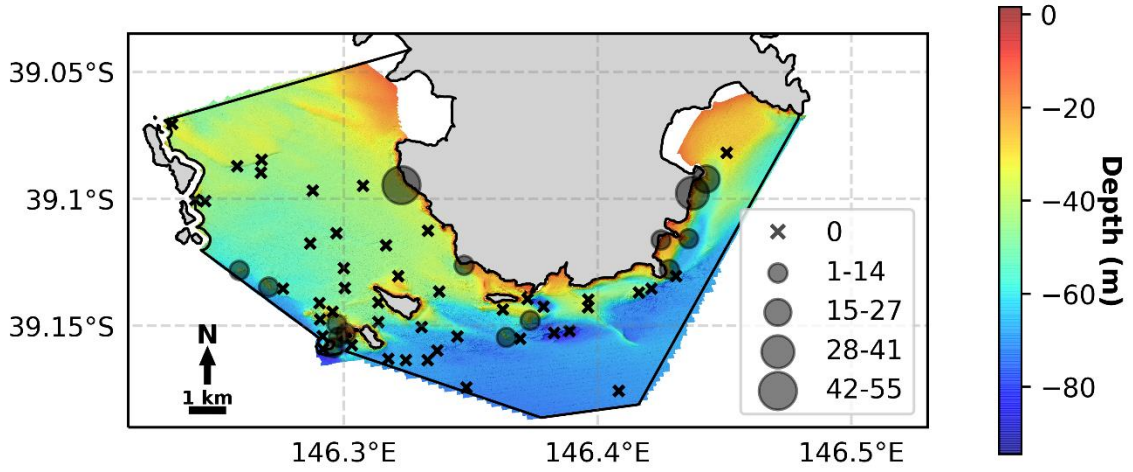

Figure 3.24: Relative abundance of Dinolestes lewini for all BRUVS deployments. The size of each site marker corresponds to the relative abundance of *Dinolestes lewini* observed at that site. These sites are overlaid on hillshaded bathymetry of the study area, coloured by depth. The black box denotes the boundary of Wilsons Promontory MNP

The distribution of *P. melbournensis* derived from the BRUVS deployments indicates it is most abundant in areas of lower relief sedimentary habitats (Figure 3.25). These patterns are consistent with other studies that show that *P. melbournensis* mostly inhabits, and feeds on prey protruding from, the sediment (Platell et al., 1997).

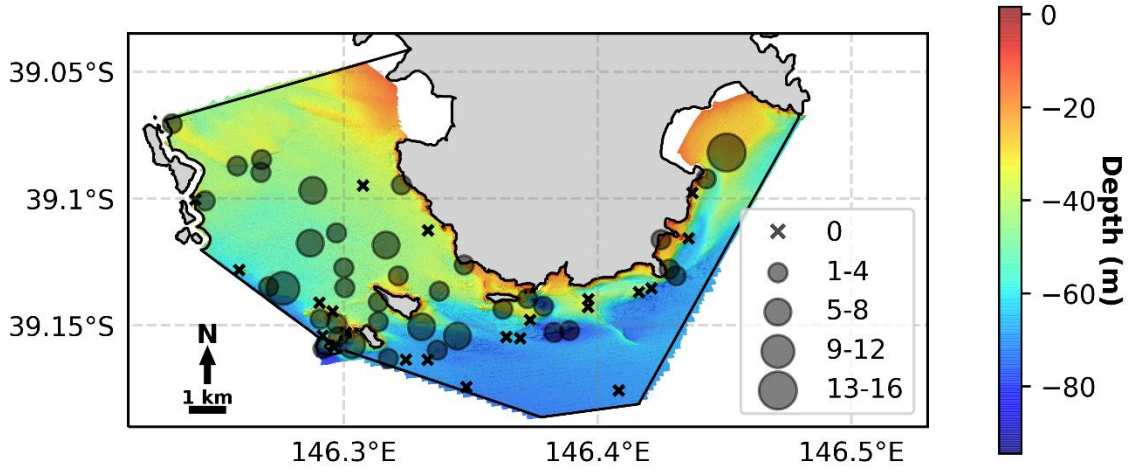

Figure 3.25: Relative abundance of *Parequula melbournensis* for all BRUVS deployments. The size of each site marker corresponds to the relative abundance of *P. melbournensis* observed at that site. These sites are overlaid on hillshaded bathymetry of the study area, coloured by depth. The black box denotes the boundary of Wilsons Promontory MNP

The commercial fishery for *M. antarcticus* makes it a heavily targeted species in Victorian waters; therefore, understanding its distribution and habitat associations is important. The BRUVS sampling within Wilsons Promontory MNP shows that *M. antarcticus* occurs across a wide depth range with the higher abundances within close proximity to reef habitat (Figure 3.26). This aligns with previous research that found them inhabiting edge areas (Barnett and Semmens, 2012). They also tend to avoid shallow habitats (Barnett and Semmens, 2012), which explains the greater abundances in deeper areas of the park.

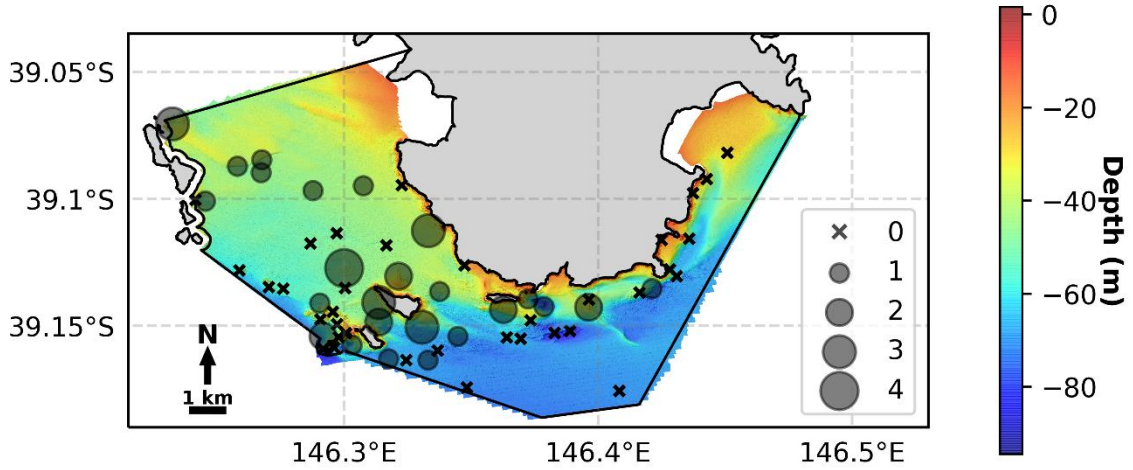

Figure 3.26: Relative abundance of *Mustelus antarcticus* for all BRUVS deployments. The size of each site marker corresponds to the relative abundance of *M. antarcticus* observed at that site. These sites are overlaid on hillshaded bathymetry of the study area, coloured by depth. The black box denotes the boundary of Wilsons Promontory MNP

3.5 Autonomous underwater vehicle

This study completed 7 surveys across Wilsons Promontory MNP to establish a baseline for monitoring sites across the park and to compare results of AUV transects with diver transects. Over 3 days, 7 surveys were completed, totalling 4.2 linear kilometres (km) of transects between depths of 9 and 75 m and obtaining 16,521 stereo pairs of downward-facing still images. The surveys provided coverage of major habitat groups within the MPA. From this data, 374 georeferenced still images were classified. To reduce effects of spatial autocorrelation, images were subset using criteria of minimum 20 seconds and 5 m separation between images.

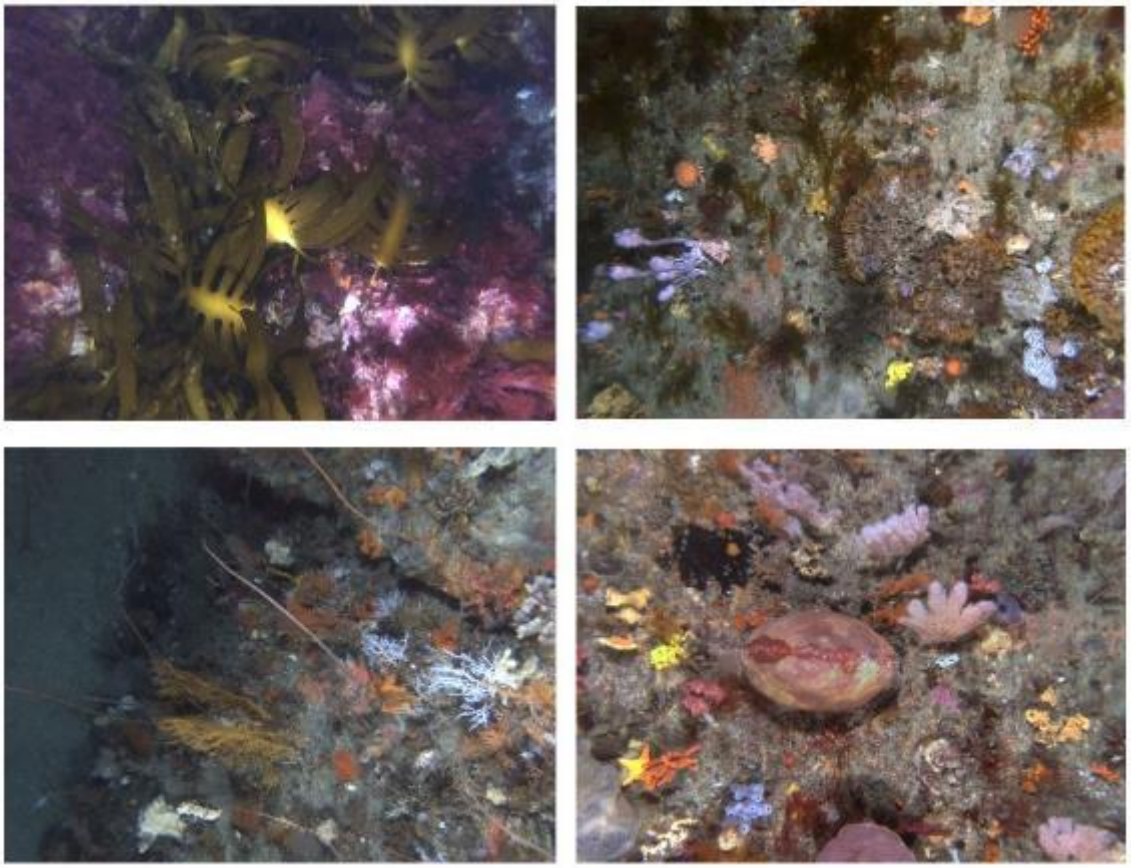

Figure 3.27: Example photo quadrats taken from the AUV *Sirius* surveys. Photo quadrats are subsequently classified using 25 random points which allows for detailed habitat classifications to be made (CATAMI classification scheme, Althaus et al., 2013)

Table 3.7: Summary of distance covered, number of transects completed and number of downward-facing stills successfully collected using the AUV *Sirius* at Wilsons Promontory MNP

	2016
Distance covered (km)	4.169
No. of transects completed	7
No. of downward-facing stills acquired	16,521
No. of classified downward-facing stills	374

Table 3.8: Summary of depth, distance and number of downward-facing stills successfully collected at each site using the AUV *Sirius* at Wilsons Promontory MNP

Site	Maximum depth (m)	Minimum depth (m)	Distance travelled (m)	Total no. of images	No. of images classified
Oberon Sth	38.63	21.43	644.57	2,266	76
Carpentaria East	45.96	19.64	664.27	2,550	73
Skull West	74.86	31.17	565.96	2,542	51
Wattle Offshore	47.73	38.73	939.77	3,652	23
Fenwick Point	16.59	9.26	143.92	517	19
Cape Wellington	40.18	16.38	663.64	2,544	76
Cape Wellington Point	62.83	11.38	547.31	2,450	56

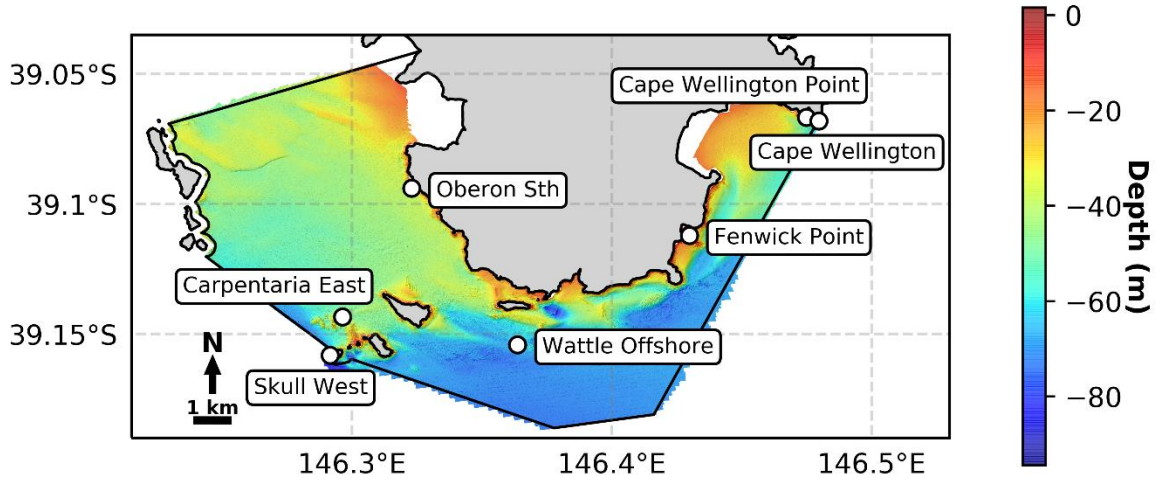

Figure 3.28: AUV sites completed across the Wilsons Promontory MNP

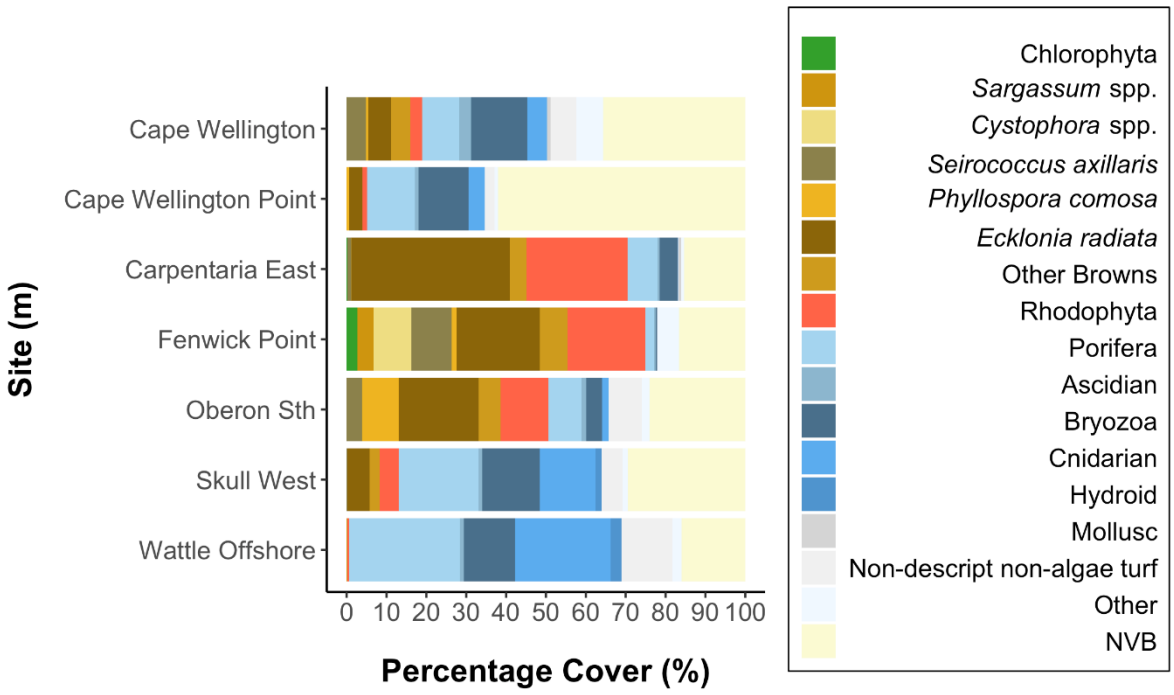

Figure 3.29: Percentage cover of broad habitat categories across all sites observed by classifying downward-facing still images collected using AUV. NVB is 'no visible biota'

3.6 Towed video and downward-facing imagery

This project achieved extensive towed video coverage across both the Wilsons Promontory and Bunurong marine national parks over 90 transects (Table 3.9). From these transects, a total distance of 47 linear kilometres was covered and 4,890 downward-facing still images acquired. From these data, 40 georeferenced still images (or the maximum number of images available) were extracted and classified for each 5 m depth stratum. This process was completed for both surveys, resulting in the classification of 923 georeferenced stills.

Table 3.9: Summary of distances covered, number of transects completed and number of downward-facing stills successfully collected using towed video in this study

	Wilsons Promontory	Bunurong	Total
Distance towed (km)	16.77	30.27	47.04
No. of transects completed	10	80	90
No. of downward-facing stills acquired	1,928	2,962	4,890
No. of classified downward-facing stills	492	431	923

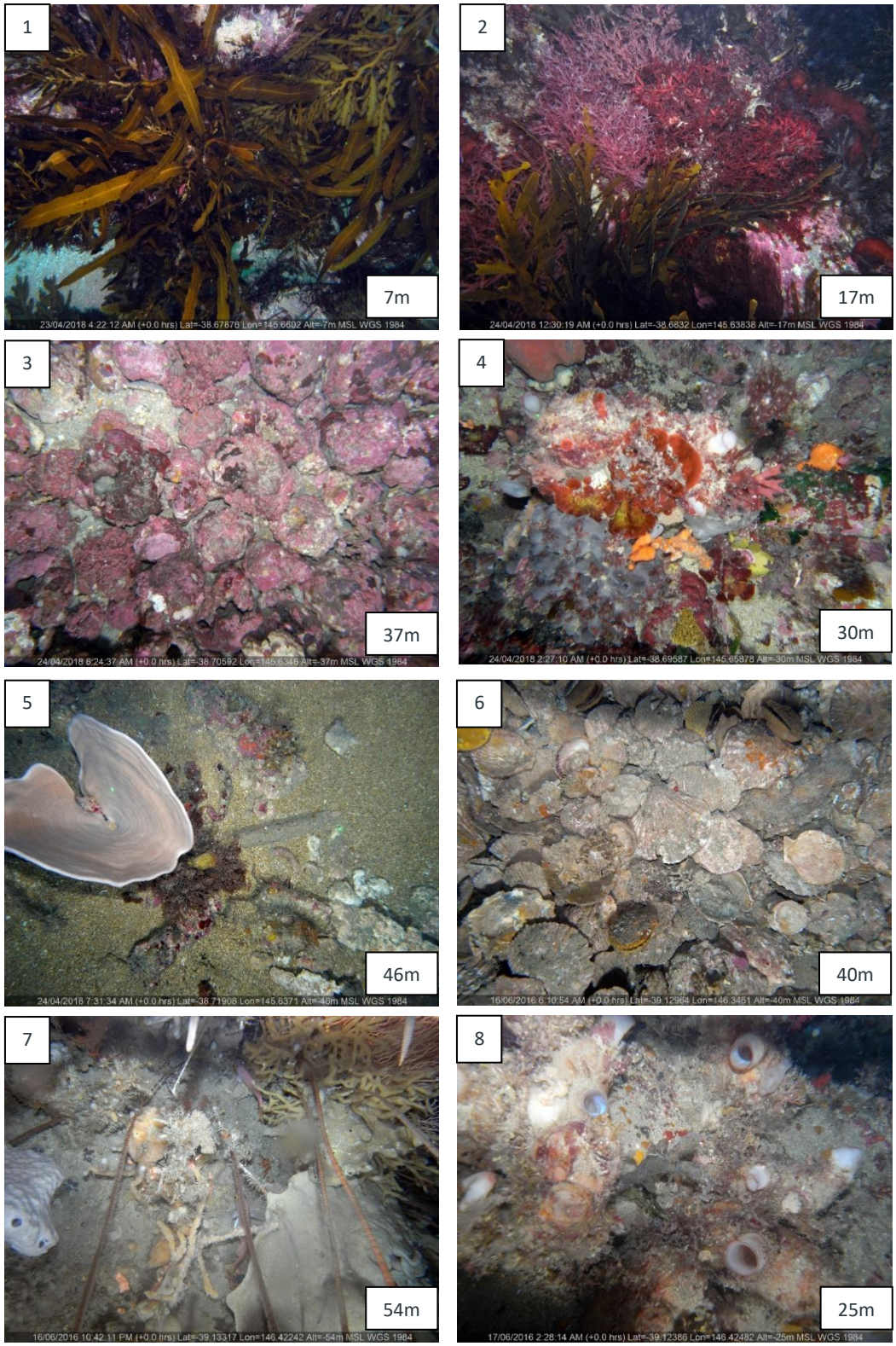

Figure 3.30: Examples of downward-facing georeferenced stills collected using towed video, showing various benthic habitat types found in Wilsons Promontory and Bunurong marine national parks. Photo quadrats are subsequently annotated using 25 random points, which results in detailed habitat classifications. Images 1–5 are from Bunurong MNP, images 6–8 are from Wilsons Promontory MNP. Images are labelled with depth in metres

3.6.1 Depth-related patterns of habitat composition

Classification of georeferenced downward-facing stills revealed varying patterns in dominant cover types between Wilsons Promontory and Bunurong MNPs (Figures 3.31, and 3.32). The subset of images classified across Wilsons Promontory MNP indicated a dominance of unvegetated areas at depths deeper than 15 m. Brown macroalgae dominates biota between 10 and 20 m depth. The 20 to 25 m depth contour shows the lowest coverage of biota for the entire park; however, slightly deeper at 25 to 30 m depth, coverage of biota returns to approximately 50%. In this zone, there is a transition of dominance from brown macroalgae to red macroalgae and sessile invertebrates. There, red algae makes up a substantial proportion of biotic cover to depths of 50 m, beyond which biota is predominantly sessile invertebrates.

In contrast, coverage in Bunurong MNP is predominantly made up of brown algae from the surface to 20 m depth. Seagrass (*Amphibolis antarctica*) is present in notable quantities at depths shallower than 10 m. Red algae makes up a substantial quantity of biotic coverage at all depths of Bunurong MNP; however, it becomes the dominant biota at depths greater than 20 m. Between depths of 25 and 45 m, much of the dominance of red algae is made up of rhodolith beds. Sessile invertebrates are not prominent at any depth within Bunurong MNP. This study also found that the 'no visible biota' category occurred over large areas throughout all depths within the park. The proportion of 'no visible biota' increased with depth: it covered 14% of the substrate between 0 and 5 m and 99% between 50 and 55 m.

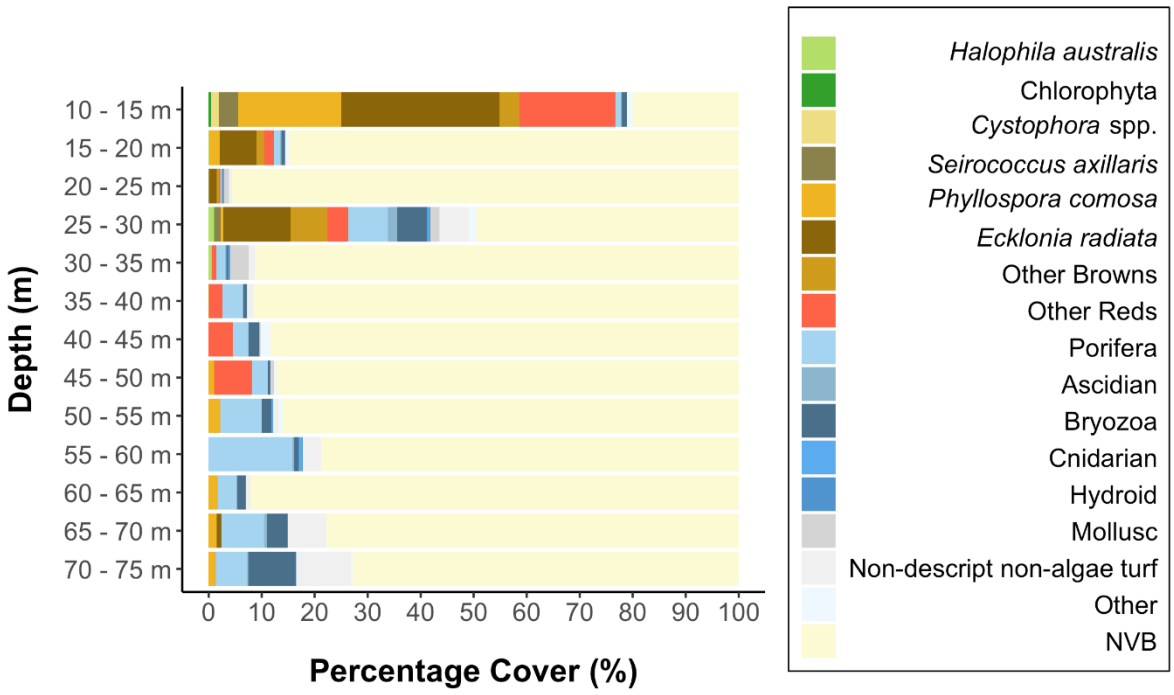

Figure 3.31: Depth zonation of broad reef habitat categories for the Wilsons Promontory MNP, observed by classifying downward-facing still images collected using towed video. NVB is 'no visible biota'

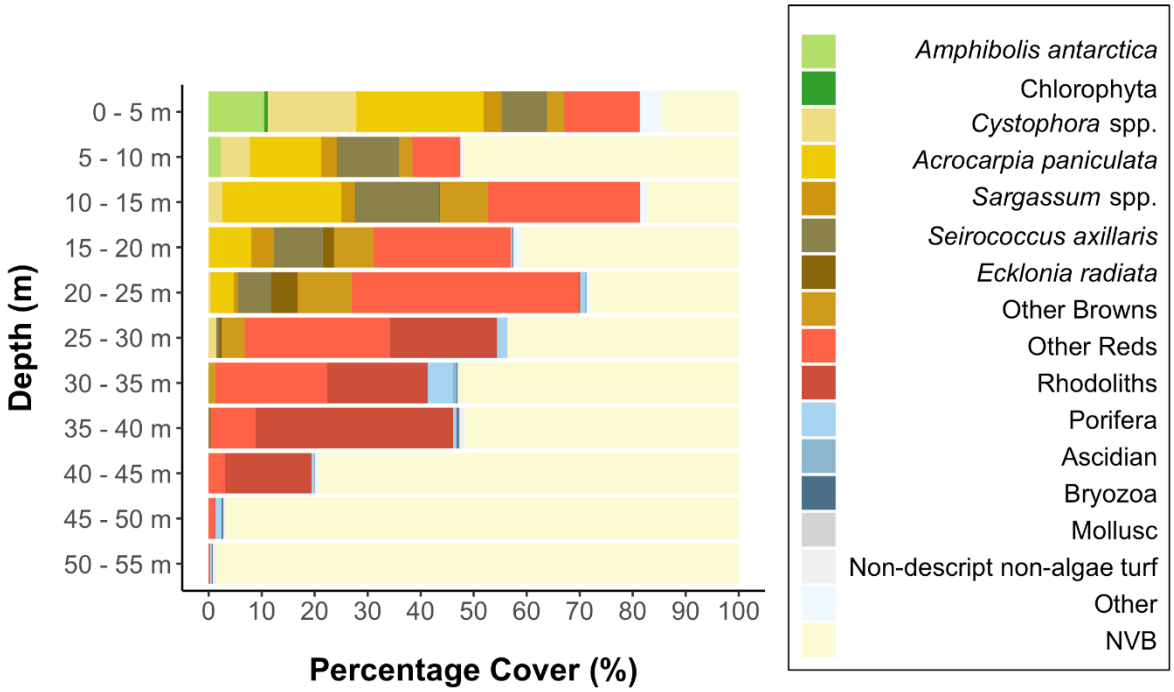

Figure 3.32: Depth zonation of broad reef habitat categories for the Bunurong MNP, observed by classifying downward-facing still images collected using towed video. NVB is 'no visible biota'

3.7 Habitat mapping

3.7.1 Wilsons Promontory habitat map and variable importance

As detailed in Section 2.6, the habitat mapping at Wilsons Promontory MNP was developed using classes derived from the new Combined Biotope Classification Scheme (CBiCS). Descriptions of the hierarchies are outlined in Section 2.6.2.

The habitat classification map for habitat complex (BC3) shows that Sublittoral mixed sediments and Sublittoral sand and muddy sand account for 90% coverage of Wilsons Promontory MNP, while High energy open-coast circalittoral rock and High energy infralittoral rock are found fringing along the headlands and islands (Figure 3.33).

The results of the biotope complex (BC4) (Figure 3.33) show the smallest class by area was Circalittoral coarse sediment, which was found in the south-western section of the study site at a mean depth of 45 m ± 9 m. The penultimate smallest class by area is Moderate to high complexity circalittoral rock with covering of small colonies and well-spaced erect sponges, which is found primarily near shore with a mean depth of 45 m ± 7 m.

The largest class by area was Sublittoral fine sand, which is distributed primarily in the east and south of the site with patches in the west. Sublittoral fine sand has a mean depth of 44 m ± 7 m. The second-largest class by area is Circalittoral mixed sediments, which is found at a mean depth of 49 m ± 8 m, deeper than Circalittoral fine sand. Circalittoral mixed sediments is found throughout the western section of Wilsons Promontory MNP with patches near the headlands in the south. The biotope complex High energy circalittoral rock with bushy branching and low erect sponges is found at a mean depth of 58 m ± 14 m with the majority located just south of the headlands. High energy *Ecklonia–Phyllospora* communities is present along the coastline and fringing off the south-western islands at a mean depth of 27 m ± 8 m. The final class, Sandy low profile reef wave surge communities, is scattered within Circalittoral mixed sediments and has a mean depth of 48 m ± 9 m.

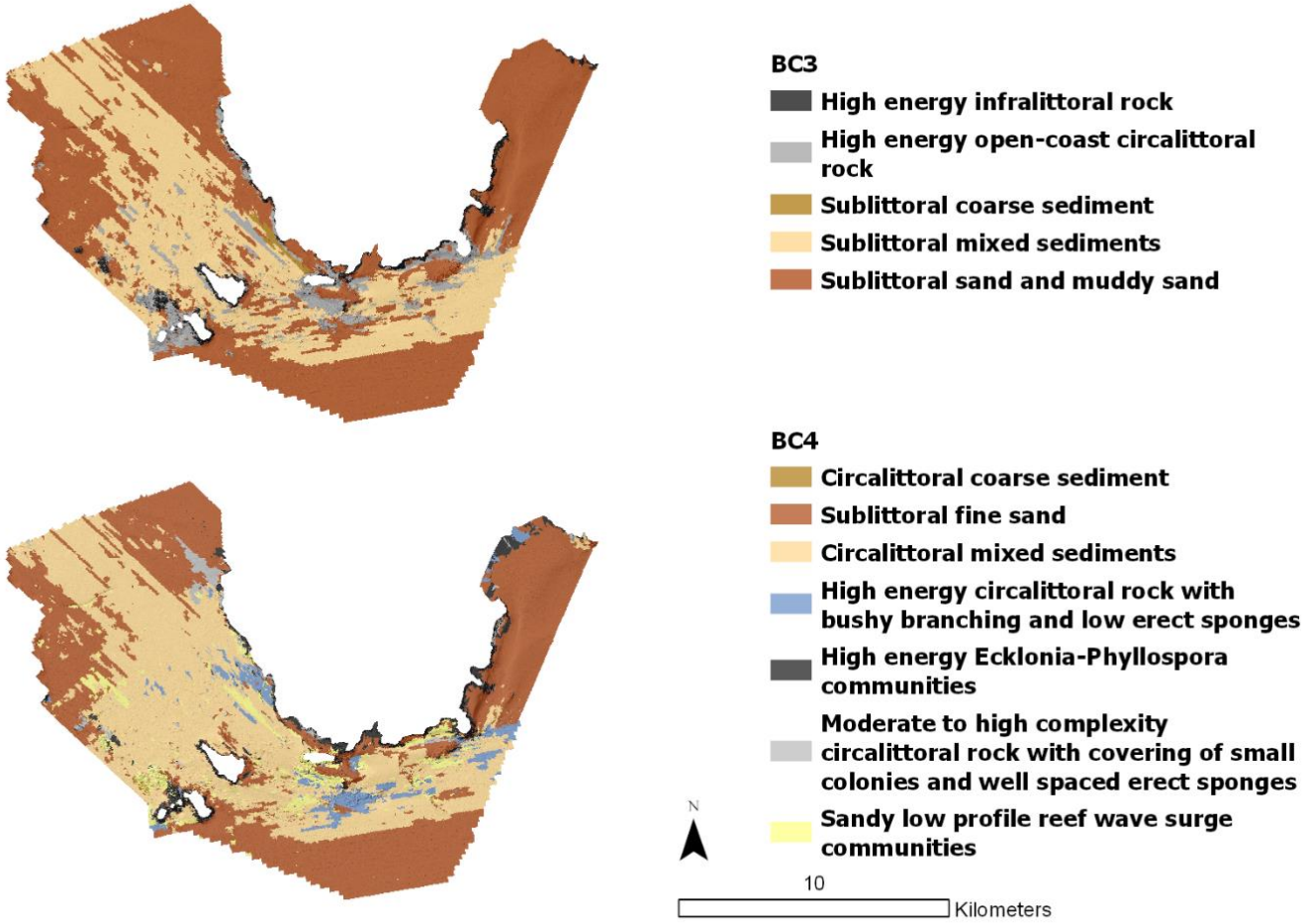

Figure 3.33: Predictive habitat maps across Combined Biotope Classification Scheme (CBiCS) hierarchies in Wilsons Promontory MNP. BC3 – Habitat complex, BC4 – Biotope complex. Created using ModelMap in R

Table 3.10: Combined Biotope Classification Scheme (CBiCS) hierarchies (BC2, BC3, BC4) used to train and validate the habitat maps for Wilsons Promontory MNP, with number of observations (*N*) for each level at BC4 – Biotope Complex

BC2 – Broad habitat	BC3 – Habitat complex	BC4 – Biotope complex	*N*
Infralittoral rock and other hard substrata (IR)	High energy infralittoral rock (James et al., 2013)	High energy *Ecklonia–Phyllospora comosa* communities (EP)	32
Circalittoral rock and other hard substrata (CR)	High energy open-coast circalittoral rock (HCR)	High energy circalittoral rock with bushy branching and low erect sponges (HCB)	71
		Moderate to high complexity circalittoral rock with covering of small colonies and well-spaced erect sponges (MCS)	32
		BC4: Sandy low profile reef wave surge communities (SLP)	
		BC5: Provisional southern Wilsons Promontory erect sponges, covering sponges, sea plume complex	79
Sublittoral sediment (SS)	Sublittoral coarse sediment (SCS)	Circalittoral coarse sediment (CCs)	51
	Sublittoral mixed sediments	Circalittoral mixed sediments (CMs)	293
	Sublittoral sand and muddy sand (Coombes et al., 2013)	Circalittoral fine sand (CLFiSa)	151
		Classes not used to produce the maps	
		Ecklonia radiata assemblages on moderate energy rock	2
		Erect octocorals on sediment	1
		High energy circalittoral reef with Bushy and hard bryozoans, sparse sponges and bramble gorgonian *Acabaria*	3
		High energy circalittoral rock with seabed covering sponges	1
		High energy lower infralittoral zone	21
		High energy *Phyllospora*	2
		Infralittoral fine sand	12
		Low to high complexity circalittoral rock with prominent sea plumes, sea whips, hydroid fans, hard bryozoans and encrusting sediment organic matrix	16
		Moderate to high complexity circalittoral rock with dense covering of *Herdmania* ascidians and few other erect forms	20
		Sessile invertebrate clumps on circalittoral biogenic gravel	1

Table 3.11: Combined Biotope Classification Scheme (CBiCS) hierarchies (BC2, BC3, BC4) used to train and validate the habitat maps for the Bunurong MNP, with number of observations (*N*) for each level at BC4 – Biotope complex

BC2 – Broad Habitat	BC3 – Habitat Complex	BC4 – Biotope Complex	*N*
Sublittoral sediment (SS)	Sublittoral sand and muddy sand	Circalittoral fine sand	46
		Infralittoral fine sand	72
	Sublittoral mixed sediments	Circalittoral mixed sediments	45
	Sublittoral rhodolith beds	Rhodolith beds in subtidal clean gravel or sand on open coasts	249
Infralittoral rock and other hard substrata (IR)	High energy infralittoral rock	High energy lower infralittoral zone	146
		High energy sandy veneer and scour turf communities	49
		High energy sub-canopy brown seaweed communities	248
Circalittoral rock and other hard substrata (CR)	High energy open-coast circalittoral rock	Sandy low profile reef wave surge communities	48
		Class not used to produce the maps	
		Amphibolis stands on high energy rock	2

When we compared modelled prediction data with validation ground truth data, habitat complex (BC3) class specific accuracies were above 60% with the exception of High energy infralittoral rock and sublittoral coarse sediments. Sublittoral sand and muddy sand had the highest user accuracy (the proportion of pixels or units where the predicted classification matched the corresponding ground truthed data) at 97.1%, and Sublittoral mixed sediments had the highest producer accuracy (the proportion of a particular category for which the ground truthed classification corresponded with the predicted data) at 87.4%. Overall accuracy for BC3 was 70.12% with a standard deviation of 0.1. Kappa (a measure of how closely the classified data match the ground truth) was 0.57. Class accuracy was reduced at the level of biotope complexes (BC4). All user accuracies for BC4 were above 50%. Three classes fell below 50% for the producer accuracies: Circalittoral coarse sediment (22.4%), Moderate to high complexity circalittoral rock with covering of small colonies and well-spaced erect sponges (4.5%), and Sandy low profile reef wave surge communities (47%). Sublittoral fine sand had the highest user accuracy at 91.2% and High energy *Ecklonia*–*Phyllospora* communities had the highest producer accuracy at 92.6%. Overall accuracy for BC4 was 70.33% with a standard deviation of 0.1.

Table 3.12**: User and producer accuracies for Habitat complex – BC3**

Class	User accuracy (%)	User standard deviation (%)	Producer accuracy (%)	Producer standard deviation (%)
High energy infralittoral rock	78.2	5.5	32.7	3.9
High energy open-coast circalittoral rock	64.7	0.2	61.1	0.7
Sublittoral coarse sediment	64.2	7.2	23.1	3.6
Sublittoral mixed sediments	65.7	0.1	87.4	0.3
Sublittoral sand and muddy sand	97.1	0.1	77.1	0.3

Table 3.13: User and producer accuracies for Biotope complex – BC4

Class	User accuracy (%)	User standard deviation (%)	Producer accuracy (%)	Producer standard deviation (%)
Circalittoral coarse sediment	64.9	7.1	22.4	3.7
Sublittoral fine sand	94.9	0.1	75.2	0.3
Circalittoral mixed sediments	65.1	0.1	88.0	0.3
High energy circalittoral rock with bushy branching and low erect sponges	91.2	0.7	56.7	0.9
High energy *Ecklonia–Phyllospora* communities	57.5	0.7	92.6	1.3
Moderate to high complexity circalittoral rock with covering of small colonies and well-spaced erect sponges	90.6	8.1	4.5	0.3
Sandy low profile reef wave surge communities	54.0	0.7	47.0	0.9

Variable importance metrics, as shown in Figure 3.34, and described in Section 2.6.4, were recorded for each CBiCS hierarchy level. The most important variables across the models were bathymetry mean for the habitat complex (BC3) and phi mean for the biotope complex (BC4) (Figure 3.34). The angular response analysis (ARA) derivatives (volume standard deviation, impedance mean and volume mean) had higher mean decrease in accuracy than other variables such as backscatter mean, backscatter standard deviation, backscatter VRM, slope and curvature. The AR derivative skewness and AR slope had low variable importance.

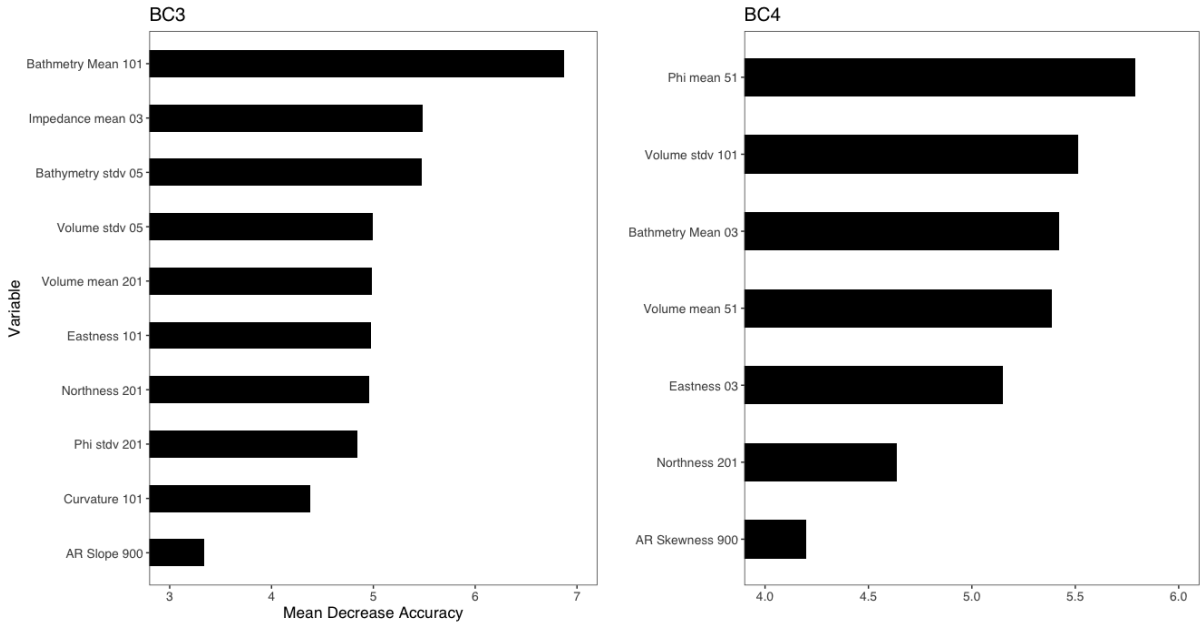

Figure 3.34: Wilsons Promontory MNP variable importance for retained model variables. Habitat complex – BC3, Biotope complex – BC4. Mean decrease in accuracy represents the RF model decrease in accuracy when that variable is removed; therefore, a larger value for mean decrease in accuracy indicates that the environmental predictor is more important

3.7.2 Bunurong habitat map and variable importance

Results from the 'randomForest' (RF) model in R indicate that Bunurong MNP is characterised by High energy infralittoral rock, ranging from 2 to 30 m depth (Figure 3.35). At the habitat complex (BC3) level, there are patches of Sublittoral sand and muddy sand near the shoreline and throughout the Sublittoral rhodolith bed class. The south-west is dominated by Sublittoral mixed sediments. Extensive rhodolith beds are present throughout the centre and western portions of the site.

The smallest class by area predicted at the biotope complex (BC4) level was Sandy low profile reef wave surge communities, which is found in the southern portion of the site at a depth of 43 $\pm$ 6 m. Infralittoral fine sand is found in patches along the shoreline. High energy sub-canopy brown seaweed communities is found throughout the High energy lower infralittoral zone, at a mean depth of 16 $\pm$ 5 m. Circalittoral fine sand and Circalittoral bare mixed sediments are found deeper than 40 m in the south and south-west portion of the site. The most dominant habitat throughout Bunurong MNP is Rhodolith beds in subtidal clean gravel or sand on open coasts at 44% coverage, primarily distributed in the park's western and central regions at a mean depth of 37 $\pm$ 4 m (Figure 3.36).

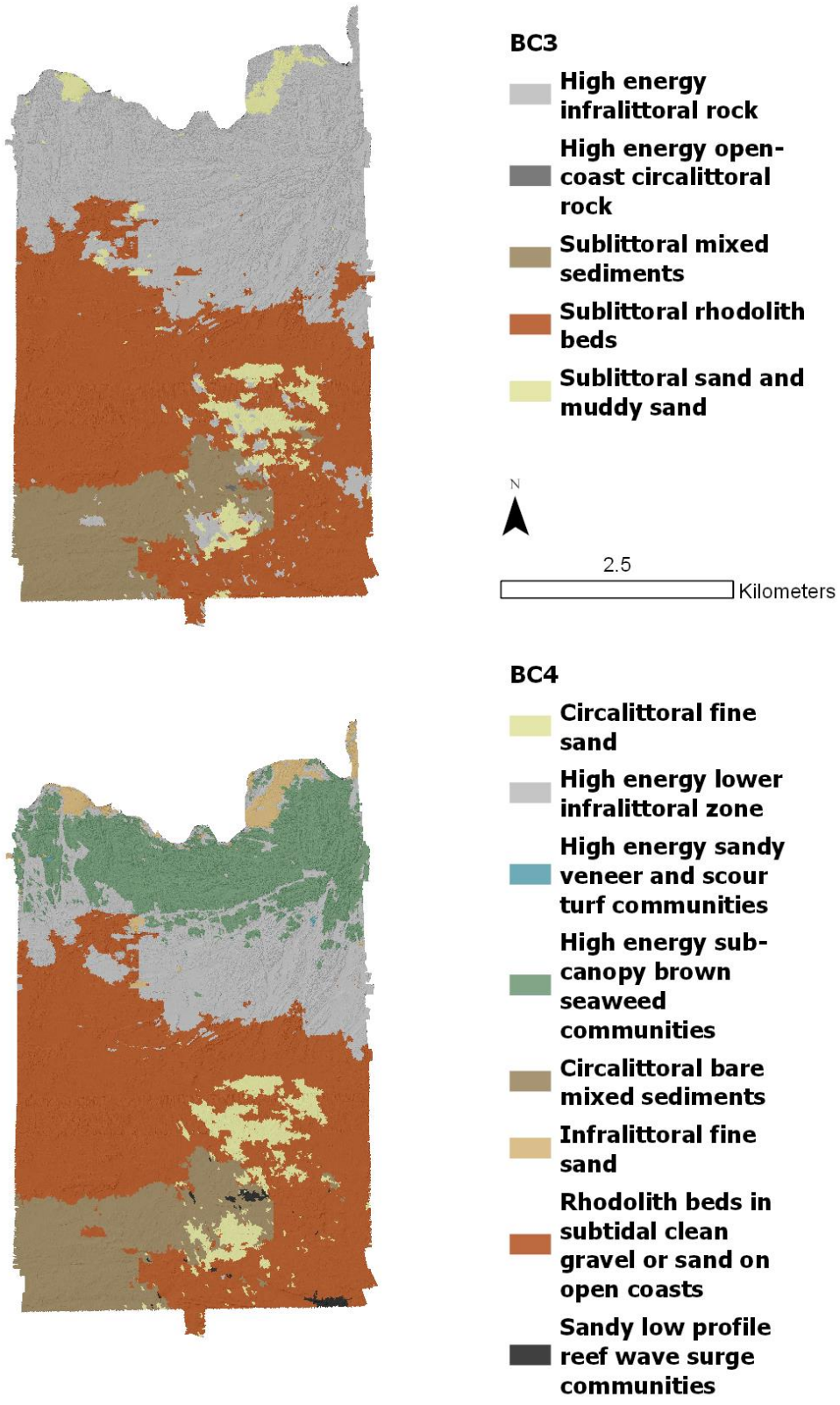

Figure 3.35: Predictive habitat maps of Bunurong MNP across both hierarchies BC3 – Habitat complex and BC4 – Biotope complex. Created using "ModelMap" in R

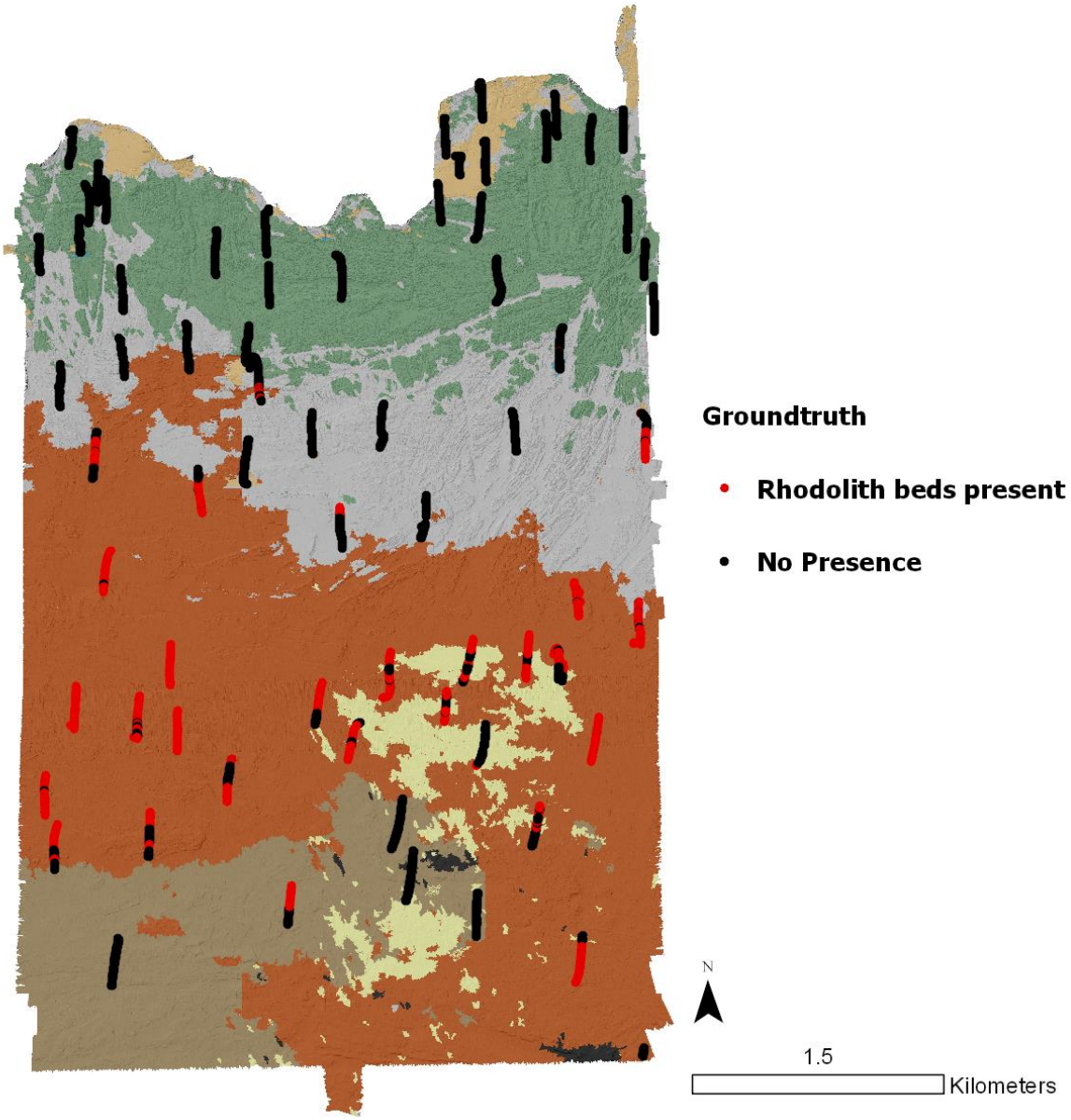

Figure 3.36: Rhodolith presence at Bunurong MNP, overlaid from towed video on classified map for Bunurong MNP at BC4 – Biotope complex

The 2 benthic habitat maps were assessed by comparing predicted classes to observed classes. CBiCS habitat complex (BC3) had the highest model accuracy at 84.3% and a kappa of 0.77. The model for biotope complex (BC4) had an overall accuracy of 76.2% and a kappa of 0.69. This means that habitat complex (BC3) fitted the data better than did biotope complex (BC4). User accuracy was above 80% for all classes except High energy open-coast circalittoral rock at 54% (Table 3.14). Producer accuracy was above 65% for all classes with the exception of Sublittoral rhodolith beds at 8.5%.

Table 3.14: User and producer accuracies for BC3 – Habitat complex

Classes	User accuracy (%)	User standard deviation (%)	Producer accuracy (%)	Producer standard deviation (%)
High energy infralittoral rock	94.7	0.1	92.0	0.1
Sublittoral mixed sediments	83.3	0.1	68.8	0.1
High energy open-coast circalittoral rock	54.0	0.1	83.0	0.1
Sublittoral sand and muddy sand	81.9	0.1	93.3	0.1
Sublittoral rhodolith beds	99.8	0.1	8.5	0.1

User accuracy for biotope complex (BC4) was generally high among classes; Infralittoral fine sand and Circalittoral mixed sediments had the lowest accuracies at 53.4% and 65.6%, respectively (Table 3.15). Producer accuracies were above 60% for 6 classes; High energy sandy veneer and scour turf communities and Rhodolith beds in subtidal clean gravel or sand on open coasts were both below 30%.

Table 3.15: User and producer accuracies for BC4 – Biotope complex

Classes	User accuracy (%)	User standard deviation (%)	Producer accuracy (%)	Producer standard deviation (%)
Circalittoral fine sand	92.2	0.1	68.9	0.1
High energy lower infralittoral zone	79.7	0.2	63.1	0.1
High energy sandy veneer and scour turf communities	69.8	1.1	28.9	1.0
High energy sub-canopy brown seaweed communities	81.0	0.0	92.5	0.0
Circalittoral mixed sediments	65.6	0.0	80.4	0.2
Infralittoral fine sand	53.4	0.0	75.0	1.0
Rhodolith beds in subtidal clean gravel or sand on open coasts	76.2	5.9	13.6	0.7
Sandy low profile reef wave surge communities	81.0	0.1	67.4	0.2

Both BC3 and BC4 found ARA derivatives impedance (measuring the interaction between density and sound speed), volume (as a measure of water column backscatter) and phi (measuring sediment grain size) to be the most important variables (Figure 3.37). For habitat complex (BC3), backscatter standard deviation and backscatter VRM were not correlated with the ARA derivatives and were the least important variables. Northness and curvature were the least important variables for biotope complex (BC4). Complexity, slope and mean backscatter were not found in any models due to correlation with more important variables.

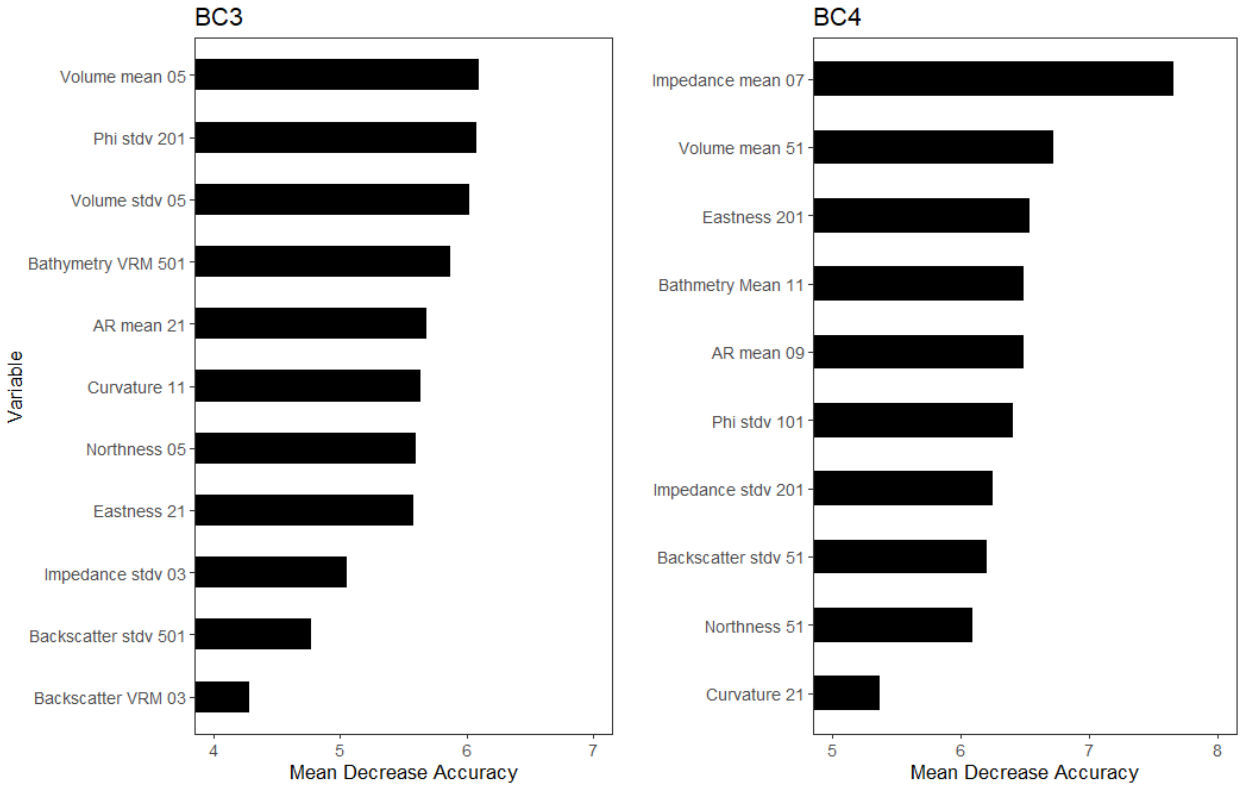

Figure 3.37: Bunurong MNP variable importance for retained model variables BC3 – Habitat complex, BC4 – Biotope complex. Mean decrease in accuracy represents the 'randomForest' model decrease in accuracy when that variable is removed; therefore, a larger value for mean decrease in accuracy indicates that the environmental predictor was more important

4. Discussion

4.1 Fisheries-independent Southern Rock Lobster survey

Fisheries-independent surveys of *Jasus edwardsii* (Southern Rock Lobster) populations within and adjacent to the Wilsons Promontory MNP do not show clear trends with respect to protection. The results showed no significant differences inside and outside the MPA. This lack of difference could be due to a number of factors including low recruitment to the whole area around Wilsons Promontory. The individuals captured in and around Wilsons Promontory were predominantly large and found in low numbers, potentially suggesting low recruitment. These low numbers are consistent with findings in other reports showing that densities have remained low since monitoring began in the early 2000s (Edmunds et al., 2011). More spatially explicit observation data across the MPA network are needed for us to better understand these spatial differences in productivity across the *J. edwardsii* populations in Victoria and the potential benefit of MPAs for increasing productivity. Access to these types of datasets would allow us to better understand how the environment and protection by MPAs affect *J. edwardsii* productivity.

Although there were no significant differences with regard to protection status, finding many large individuals in the survey suggests the area may export larval *J. edwardsii* that contribute to populations outside the study area. *J. edwardsii* has a complex early life cycle and can spend 12 to 24 months within oceanic waterbodies undergoing 11 larval stages before settling (Linnane et al., 2014; Thomas et al., 2000). Previous studies have suggested that Australian *J. edwardsii* populations are responsible for some trans-Tasman larval flow that contributes to and possibly maintains New Zealand populations (Chiswell et al., 2003; Morgan et al., 2013). Our study, however, inexplicably found a lack of sub-legal-size lobsters both inside and outside the MPA. This could suggest a reduced supply of recruits to this population, which could be monitored by repeating these surveys through time. Future monitoring could introduce juvenile-specific sampling methods such as puerulus collectors. The low number of pre-recruit lobster recorded could also arise from larger lobsters excluding the smaller lobsters from traps (Frusher and Hoenig, 2001; Miller, 1990). This type of information is important for understanding which marine protected areas are likely to be sources or sinks for populations of *J. edwardsii* and where management or compliance efforts should be targeted.

Jasus edwardsii are obligate crevice dwellers and are found on all rock types and geomorphological structures from the intertidal zone to 200 m deep, provided there is suitable shelter (Booth, 1997; Edmunds, 1995; MacDiarmid et al., 1991). They reside in ‘dens’ within crevices or under ledges formed by reefs and are important predators that forage on slow-moving benthic invertebrate prey such as bivalves, sea urchins and abalone (Edmunds, 1995; Jernakoff et al., 1987). However, our methods to associate *J. edwardsii* with characteristics of the seafloor habitat were unsuccessful in Wilsons Promontory MNP. The lobsters showed no strong relationships with the structure of the seafloor, likely due to the lack of structural variability between the targeted habitats detected by our multibeam

sonar system. The 2-dimensional derivatives of the bathymetry may not be adequately capturing important Southern Rock Lobster habitat within this park. Although crevices and shelter are often associated with more complex reef habitat, we recognise that our methods did not measure differences in shelter availability directly. This study assumed that substratum complexity indices were related to lobster shelter and foraging habitats, and we recognise that these analyses could be improved in the future by including more direct geomorphological descriptions, such as those of Harrington and Hovel (2016).

These results provide an appropriate baseline for future studies documenting changes in this marine national park to assess how the population responds to protection, recruitment and a changing climate over time. Continued future sampling of this and other MPAs will provide a more conclusive understanding of how *J. edwardsii* are responding to complete removal of fishing pressure within MPAs across the state.

4.2 Large mobile fish (including sharks and rays)

Fish assemblages within and adjacent to Wilsons Promontory MNP were observed using baited remote underwater video stations (BRUVS). These fish assemblages have previously only been monitored using Subtidal Reef Monitoring Program underwater visual census techniques. One identified limitation of diving methods is the shallower depth range that can be monitored (Langlois et al., 2018). The importance of mesophotic reefs (low-light reefs in the transition zone between well-lit shallower waters and dark deep water) is now well accepted in the literature (Loya et al., 2016). In comparison with tropical mesophotic systems, little is known about temperate mesophotic ecosystems (Williams et al., 2019) and more data are needed. Moore et al. (2010) found species richness of a temperate fish assemblage increased with depth. They found that greatest species richness was present at depths between 20 and 50 m, which are generally inaccessible for underwater visual census techniques. This depth range also coincides with a large portion of reef within the Wilsons Promontory MNP, and BRUVS can help explain these patterns across broad networks of MPAs.

This study established a baseline for building a time series to monitor fish assemblages over the entire depth range of Wilsons Promontory MNP using BRUVS. Including BRUVS in monitoring also let us make spatially explicit models for various diversity metrics and abundance of key species throughout the park; this was aided by the distribution of sample locations across observed environmental gradients. Reaching the same density of field locations using underwater visual census methods would not be feasible. Our approach, driven by classifications of the seabed structure provided by sonar technologies, allowed us to develop a spatially balanced design across the environmental variability of the site.

An advantage of distribution modelling approaches, such as those used in this study, is their ability to predict patterns in abundance and biodiversity beyond sampled locations if relationships with environmental drivers can be inferred (Araújo and Guisan, 2006; Sequeira et al., 2016). Distribution modelling can be relevant for a range of applications such as

tracking invasive species and researching effects of climate change (Elith and Graham, 2009). This study, for example, predicted hotspots of species richness and abundance across an area of over 150 km^2, which covered Wilsons Promontory MNP. Park authorities can now use this knowledge to target diversity assessments and identify sites of high biodiversity or public interest not previously visited.

Furthermore, stakeholders are often interested in community-level metrics of assemblage patterns, such as relationships between biodiversity patterns and the surrounding environment (Guisan and Thuiller, 2005). Sequeira et al. (2016) suggested that efficient management tools should focus on improving the predictive ability of biodiversity distribution models rather than studying and mapping each species individually. Our findings indicate that BRUVS provide sufficient information to reliably generate spatially explicit models of entire assemblages, functional groups and species, thereby maximising our understanding of the dynamics within the assemblage and letting us test the model's relevance to known ecology.

4.3 Classification of the benthic habitat

Autonomous underwater vehicle and towed video classification

This project used autonomous underwater vehicle (AUV) surveys in Wilson Promontory MNP and towed video surveys in both Wilsons Promontory MNP and Bunurong MNP. With its ability to provide high taxonomic resolution and extensive spatial coverage across the MPA, the downward-facing stills imagery collected using these methods was used to classify the benthic habitat and to understand community structure throughout the park. Bunurong MNP has a reasonably uniform and gentle depth gradient throughout the park with extensive contiguous reef areas across a wider depth range. In contrast, much of Wilsons Promontory MNP is dominated by sediment with patchier reefs clustered in shallower areas that are predominantly extensions of granitic outcrops. These differences between the 2 parks in their depth range and reef structure resulted in differences in the benthic species and assemblages observed. Although both parks are dominated by brown macroalgae in areas shallower than 20 m, most depth classes in Wilsons Promontory MNP deeper than 20 m are dominated by sediments with sparse sessile invertebrates. Bunurong MNP is dominated by red algae below 20 m and has over 50% coverage of biota until around 40 m depth. Bunurong MNP also has a large region dominated by rhodolith beds between 25 and 40 m depth.

The AUV *Sirius* had the advantage of being able to capture imagery with high frequency, allowing for the generation of photomosaic images. However, we used these data in a similar way to our use of towed video; for both, we classified a subset of downfacing-stills. Future work is needed to evaluate the benefits of generating photomosaics that also generate digital surface models like the UAV approach presented. These benefits are likely to be generated through time series collection where habitat fragmentation metrics beyond the individual stills frame will provide value.

Predictive habitat mapping

Random forest models performed relatively well in developing habitat maps for Wilsons Promontory MNP and Bunurong MNP; the models for Bunurong MNP performed slightly better. In Wilsons Promontory MNP, both levels of the CBiCS hierarchy (BC3 – Habitat complex and BC4 – Biotope complex) had around 70% accuracy while the Bunurong MNP habitat maps had accuracies of 76% for BC3 and 84% for BC4. These accuracies mean that the habitats classified from our models match well with the habitats identified in the reserved dataset, providing high confidence in the habitat maps we have developed for these sites. The slightly lower performance in the Wilsons Promontory MNP is likely due to the predominance of sedimentary substrate, which is harder to differentiate across the bathymetry-derived variables. However, incorporating those variables from the angular response analysis helped to classify variations in sediment types, which was important in the models for both MPAs. Previous studies have shown that combining bathymetric and backscatter derivatives results in more accurate habitat classifications than using bathymetric derivatives alone (Che Hasan et al., 2012; Rattray et al., 2009). Backscatter derivatives are used less often in predictive habitat mapping than bathymetric derivatives, but multiple studies demonstrate that backscatter derivatives improve the accuracy of biotic habitat classifications (Che Hasan et al., 2012; Che Hasan et al., 2014; Ierodiaconou et al., 2018; Rattray et al., 2009).

The habitat maps resulting from these analyses can help prioritise management within MPAs by providing more comprehensive information on the types of habitats available and their distributions. The predictive habitat maps developed for Wilsons Promontory MNP show that most of the site is dominated by sediment with small outcroppings of rocky reefs along the shores of the islands and mainland. Bunurong MNP contains a large expanse of reef in the infralittoral zone with a large area of rhodolith beds in the coarse sediments offshore from the reef in deeper regions of the park. Due to the variation in fish and assemblages associated with these different benthic classifications, there is the potential to combine these habitat maps with the BRUVS data to further refine the estimates of fish diversity and distributions described in Section 4.2.

Section B Unmanned aerial vehicle intertidal surveys

5. Introduction

Increasing pressures on coastal zones from climate change and coastal development, highlight the need to effectively monitor intertidal environments at scales capable of informing management decisions. Monitoring coastal habitats is multifaceted and uses a variety of data collection methods to characterise topographic structure and species distributions on subtidal reefs, including traditional visual observational studies on intertidal and subtidal rocky reefs and sandy beaches (Dayton, 1975); marine remote-sensing technologies, such as underwater video monitoring and bathymetry from ship-based sonar; and aerial-based LiDAR approaches (Ierodiaconou et al., 2011; Young and Carr, 2015; Zavalas et al., 2014). Fundamental to conserving marine biodiversity into the future is an understanding of natural spatial and temporal variability in intertidal reef biota and whether improved resilience to natural and anthropogenic disturbances may be achieved via management strategies, such as implementation of marine protected areas.

Intertidal reefs are dynamic and physiologically stressful ecosystems that can vary greatly in community structure over small spatial scales due to the mosaic of habitats created by biotic and abiotic influences (Airoldi, 2003). Logistical constraints of monitoring intertidal reef biota during periods of emersion at low tide and variable wave exposure mean that replicated sampling of these areas can be challenging and time consuming. Intertidal reef monitoring traditionally involves targeting small areas of the reef using quadrats, or along transects, often stratified by reef zonation, collecting data on species richness, abundance and community composition (Underwood, 2000). Although this provides an insight into community structure, it is labour intensive, captures only a small area of the reef under study, and generally does not collect information on the fine-scale variations in reef structure that may influence the distribution of assemblages observed. Gathering geomorphological data on the entire reef could help determine how differences in reef topography drive differences in species distributions across broader spatial scales and provide new insights into the spatial configuration of patterns observed.

Remote sensing of the earth and oceans has traditionally been performed by satellites and manned aircraft. Although these traditional methods of remote sensing can capture data over broad spatial scales, there are major limitations when applied to monitoring intertidal reefs. These include the inability to provide high-resolution imagery required to map fine-scale heterogeneity (i.e. centimetre scale), inherently high costs associated with acquisition, limitations in terms of temporal collection due to orbits, and weather and associated constraints due to cloud cover (Anderson and Gaston, 2013).

Unmanned aerial vehicles (UAVs), or drones, are beginning to bridge the disparity in scale between traditional remote-sensing methods and on-ground monitoring techniques in various ecosystems (Anderson and Gaston, 2013). The ability to collect remote-sensing data on demand, using low-cost platforms and sensors, provides new opportunities in the field of ecology to better understand patterns and the processes driving them. Flying at lower altitudes (<100 m) than traditional remote-sensing methods allows for data capture below

cloud cover, finer spatial resolution (sub centimetre) in outputs and reduced costs (Feng et al., 2015). These advantages allow rapid collection of high-resolution data at precisely designed temporal scales, which has seen UAVs emerge as an important tool in environmental conservation and monitoring (Allan et al., 2015; Koh and Wich, 2012).

The potential of UAVs for environmental assessment and monitoring is increasingly being demonstrated, and the impacts of environmental disturbances can be assessed rapidly because of the ease of deployment and portability of UAVs (DeBusk, 2010). Recent studies show the advantage of using UAVs in forest and crop monitoring (Vega et al., 2015; Zahawi et al., 2015), monitoring coastal erosion (Bellezza Quarter et al., 2014; Turner et al., 2016), and quantification of submerged vegetation in shallow water (Casado et al., 2015). UAV systems can also use multispectral sensors to assist with identification of species and vegetation health via spectral classifications (Pérez-Ortiz et al., 2015) and can be deployed to perform population censuses of species in remote or difficult-to-access areas (Chabot and Bird, 2015; Christiansen et al., 2016; Hodgson et al., 2016).

While UAVs have been used to assess broadscale coastal morphology along beaches and sand dunes (Gonçalves and Henriques, 2015; Turner et al., 2016), applications to intertidal reef systems to investigate community structure have been limited, although a few studies have considered innovative ways to capture intertidal reefs at a much higher resolution using low-altitude remote-sensing platforms. For example, a blimp fitted with a multispectral sensor was deployed to map an intertidal reef from an altitude of 80 m to estimate algal biomass using normalised difference vegetation indices (NDVI) and topographic heterogeneity of the reef for scale-dependent analyses of algal biomass–topography relationships (Guichard et al., 2000). Another study used a kite to collect imagery of a reef and construct high-resolution (5 cm) 3D models to characterise the geomorphology of the reef and collect multispectral data over hundreds of metres (Bryson et al., 2013).

The ability to use low-cost multirotor platforms with autopilot systems provides distinct advantages for low-altitude imagery platforms for intertidal reefs, including improved efficiency using predetermined flight paths for data collection, which is critical to maximise survey time available at low tides. Off-the-shelf UAV platforms, easily accessible to the hobbyist, also provide the potential to enhance data output through citizen science programs, with low-cost platforms capable of autonomous programmed flight now common in the marketplace (Allan et al., 2015; Raoult et al., 2016). This readily available technology will allow citizen scientists access to pre-programmed flight paths, smart ground control targets to allow for centimetre precision, and web-based workflows to automate data upload to central depositories for cloud processing and data dissemination. Over networks, this could provide scientists with high-frequency image capture to monitor change that would not be possible using scientific teams alone. While yet to be fully exploited for citizen science, there is great potential for such UAV approaches to be effective in providing high-frequency temporal data collection over targeted areas if adequate training and quality

control can be provided and flight regulatory requirements for small UAVs can be met (Allan et al., 2015).

There is also a need to quantify the detectability of species when using UAV surveys compared to traditional approaches to determine the value of low-cost UAVs to complement, or potentially replace, more field-intensive ground-based approaches. Through accurate georeferencing of imagery mosaics, UAVs provide the potential to identify subtle shifts in species distribution with repeat surveys. In addition, digital surface models from UAV surveys make it possible to collect data on the variation in geomorphic features, such as subtle changes in elevation and complexity that have been found to influence biotic assemblages (Longtin et al., 2009), and susceptibility to sea level rise with a changing climate (Helmuth et al., 2006).

This study assesses the potential for UAVs to accurately monitor intertidal reefs. This was achieved by comparing dominant algal communities measured using on-ground quadrat surveys to those extracted from UAV-captured photogrammetry. Fine-scale geomorphic features derived from UAV data capture are also used to determine environmental drivers of biological variation on the reef. UAV geomorphic features representing variations in reef structure were compared to species counts from on-ground quadrat surveys to determine their influence on intertidal macroalgae and invertebrate assemblages. Automated unsupervised classification of canopy-forming macroalgae was also tested to explore the potential for full unmanned intertidal reef census.

6. Methods

6.1 Unmanned aerial vehicle surveys of intertidal reefs

6.1.1 Study sites

Study sites were identified from the Parks Victoria Intertidal Reef Monitoring Program to represent intertidal reefs from open coast to embayments along a longitudinal gradient. Four regions were chosen on the Victorian coast, each containing a site within a marine protected area (MPA) and a corresponding non-protected reference site (Table 6.1, Figure 6.1) (see Murfitt et al. (2017) for more details). Surveys were undertaken at low tides between 0.12 and 0.26 m.

Table 6.1: Details of survey sites

Region (see Figure 6.1)	Study site	MPA or REF	Position
Warrnambool	Pickering Point	Merri MS MPA	−38°24’S, 142°28’E
Warrnambool	Shelly Beach	Merri REF	−38°24’S, 142°28’E
Port Phillip Heads	Point Lonsdale	Port Phillip Heads MNP MPA	−38°17’S, 144°36’E
Port Phillip Heads	Cheviot Beach	Port Phillips Heads REF	−38°18’S, 144°39’E
Beaumaris	Ricketts Point	Ricketts Point MS MPA	−37°59’S, 145°01’E
Beaumaris	Halfmoon Bay	Ricketts Point REF	−37°58’S, 145°05’E
Flinders	Mushroom Reef	Mushroom Reef MS MPA	−38°29’S, 145°01’E
Flinders	West Flinders	Mushroom Reef REF	−38°28’S, 145°06’E

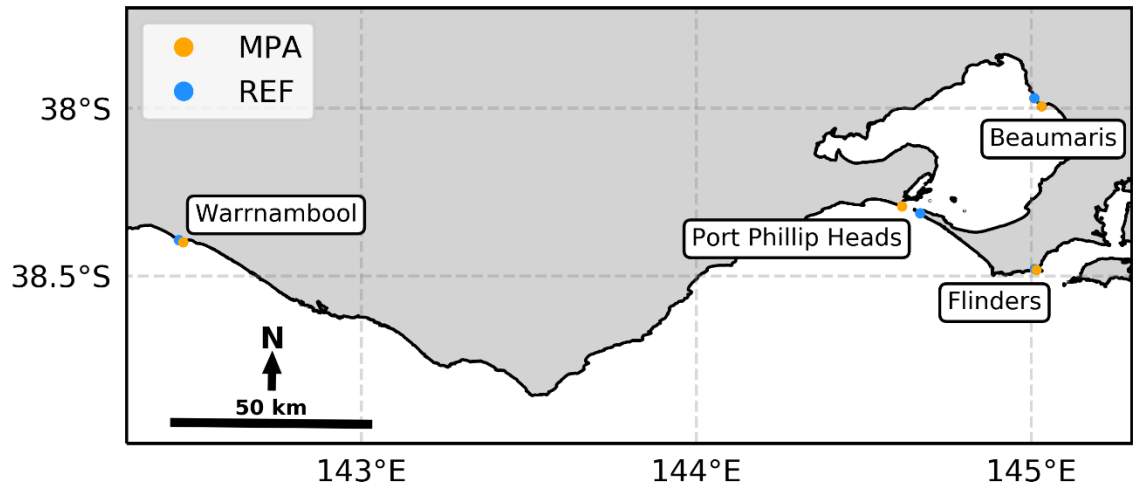

Figure 6.1: Study sites at the 4 regions along the coast of Victoria, Australia, showing sites inside marine protected areas (MPA) and reference sites outside MPAs (REF)

6.1.2 Unmanned aerial vehicle surveys

Unmanned aerial vehicle (UAV) surveys were conducted using a Swellpro Splashdrone quadcopter, measuring 32 cm (w) × 25 cm (h), with total weight of 2.5 kg. The UAV was fitted with an open-source ArduPilot flight control system to allow for autonomous flight along pre-prepared flight paths. The UAV was fitted with a waterproof Canon D30 sensor, with a resolution of 4,592 × 3,056 pixels and an automated trigger system capable of capturing high-quality images every 2 seconds. The entire airframe and payload is waterproof for use in coastal and marine environments, which allows for a safe emergency landing in the ocean if necessary.

Mission Planner software (v. 1.3.35) was used to prepare flight paths for each site and monitor progress during UAV data capture. Flight missions were flown at an altitude of 10 m above Australian Height Datum (AHD) and a speed of 2 m/s. UAV flight paths were designed in a cross-hatch pattern to allow for greater overlap in imagery; the cross-hatch design had a 60% overlap and 40% sidelap to ensure high data redundancy. For larger sites, multiple flights were required due to limited battery endurance (15 minutes). To ensure the greatest spatial capture of the exposed intertidal reef, surveys were carried out on days with low wind speed (<15 knots) and low tides (0.12 to 0.25 m above AHD to ensure the key ecological indicator *Hormosira banksii* was captured). UAV flights were undertaken immediately after the tide had receded to maximise coverage that could be achieved before the incoming tide, and low tide times were selected to avoid glare from the high sun close to midday.

For accurate georeferencing of imagery, ground control points (GCPs) (black and white 30 cm × 30 cm checkerboard targets) were deployed at each site. The centre of each GCP was recorded using Topcon HiPer-S real-time kinematic global positioning system (RTK GPS), with <2 cm precision for latitude, longitude and elevation. This precision was achieved by streaming real-time corrections via the 4G cellular network from the GPSNET base station network.

6.1.3 Unmanned aerial vehicle image processing

Images collected from UAV flights were geotagged with Mission Planner (v. 1.3.35) prior to photogrammetric processing using Pix4Dmapper software (v. 2.1.53). GCPs were added to each project and manually tied to several images to produce a georeferenced orthomosaic. This allowed for vertices of the on-ground quadrats recorded with RTK GPS to be located with high precision for extraction of UAV virtual quadrats. Full processing was initiated in Pix4Dmapper software (v. 2.1.53), which searched for matching points in uploaded images and calibrated the position and orientation of image capture, calculated 3D coordinates of images to create a point cloud, and generated a digital surface model (DSM) and georeferenced orthomosaic for each of the 8 sites (Figure 6.2).

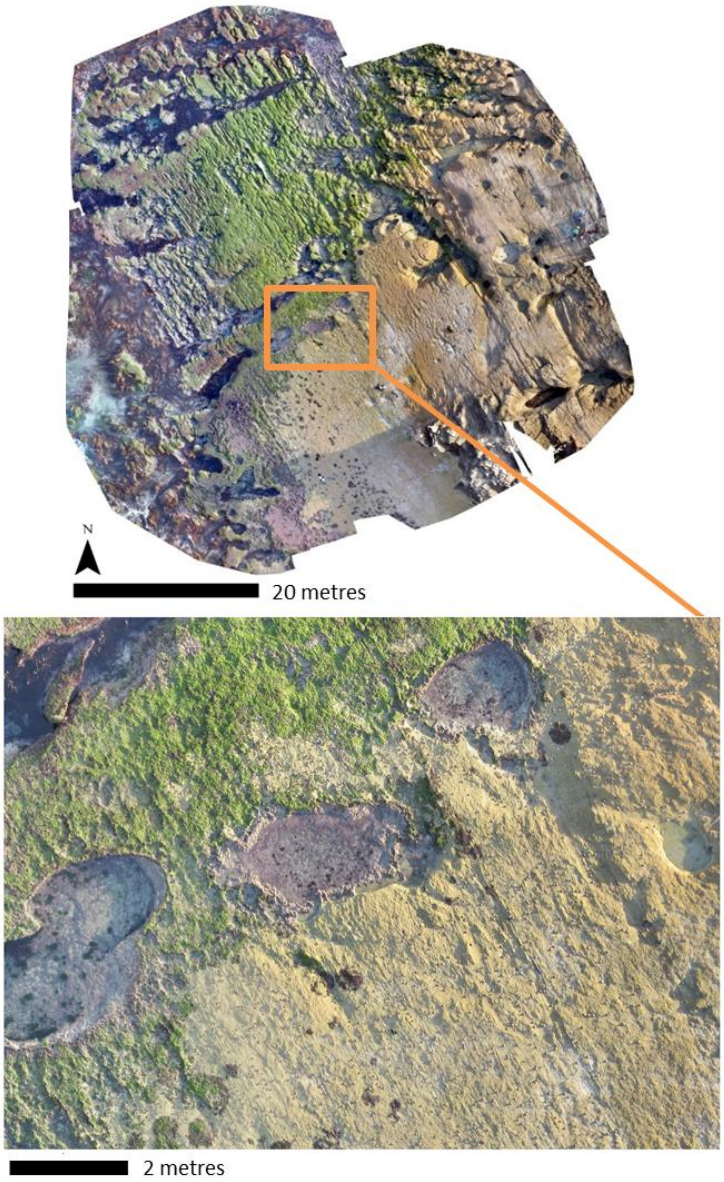

Figure 6.2: Orthomosaic of Shelly Beach site in Warrnambool, inset showing a detailed section of the reef, derived from 10 m altitude unmanned aerial vehicle (UAV) flight

Orthomosaics for each site were imported into ArcMap (v. 10.4.1) along with RTK GPS data points from the coordinates of on-ground quadrat corners to allow for data co-location. UAV virtual quadrats were exported into Coral Point Count software (v. 4.1), and a 50-point grid (in keeping with IRMP methods) was created to quantify percentage cover of dominant algae (Figure 6.3). After preliminary UAV surveys at 2 of the sites, it was decided to classify the algal taxa into 4 dominant and easily recognised groups (*Hormosira banksii*, turfing rhodophytes, chlorophytes and encrusting corallines). This classification alleviated issues with identifying species of similar morphology, limitations of the sensor, and in some cases, insufficient resolution for confidently differentiating species.

Secondary products were derived from the DSM to characterise the structural complexity of the intertidal reef likely to influence biotic assemblages. DSM resolution for all sites was resampled to 5 cm in the horizontal plane from an average output resolution of 0.29 cm for comparable analysis and to reduce the influence of micro roughness by fine-scale biological

components, such as macroalgae. Environmental variables were derived from the UAV virtual quadrats using Benthic Terrain Modeller 3.0 in ArcMap (v. 10.4.1). The mean elevation, vector ruggedness measure (VRM), aspect (northness and eastness), and distance to seaward reef edge, were calculated for each quadrat at all sites using a 3 × 3 kernel.

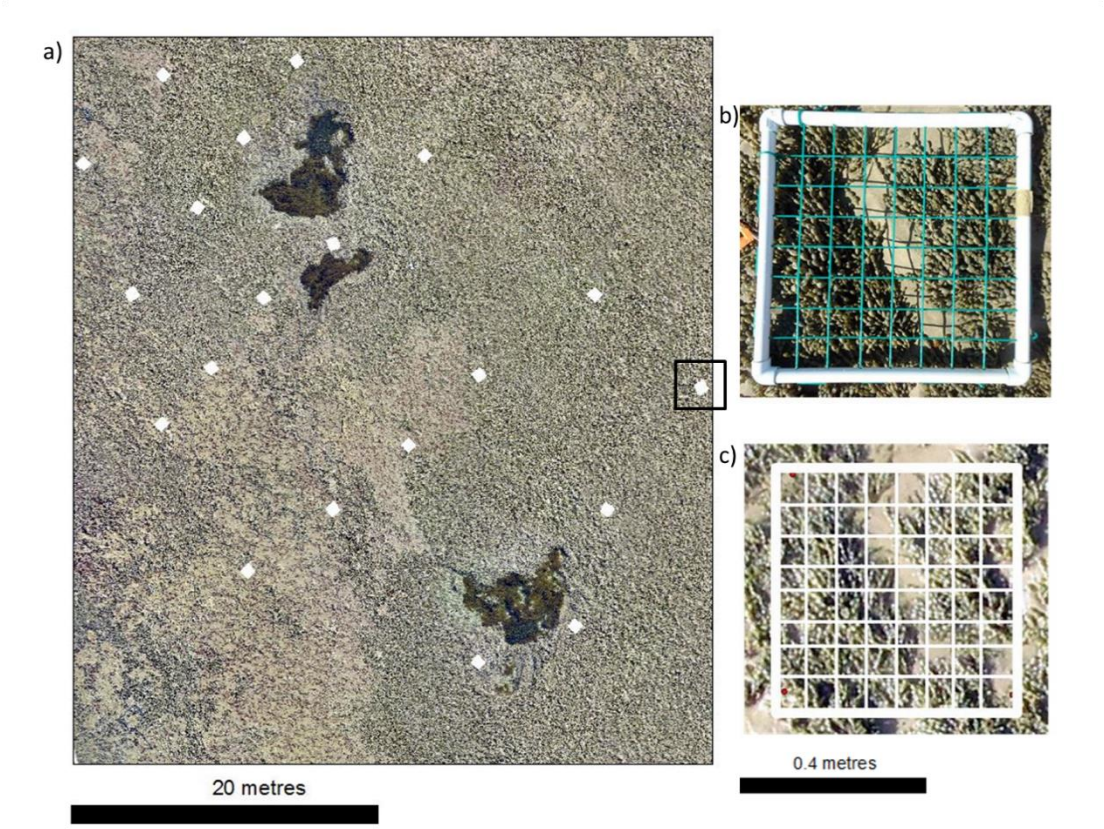

Figure 6.3: Example orthomosaic and virtual quadrats used to quantify % cover of *Hormosira banksii* (a) section of Cheviot Beach orthomosaic with position virtual quadrats shown in white (virtual quadrat positions were determined based on the position of the corners of on-ground quadrats), (b) photo of on-ground quadrat, and (c) extracted UAV virtual quadrat with point count grid overlay. The dominant canopy-forming alga *H. banksii* is seen in each image

6.1.4 On-ground quadrat surveys

On-ground quadrat data were collected in accordance with the Parks Victoria Intertidal Reef Monitoring Program, and where possible completed during the same tide as the UAV surveys. At each site, 25 existing fixed-position quadrats were surveyed along 5 transects running from the high to low shoreline using a 0.25 square metre (m^2), 50-point quadrat, recording percentage covers of algae and sessile invertebrates, abundances of mobile invertebrates and photo quadrats. A total of 198 quadrats were surveyed over the 8 sites (25 quadrats surveyed at each site) except Point Lonsdale and Mushroom Reef (n = 24 quadrats per site) where restricted low-water time resulted in an individual quadrat being missed at each location. Algae and invertebrates were identified to the lowest possible taxonomic level. Coordinates of quadrat corners were recorded with RTK GPS for co-location within the UAV orthomosaic.

6.1.5 Automated macroalgal classification

The potential for a full-reef census with automated classification was tested using ISO Cluster Unsupervised Classification in ArcMap (v. 10.4.1) on the Point Lonsdale site using the dominant fucoid *H. banksii*. A section of the site (2,935.74 m^2 in area) was clipped for the analysis and resampled to 1 cm resolution to assess the potential resolution of higher altitude flights. Fifty 0.25 m^2 virtual quadrats were randomly selected to quantify percentage cover using manual and ISO image-classification approaches. Percentage cover of the manual and ISO-automated quadrats were then extrapolated to estimate percentage cover of the section. They were compared with full-coverage ISO image classification for the section to determine the potential of upscaling percentage cover estimates from traditional survey approaches. Percentage cover of manually and automatically classified *H. banksii* cover in the 50 virtual quadrats was compared by linear regression and paired t-tests in R statistical software (R Core Team, 2013).

6.1.6 Comparison of assemblage data collected by UAV and on-ground quadrat surveys

Algal assemblage groups were compared among regions, parks, and methods using a mixed-model permutational multivariate analysis of variance (Anderson et al., 2008) in PRIMER (v. 7.0.11) with the PERMANOVA+ add on. Data were square-root transformed to account for variation in species abundances and prevent undue influence from a small number of very common taxa (Kruskal, 1964) and then tested with unlimited permutations of data using Bray–Curtis similarity matrices (Warwick and Clarke, 1991). The statistical design had 4 crossed factors: Region (4 levels, random), Park (2 levels: MPA and reference, fixed), Method (2 levels: on-ground quadrats and UAV, fixed) and Quadrat (25 levels, fixed). Tests for homogeneity of dispersions within factors were performed using PERMDISP (Anderson et al., 2008) with distance to centroids. Pairwise analyses were conducted between on-ground and UAV virtual quadrat methods for significant interaction terms, and similarity percentages (SIMPER) were calculated to determine species making the greatest contribution to the dissimilarities between survey methods. Non-metric multidimensional scaling (nMDS) (Clarke, 1993) was used to visualise the differences in assemblages detected using the 2 survey methods. Ordinations were accepted if stress values were <0.20 (Kruskal, 1964). Time taken to complete all on-ground quadrats was compared to time taken to complete UAV survey, extraction of virtual quadrats and virtual quadrat analysis combined through paired t-tests in R statistical software (R Core Team, 2013). Time was calculated from the commencement of the first to the completion of the final quadrat for on-ground counts. UAV surveys were calculated by flight time combined with time taken for extraction of UAV virtual quadrats, and algal percentage cover analysis in Coral Point Count software (v. 4.1). Processing times for UAV data capture were not included, as this process is semi-autonomous after the initial upload of data.

6.1.7 Geomorphological and environmental influence on assemblage structure

Environmental variables were checked for correlation in PRIMER through draftsman plots, and multicollinearity measured by variance inflation factor (VIF) with all variables used showing VIF values <5. Environmental variables were then normalised to account for variation in units, and their influence on intertidal community assemblages were tested with BIOENV analyses. BIOENV tests were run to address the influence of MPA and reference sites on assemblage structure. To determine the percentage contribution environmental variables had on biotic assemblages, distance-based linear model multivariate analysis (DistLM) was performed. Distance-based redundancy analyses (dbRDA) with environmental variable overlays were used to visually analyse the influence of environmental variables on assemblage structure across the sites (Cortes et al., 2011).

7. Results

7.1 Unmanned aerial vehicle surveys of intertidal reefs

Digital outputs created from the UAV imagery had an average resolution of 0.29 ± 0.01 cm; geolocation accuracy had an average of 0.61 ± 0.18 cm, 0.65 ± 0.24 cm, and 1.19 ± 0.42 cm for latitude, longitude and altitude, respectively, for all 8 survey sites (Table 7.1).

Table 7.1: Information from the Pix4Dmapper processing of all 8 UAV surveys, including the number of ground control points (GCPs) used at each site for georeferencing and RMSE in X, Y and Z axes of the GCP locations

Site MPA or REF	No. of calibrated images	Ground resolution[1]	Area (ha)	No. of GCPs	RMSE X[1]	RMSE Y[1]	RMSE Z[1]
Pickering Point Merri MS MPA	256	0.34	0.726	4	0.007	0.228	0.390
Shelly Beach Merri REF	144	0.33	0.344	4	0.393	0.376	1.082
Point Lonsdale Port Phillip Heads MNP MPA	950	0.26	1.438	3	0.202	0.483	0.967
Cheviot Beach Port Phillips Heads REF	564	0.28	0.883	8	1.445	2.283	3.819
Ricketts Point Ricketts Point MS MPA	325	0.25	0.446	4	0.718	0.329	0.638
Halfmoon Bay Ricketts Point REF	200	0.27	0.149	5	0.669	0.492	1.812
Mushroom Reef Mushroom Reef MS MPA	268	0.29	0.789	5	0.290	0.481	0.132
West Flinders Mushroom Reef REF	270	0.27	0.583	5	1.187	0.539	0.684

Note: **1 Cox et al. (2012)**

UAV flights and preparation took an average of 13.7 ± 4.8 minutes to complete, plus 49.9 ± 4.4 minutes post-processing per site (total 63.6 ± 5.0 minutes per site), while the average time taken to complete all on-ground quadrats per site was 126.3 ± 8.1 minutes. Overall, UAV surveys took significantly less time to complete than on-ground quadrat surveys (t = 8.757, P = <0.001), with UAV survey time at approximately half that of the on-ground survey time. However, the UAV remote-sensing data only quantifies a single stratum of algal cover, whereas the data collected from the on-ground quadrats include the understorey and provide greater detail of community assemblages.

Reliable identification of intertidal biota from UAV virtual quadrats is limited by image resolution and reduced by canopy-forming species obscuring the understorey; thus ground surveys, as expected, provide the additional benefits of identifying understorey communities including invertebrates. For comparisons between on-ground quadrat and UAV virtual quadrats, algal taxa were classified into 4 major groups (*Hormosira banksii*, turfing rhodophytes, chlorophytes and encrusting corallines), and invertebrate taxa were excluded.

Differences of algal assemblages detected by the UAV and on-ground methods were not consistent when comparing reference sites and sites inside the MPAs, partly due to differences in dispersion between algal groups (PERMANOVA Park × Method interaction: Pseudo-$F_{(3,395)}$ = 55.49, $P_{(perm)}$ = <0.001; PERMDISP $F_{(3,392)}$ = 8.583, $P_{(perm)}$ = <0.001). Similarly, the differences in the composition and percentage cover of algal groups between reference sites (REF) and sites inside marine protected areas (MPA) were not consistent among regions (PERMANOVA Region × Park interaction: Pseudo-$F_{(3,395)}$ = 101.07, $P_{(perm)}$ = <0.001; PERMDISP $F_{(7,388)}$ = 40.58, $P_{(perm)}$ = <0.001; Table 7.1, Appendixes 4 and 5).

Pairwise analysis showed no significant difference in algal assemblages at MPA sites between the UAV virtual quadrat method and the on-ground quadrat method (t = 0.489, $P_{(perm)}$ = 0.710). However, the analysis showed a significant difference between the 2 methods among reference sites (t = 12.164, $P_{(perm)}$ = 0.001). SIMPER analysis of reference site data indicated that the dissimilarity between the 2 quadrat methods was explained by turfing rhodophytes (39.6%) and *H. banksii* (35. 4%).

Table 7.2: Mean percentage cover (± SE) of 4 major algal groups recorded in on-ground quadrats and UAV remotely sensed virtual quadrats for each site. All sites had 25 quadrats, except Point Lonsdale and Mushroom Reef (*n* = 24)

	On-ground quadrats				UAV virtual quadrats			
Site **MPA or REF**	*Hormosira banksii*	Turfing rhodophytes	Encrusting corallines	Chlorophytes	*Hormosira banksii*	Turfing rhodophytes	Encrusting corallines	Chlorophytes
Pickering Point **Merri MS MPA**	3.36 ± 1.55	15.56 ± 2.40	-	0.92 ± 0.30	3.76 ± 1.90	23.84 ± 2.79	-	1.56 ± 0.57
Shelly Beach **Merri REF**	-	17.36 ± 4.04	1.04 ± 0.74	20.44 ± 3.84	-	5.8 ± 2.01	-	14.12 ± 2.61
Point Lonsdale **Port Phillip Heads MNP MPA**	37.92 ± 2.39	0.88 ± 0.55	-	0.38 ± 0.33	37.17 ± 2.55	0.17 ± 0.16	-	0.08 ± 0.08
Cheviot Beach **Port Phillips Heads REF**	34.48 ± 3.08	12.40 ± 1.90	0.60 ± 0.28	5.52 ± 1.57	34.64 ± 3.29	2.48 ± 0.94	-	-
Ricketts Point Ricketts Point MS MPA	8.32 ± 2.33	0.16 ± 0.12	-	2.04 ± 0.83	10.52 ± 2.92	0.28 ± 0.12	-	0.32 ± 0.15
Halfmoon Bay Ricketts Point REF	-	7.76 ± 1.84	-	0.64 ± 0.39	-	5.12 ± 1.39	-	-
Mushroom Reef Mushroom Reef MS MPA	3.42 ± 1.49	0.38 ± 0.16	0.29 ± 0.29	-	2.75 ± 1.11	0.21 ± 0.14	2.96 ± 1.40	-
West Flinders Mushroom Reef REF	11.12 ± 1.94	19.92 ± 3.11	0.80 ± 0.29	0.08 ± 0.08	8.76 ± 1.98	3.96 ± 0.92	0.20 ± 0.10	-

7.1.1 Geomorphological and environmental influence on assemblage structure

Elevation and distance to seaward reef edge were the most influential environmental features; elevation was the best explanation for algal taxa occurrence (ρ = 0.17), and a combination of elevation and distance to seaward reef edge explained the most variation for invertebrate assemblages (ρ = 0.31).

Distance-based linear models (DistLM) showed that 19.7% and 15.9% of the total variation in assemblage composition was attributable to environmental derivatives for algae and invertebrates, respectively. Elevation explained the greatest percentage of variation (14.9%) in the algal assemblages (r = 0.799, *P* = 0.001), with seaward reef edge explaining 4.5% of the variation (r = −0.860, *P* = 0.001) (Figure 7.1a). Invertebrate assemblage variation was principally explained by distance to seaward reef edge (9.8%; r = 0.982, *P* = 0.001) and elevation (4.8%; r = 0.991, *P* = 0.001) (Figure 7.1b). Vector ruggedness measure (VRM) was also significant for invertebrate assemblages (r = −0.928, *P* = 0.023); however, it only explained 0.7% of the total variation.

7.1.2 Automated macroalgal classification

Linear regression of the UAV imagery for Point Lonsdale showed a significant positive relationship between the manual and ISO-automated classifications of *H. banksii* cover (R^2 = 0.64, *P* < 0.001; Appendix 4). However, there was a significant difference between the manual and ISO-automated classifications in percentage cover of *H. banksii* (paired t-test t = 3.866, *P* < 0.001), with the automated classification underestimating cover by approximately 27%. Extrapolation of *H. banksii* cover from the 50 virtual quadrats to the clipped section of the Point Lonsdale site (see Section 6.1.5) estimated that percentage cover was 57.95% for manually classified and 46.95% for ISO cluster unsupervised classification (Figure 7.2). The extrapolation of the 50 ISO virtual quadrats resulted in similar percentage cover (~47%) to the ISO classification of the entire clipped section. Cover of *H. banksii* from on-ground quadrat surveys in the section (*n* = 14) were also extrapolated to the clipped section at 63.71%.

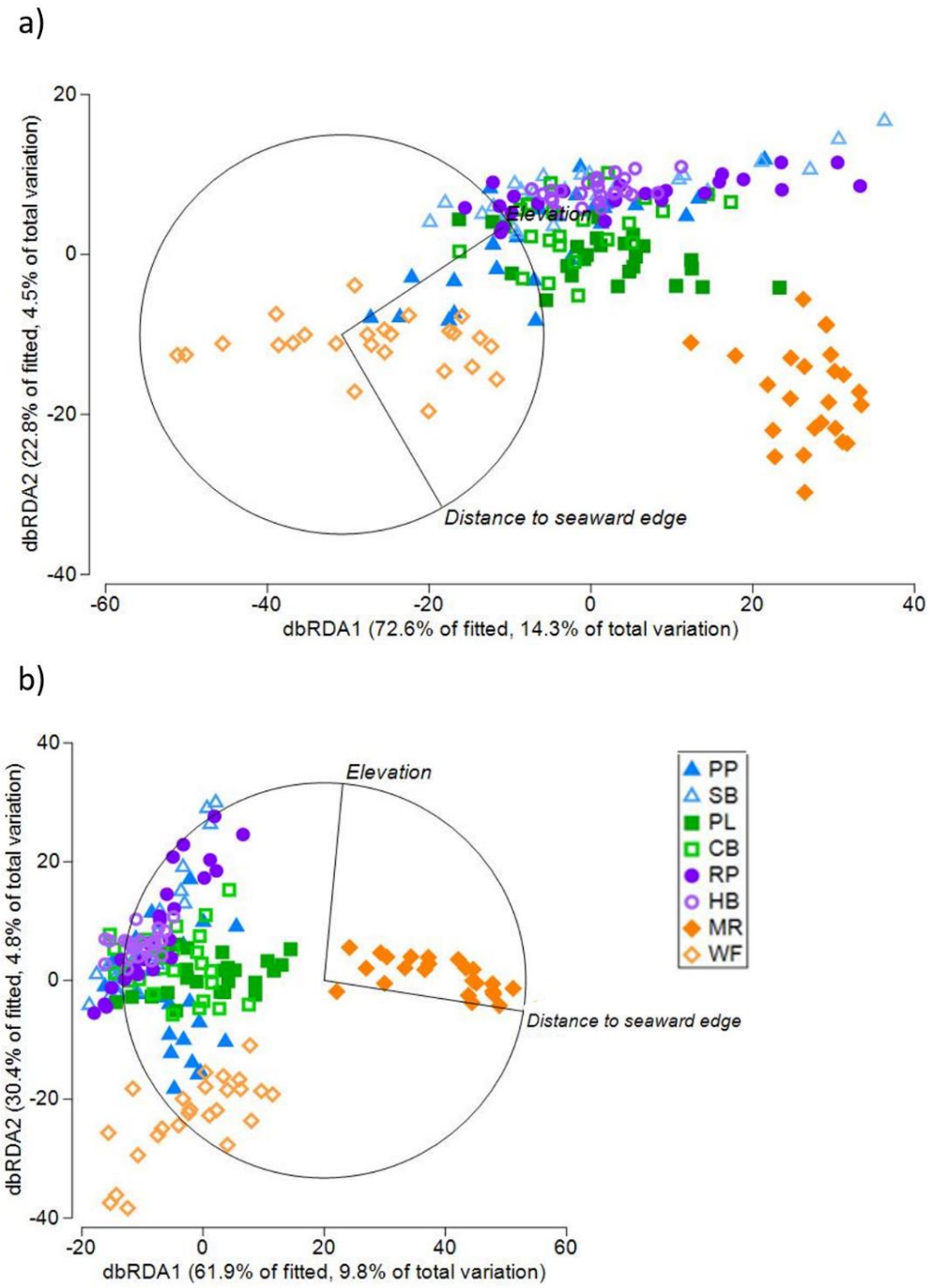

Figure 7.1: Distance-based redundancy analysis (dbRDA) ordination describing the relationship between UAV-derived environmental variables and a) algal percentage cover and b) invertebrate abundances from on-ground quadrat DistLM classified by site. Vectors depict the effect of environmental variables influencing presence of algae and invertebrates, with length of vector representing the strength of effect. Axes show percentage of variation: a) elevation (dbRDA1) and distance to seaward reef edge (dbRDA2), and b) distance to seaward reef edge (dbRDA1) and elevation (dbRDA2). Sites: PP = Pickering Point, SB = Shelly Beach, PL = Point Lonsdale, CB = Cheviot Beach, RP = Ricketts Point, HB = Halfmoon Bay, MR = Mushroom Reef, WF = West Flinders; Park: MPA = closed symbol, reference = open symbol

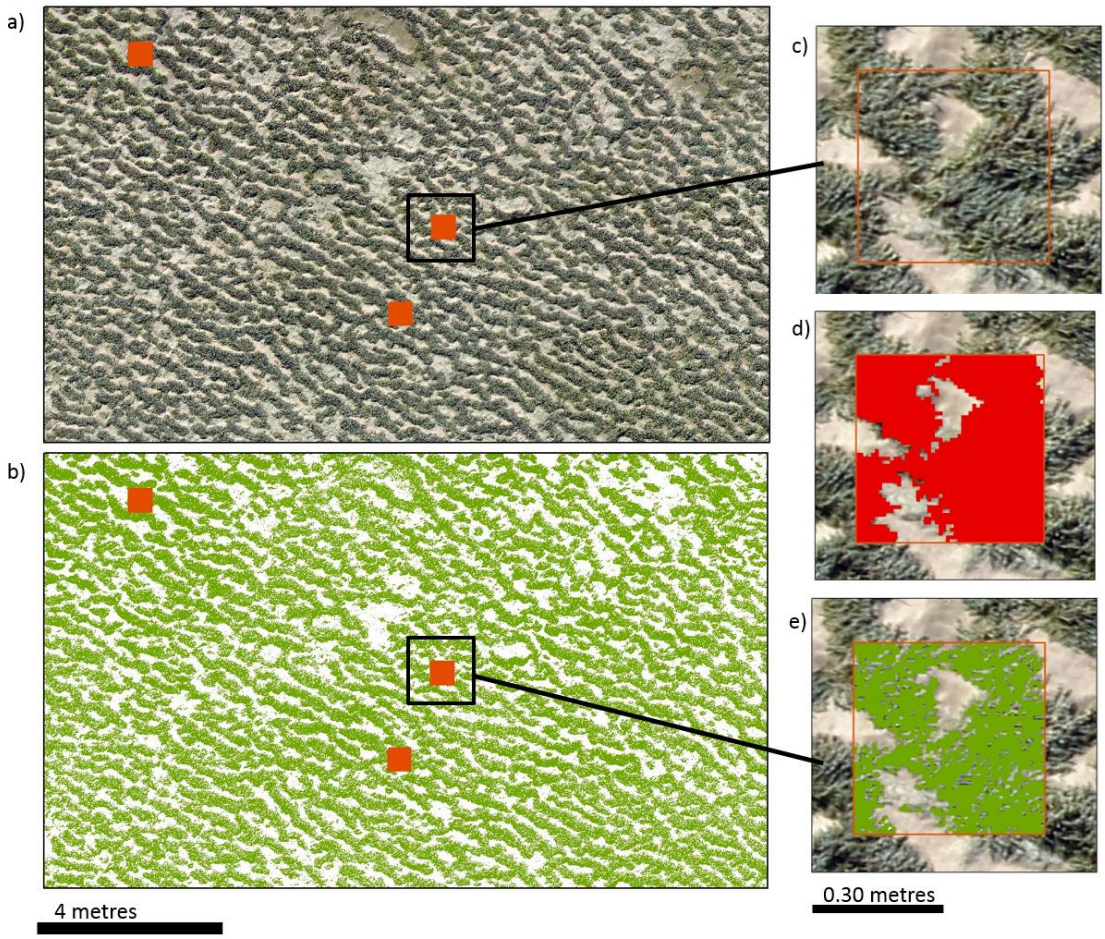

Figure 7.2: Examples of ISO unsupervised classification and manual classification of virtual quadrats of *Hormosira banksii*: a) section of Point Lonsdale site showing 0.25 m^2 quadrats used for automated classification, b) same section shown as ISO unsupervised classification with *H. banksii* represented in green, c) one of the 50 random quadrats across the site, d) manual classification of *H. banksii* (red) for comparison with automated classification, e) ISO classification of *H. banksii* (green) from the same quadrat

8. Discussion

8.1 Unmanned aerial vehicle surveys of intertidal reefs

Use of UAVs in the present study reveals the potential for high-resolution remote sensing to be implemented into current intertidal monitoring efforts through simultaneous estimation of algal canopy cover and quantification of fine-scale geomorphological attributes of entire intertidal reefs. The present study expands on knowledge gained from on-ground surveys to encompass broader spatial scales, giving insight into the distribution and abundance of biota across intertidal reefs. Important findings include that quantification of dominant, canopy-forming macroalgae from the UAV imagery is similar to that from on-ground measures; UAV surveys can capture fine-scale (Cox et al., 2012) geomorphological variables of the whole reef; and automated classification approaches have the potential of upscaling to a full-reef census. In addition, the information provided by the UAVs requires about half the time needed for manually surveying intertidal reefs using quadrats.

Results showed no significant difference between UAV and on-ground methods for macroalgal canopy cover estimates at MPA sites, driven by dominance of the fucoid *Hormosira banksii*. Canopy-forming algae are often associated with other intertidal biota, and shifts of these species could influence species composition on the reef (Lilley and Schiel, 2006), so the ability to easily identify the *H. banksii* canopy in UAV surveys is an advantage of using this technique to monitor intertidal reefs. Additionally, extrapolation of *H. banksii* from the on-ground quadrats showed larger estimates of percentage cover when extrapolated to the clipped section at Point Lonsdale than the ISO-automated classification for the area; however, this might have been influenced by quadrat placement at the site. Quadrat placement along a stratified habitat design may allow for a more balanced estimate when extrapolating to the entire reef. Estimations may also improve through machine learning techniques and classification, the use of multispectral sensors to help discriminate between biota, and opportunities to better evaluate relationships between UAV-based estimates and on-ground condition.

Additional information provided by the UAV data, including on the structure of the intertidal zone, aids in assessing how species are distributed across variations in the geomorphology of the substrate. As intertidal assemblages change from low to high on the shore, variations in reef features, including elevation, may become important across a range of scales. The multi-scale geomorphic structure of the reef, captured by the UAV, allowed for testing of how these features influenced distribution of distinct algal and invertebrate assemblages. Combining fine-scale structural information with detailed assemblage data from on-ground quadrat surveys revealed elevation and distance to seaward reef edge were the strongest physical drivers of observed species distributions. Elevation was the most important variable for algae, and a combination of elevation and distance to seaward reef edge was the most important for invertebrates. These results support previous studies revealing the

importance of elevation for species of the intertidal environment (Heaven and Scrosati, 2008; Hollenbeck et al., 2014). Low-shore intertidal reef has a longer inundation period than sites higher on the shore, reducing exposure to stressors such as desiccation and UV radiation. Understorey species further from the shoreline rely on canopy-forming species to ameliorate changeable environmental conditions (Coombes et al., 2013; Watt and Scrosati, 2013), although also see Pocklington et al. (2019) about the influence of canopy cover on this relationship.

Despite the added benefit of capturing the geomorphological attribute of the intertidal platform, the limitation of UAV data in not being able to image the aspects of the assemblage under the canopy results in an incomplete biological assessment. However, the quadrat surveys provide very thorough observations of targeted sections of the reef and have the potential to be extrapolated based on species' relationships with both biogenic and physical attributes of the intertidal platform.

Intertidal reefs often exhibit a high degree of heterogeneity due to the dynamic environment, and it is important that the monitoring technique used can assess the varied habitat types across these reefs. The results of this study show that although UAVs may not be able to replace on-ground monitoring techniques on intertidal reefs, they provide a complementary data source giving a more comprehensive understanding of intertidal reef assemblages. UAV surveys could be undertaken more frequently to assess landscape-scale changes in the canopy-forming algal community as an indicator of reef health, with reductions in the number of quadrats required. Collecting data on both the intertidal assemblages and the fine-scale geomorphological features of the reef (such as topographical complexity of the reef at centimetre resolutions) will assist with future management strategies by providing information on the susceptibility of these habitats to pressures such as sea level rise.

UAVs are becoming increasingly efficient to deploy in the field due to decreasing costs and increased performance and ease of use. Despite the benefits of cost savings in image acquisition, there are challenges in detecting objects by their spectral properties from aerial imagery. Data resolution, image clarity, flying height, timing of image capture, camera angle, and flight direction are just some of the considerations (Joyce et al., 2018). In intertidal environments, these considerations are further compounded by the need to consider tidal conditions, sun glint and shadows on imagery. We found that imagery obtained in bright sunlight at low tide was better suited to object-based approaches. Excessive image blur in low-light data capture or moving water on the platform led to poor classifications. Bright sunny conditions decrease image blur in final orthomosaics but are problematic as they increase the incidence of sun glint from standing water on the platform and deepen areas of shadow. Additionally, there is significant effort and cost involved in processing and automated interpretation of large sets of high-resolution imagery (Joyce et al., 2018).

Adding UAV surveys to existing intertidal monitoring programs provides benefits in terms of the full-platform imagery and topographic coverage that can be achieved. This approach also has the potential to better inform on-ground monitoring programs to ensure representative observations are achieved that capture the observed environmental gradients. This can assist in prioritising survey areas for monitoring, such as areas of high visitation or regions close to potential disturbance such as drains. In this study, we used low-cost UAV components comparable to devices currently in vogue with recreational drone users. This poses enormous opportunities to increase temporal data capture to determine trends, including seasonality, by implementing intertidal reef monitoring citizen science programs. Sea Search is one such program that relies on volunteers and community groups to observe intertidal reefs through quadrat surveys; it benefits both the local community and scientific researchers through sharing of knowledge and creating partnerships between these groups (Koss et al., 2009). Studies have also shown that 'non-expert' volunteers are able to collect intertidal biota data within the same variation range as occurs between researchers (Cox et al., 2012). Already, consumer multirotors such as DJIs phantom 4 are capable of autonomous flight and have been integrated seamlessly into photogrammetry software such as Pix4D with specialist apps developed (PIX4DCapture) allowing for cloud-based upload, data processing and storage. New laws regarding operation of UAVs and certification requirements are also making it easier for state organisations, such as Parks Victoria, to explore the application of these sensor platforms for monitoring programs. This includes flying UAVs up to 2 kg without the operator requiring Civil Aviation Safety Authority certification (Casado et al., 2015) , as applies under the Civil Aviation Safety Regulations 1998 (Commonwealth) to 'excluded' remotely piloted aircraft operating under certain conditions. UAV's have already been adopted by citizen scientists as part of the Victorian Coastal Monitoring program in which community groups are mapping coastal erosion at 15 sites across the state every 4 to 6 weeks. Combined with increased endurance through improvements in battery technology and miniaturisation of sensor technology, there is an opportunity for UAV technology become a part of sustained monitoring programs in the intertidal zone across the marine parks estate. Currently, Parks Victoria do not permit the operation of UAVs under the Excluded Category within their managed land; only operations conducted under a Remote Operators Certificate (ReOC) are permitted. The cost of a ReOC is likely untenable for most community groups, halting the potential of UAV citizen science on land managed by Parks Victoria.

9. References

Airoldi, L 2003, 'Effects of patch shape in intertidal algal mosaics: roles of area, perimeter and distance from edge', *Marine Biology*, vol. 143, no. 4, pp. 639-50.

Allan, BM, Ierodiaconou, D, Nimmo, DG, Herbert, M and Ritchie, EG 2015, 'Free as a drone: ecologists can add UAVs to their toolbox', *Frontiers in Ecology and the Environment*, vol. 13, no. 7, pp. 354-5.

Althaus, F, Hill, N, Ferrari, R et al. 2015, 'A standardised vocabulary for identifying benthic biota and substrata from underwater imagery: the CATAMI classification scheme', *PLOS ONE*, vol. 10, no. 10, e0141039.

Anderson, DR, Burnham, KP and Thompson, WL 2000, 'Null hypothesis testing: problems, prevalence, and an alternative', *The Journal of Wildlife Management*, vol. 64, no. 4, pp. 912-23.

Anderson, K and Gaston, KJ 2013, 'Lightweight unmanned aerial vehicles will revolutionize spatial ecology', *Frontiers in Ecology and the Environment*, vol. 11, no. 3, pp. 138-46.

Anderson, MJ, Gorley, RN and Clarke, KR 2008, *'PERMANOVA+ for PRIMER: guide to software and statistical methods*'. PRIMER-E, Plymouth, UK.

Arachchige Weerarathne, I, Monk, J and Barrett, N 2021, 'Sample-size requirements for accurate length–frequency distributions of mesophotic reef fishes from baited remote underwater stereo video', *Ecological Indicators*, vol. 122, 107262.

Araújo, MB and Guisan, A 2006, 'Five (or so) challenges for species distribution modelling', *Journal of Biogeography*, vol. 33, no. 10, pp. 1677-88. doi:10.1111/j.1365-2699.2006.01584.x

Austin, MP 1998, 'An ecological perspective on biodiversity investigations: examples from Australian eucalypt forests', *Annals of the Missouri Botanical Garden*, vol. 85, no. 1, pp. 2-17.

Awruch, CA, Pankhurst, NW, Frusher, SD and Stevens, JD 2009, 'Reproductive seasonality and embryo development in the draughtboard shark *Cephaloscyllium laticeps*', *Marine and Freshwater Research*, vol. 60, no. 12, pp. 1265-72.

Barkby, S, Williams, S, Pizarro, O and Jakuba, M 2009, 'An efficient approach to bathymetric SLAM', in *2009 IEEE/RSJ International Conference on Intelligent Robots and Systems*, pp. 219-24.

Barley, SC, Meekan, MG and Meeuwig, JJ 2017, 'Species diversity, abundance, biomass, size and trophic structure of fish on coral reefs in relation to shark abundance', *Marine Ecology Progress Series*, vol. 565, pp. 163-79.

Barnett, A and Semmens, JM 2012, 'Sequential movement into coastal habitats and high spatial overlap of predator and prey suggest high predation pressure in protected areas', *Oikos*, vol. 121, no. 6, pp. 882-90.

Barton 2018 MuMIn: Multi-Model Inference. R package version 1.43.17. https://cran.r-project.org/web/packages/MuMIn/

Bellezza Quater, P, Grimaccia, F and Masini, A 2014, 'Airborne unmanned monitoring system for coastal erosion assessment', in G Lollino, A Manconi, J Locat, Y Huang and M Canals Artigas (eds), *Engineering geology for society and territory – Volume 4: Marine and coastal processes*, Springer International Publishing, Switzerland, pp. 115-20.

Bewley, MS, Nourani-Vatani, N, Rao, D, Douillard, B, Pizarro, O and Williams, SB 2015, 'Hierarchical classification in AUV imagery', in L Mejias, P Corke and J Roberts (eds), *Field and service robotics*, Springer Tracts in Advanced Robotics, vol. 105., Springer, Cham, pp. 3-16.

Bjørnstad, O 2009, ncf: spatial nonparametric covariance functions. R package ver. 1.1-3. https://cran.r-project.org/web/packages/ncf/

Blaschke, T 2010, 'Object based image analysis for remote sensing', *ISPRS Journal of Photogrammetry and Remote Sensing*, vol. 65, no. 1, pp. 2-16.

Bolker, BM, Brooks, ME, Clark, CJ, Geange, SW, Poulsen, JR, Stevens, MHH and White, J-SS 2009, 'Generalized linear mixed models: a practical guide for ecology and evolution', *Trends in Ecology and Evolution*, vol. 24, no. 3, pp. 127-35.

Booth, JD 1997, 'Long-distance movements in *Jasus* spp. and their role in larval recruitment', *Bulletin of Marine Science*, vol. 61, no. 1, pp. 111-28.

Bryson, M, Johnson-Roberson, M, Murphy, RJ and Bongiorno, D 2013, 'Kite aerial photography for low-cost, ultra-high spatial resolution multi-spectral mapping of intertidal landscapes', *PlOS ONE*, vol. 8, no. 9, e73550.

Casado, MR, Gonzalez, RB, Kriechbaumer, T and Veal, A 2015, 'Automated identification of river hydromorphological features using UAV high resolution aerial imagery', *Sensors*, vol. 15, no. 11, pp. 27969-89.

Chabot, D and Bird, DM 2015, 'Wildlife research and management methods in the 21st century: where do unmanned aircraft fit in?', *Journal of Unmanned Vehicle Systems*, vol. 3, no. 4, pp. 137-55.

Che Hasan, R, Ierodiaconou, D and Laurenson, L 2012, 'Combining angular response classification and backscatter imagery segmentation for benthic biological habitat mapping', *Estuarine, Coastal and Shelf Science*, vol. 97, pp. 1-9.

Che Hasan, R, Ierodiaconou, D, Laurenson, L and Schimel, A 2014, 'Integrating multibeam backscatter angular response, mosaic and bathymetry data for benthic habitat mapping', *PlOS ONE*, vol. 9, no. 5, e97339.

Chiswell, SM, Wilkin, J, Booth, JD and Stanton, B 2003, 'Trans-Tasman Sea larval transport: is Australia a source for New Zealand rock lobsters?', *Marine Ecology Progress Series*, vol. 247, pp. 173-82.

Christiansen, F, Dujon, AM, Sprogis, KR, Arnould, JPY and Bejder, L 2016, 'Noninvasive unmanned aerial vehicle provides estimates of the energetic cost of reproduction in humpback whales', *Ecosphere*, vol. 7, no. 10, e01468.

Clarke, KR 1993, 'Non-parametric multivariate analyses of changes in community structure', *Australian Journal of Ecology*, vol. 18, no. 1, pp. 117-43.

Coombes, MA, Naylor, LA, Viles, HA and Thompson, RC 2013, 'Bioprotection and disturbance: seaweed, microclimatic stability and conditions for mechanical weathering in the intertidal zone', *Geomorphology*, vol. 202, pp. 4-14.

Cortes, RM, Varandas, S, Teixeira, A, Hughes, SJ, Magalhães, M, Barquín, J, Álvarez-Cabria, M and Fernández, D 2011, 'Effects of landscape metrics and land-use variables on macroinvertebrate communities and habitat characteristics', *Limnetica*, vol. 30, no. 2, pp. 347-62.

Cox, TE, Philippoff, J, Baumgartner, E and Smith, CM 2012, 'Expert variability provides perspective on the strengths and weaknesses of citizen-driven intertidal monitoring program', *Ecological Applications*, vol. 22, no. 4, pp. 1201-12.

Cutler, DR, Edwards Jr, TC, Beard, KH, Cutler, A, Hess, KT, Gibson, J and Lawler, JJ 2007, 'Random forests for classification in ecology', *Ecology*, vol. 88, no. 11, pp. 2783-92.

Daley, R, Stevens, JD and Last, PR 2003, *Preparation of a field guide to sharks and rays caught by Australian fisheries*. CSIRO Marine Research and Fisheries Research and Development Corporation, Australia

Dayton, PK 1975, 'Experimental evaluation of ecological dominance in a rocky intertidal algal community', *Ecological Monographs*, vol. 45, no. 2, pp. 137-59.

DeBusk, WM 2010, 'Unmanned aerial vehicle systems for disaster relief: Tornado Alley', AIAA 2010-3506, AIAA Infotech@Aerospace 2010, American Institute of Aeronautics and Astronautics, p. 3506.

Devillers, R, Pressey, RL, Grech, A, Kittinger, JN, Edgar, GJ, Ward, T and Watson, R 2015, 'Reinventing residual reserves in the sea: are we favouring ease of establishment over need for protection?', *Aquatic Conservation: Marine and Freshwater Ecosystems*, vol. 25, no. 4, pp. 480-504.

Diesing, M, Mitchell, P and Stephens, D 2016, 'Image-based seabed classification: what can we learn from terrestrial remote sensing?', *ICES Journal of Marine Science*, vol. 73, no. 10, pp. 2425-41.

Dormann, CF, Elith, J, Bacher, S et al. 2013, 'Collinearity: a review of methods to deal with it and a simulation study evaluating their performance', *Ecography*, vol. 36, no. 1, pp. 27-46.

Edmunds, M 1995, 'The ecology of the juvenile Southern Rock Lobster, *Jasus edwardsii* (Hutton 1875) (Palinuridae)', PhD thesis, University of Tasmania.

Edmunds, M and Flynn, A 2015, *A Victorian marine biotope classification scheme*. Report to Deakin University and Parks Victoria. Australian Marine Ecology Report No. 545.

Edmunds, MJ, Stewart, K and Pritchard, K 2011, *Victorian Subtidal Reef Monitoring Program: the reef biota in the Port Phillip Bay marine sanctuaries.* Parks Victoria Technical Series No. 67, Parks Victoria, Melbourne.

Eigenraam, M, McCormick, F and Contreras, Z 2016, *Marine and coastal ecosystem accounting: Port Phillip Bay*, State of Victoria, Department of Environment, Land, Water and Planning.

Elith, J and Graham, CH 2009, 'Do they? How do they? WHY do they differ? On finding reasons for differing performances of species distribution models', *Ecography*, vol. 32, no. 1, pp. 66-77.

Fahrulian F, Manik HM, Jaya I and Udrekh U 2016, 'Angular range analysis (ARA) and K-means clustering of multibeam echosounder data for determining sediment type', *ILMU KELAUTAN: Indonesian Journal of Marine Sciences*, vol. 21, no. 4, pp. 177-84.

Feng, Q, Liu, J and Gong, J 2015, 'UAV remote sensing for urban vegetation mapping using random forest and texture analysis', *Remote Sensing*, vol. 7, no. 1, 1074-94.

Fonseca L, Brown C, Calder B, Mayer L, Rzhanov Y 2009, 'Angular range analysis of acoustic themes from Stanton Banks Ireland: a link between visual interpretation and multibeam echosounder angular signatures', *Applied Acoustics*, vol. 70. no. 10, pp. 1298-304.

Foster, SD, Monk, J, Lawrence, E, Hayes, KR, Hosack, GR and Przeslawski, R 2018, *Statistical considerations for monitoring and sampling*, in R Przeslawski and S Foster (eds), *Field manuals for marine sampling to monitor Australian waters*, National Environmental Science Programme (NESP), pp. 23-41.

Freeman, EA, Frescino, TS and Moisen, GG 2018, ModelMap: an R package for model creation and map production. https://cran. r-project.org/web/packages/ModelMap/vignettes/VModelMap. pdf

Friedlander, AM and Parrish, JD 1998, 'Habitat characteristics affecting fish assemblages on a Hawaiian coral reef', *Journal of Experimental Marine Biology and Ecology*, vol. 224, no. 1, pp. 1-30.

Frusher, SD and Hoenig, JM 2001, 'Impact of lobster size on selectivity of traps for southern rock lobster (*Jasus edwardsii*)', *Canadian Journal of Fisheries and Aquatic Sciences*, vol. 58, no. 12, pp. 2482-9.

Galaiduk, R, Radford, BT, Wilson, SK and Harvey, ES 2017, 'Comparing two remote video survey methods for spatial predictions of the distribution and environmental niche suitability of demersal fishes', *Scientific Reports*, vol. 7, no. 1, 17633.

Gonçalves, JA and Henriques, R 2015, 'UAV photogrammetry for topographic monitoring of coastal areas', *ISPRS Journal of Photogrammetry and Remote Sensing*, vol. 104, pp. 101-11.

Guichard, F, Bourget, E and Agnard, J-P 2000, 'High-resolution remote sensing of intertidal ecosystems: a low-cost technique to link scale-dependent patterns and processes', *Limnology and Oceanography*, vol. 45, no. 2, pp. 328-38.

Guisan, A and Thuiller, W 2005, 'Predicting species distribution: offering more than simple habitat models', *Ecology Letters*, vol. 8, no. 9, pp. 993-1009.

Harrington, AM and Hovel, KA 2016, 'Patterns of shelter use and their effects on the relative survival of subadult California spiny lobster (*Panulirus interruptus*)', *Marine and Freshwater Research*, vol. 67, no. 8, pp. 1153-62.

Hart, SP and Edmunds, MJ 2005, *Parks Victoria standard operating procedure: biological monitoring of intertidal reefs*, Parks Victoria Technical Series No. 21, Parks Victoria.

Heaven, CS and Scrosati, RA 2008, 'Benthic community composition across gradients of intertidal elevation, wave exposure, and ice scour in Atlantic Canada', *Marine Ecology Progress Series*, vol. 369, pp. 13-23.

Helmuth, B, Mieszkowska, N, Moore, P and Hawkins, SJ 2006, 'Living on the edge of two changing worlds: forecasting the responses of rocky intertidal ecosystems to climate change', *Annual Review of Ecology, Evolution, and Systematics*, vol. 37, no. 1, pp. 373-404.

Hijmans, RJ and van Etten, J 2014, 'raster: Geographic data analysis and modeling', R package version, 2 (8). https://cran.r-project.org/web/packages/raster/

Hodgson, JC, Baylis, SM, Mott, R, Herrod, A and Clarke, RH 2016, 'Precision wildlife monitoring using unmanned aerial vehicles', *Scientific Reports*, vol. 6, no. 1, 22574.

Hollenbeck, JP, Olsen, MJ and Haig, SM 2014, 'Using terrestrial laser scanning to support ecological research in the rocky intertidal zone', *Journal of Coastal Conservation*, vol. 18, no. 6, pp. 701-14.

Hou Z, Chen Z, Wang J, Zheng X, Yan W, Tian Y and Luo Y 2018, 'Acoustic impedance properties of seafloor sediments off the coast of Southeastern Hainan, South China Sea', *Journal of Asian Earth Sciences*, vol. 154, pp. 1-7.

Ierodiaconou, D, Monk, J, Rattray, A, Laurenson, L and Versace, VL 2011, 'Comparison of automated classification techniques for predicting benthic biological communities using hydroacoustics and video observations', *Continental Shelf Research*, vol. 31, no. 2, pp. S28-S38.

Ierodiaconou, D, Schimel, ACG, Kennedy, D, Monk, J, Gaylard, G, Young, M, Diesing, M and Rattray, A 2018, 'Combining pixel and object based image analysis of ultra-high resolution multibeam bathymetry and backscatter for habitat mapping in shallow marine waters', *Marine Geophysical Research*, vol. 39, no. 1-2, pp. 271-88.

IMOS (Integrated Marine Observing System) 2018, AVHRR L3S SST, retrieved 28 September 2018, http://rs-data1-mel.csiro.au/imos-srs/sst/ghrsst/L3S-1m/

Jackson DR and Briggs KB 1992, 'High-frequency bottom backscattering: roughness versus sediment volume scattering', *The Journal of the Acoustical Society of America*, vol. 92, no. 2, pp. 962-77.

Jackson DR, Winebrenner DP and Ishimaru A 1986, 'Application of the composite roughness model to high-frequency bottom backscattering', *The Journal of the Acoustical Society of America*, vol. 79, no. 5, pp. 1410-22.

James, G, Witten, D, Hastie, T and Tibshirani, R 2013, *An introduction to statistical learning*, Springer.

Jernakoff, P, Phillips, BF and Maller, RA 1987, 'A quantitative study of nocturnal foraging distances of the western rock lobster *Panulirus cygnus* George', *Journal of Experimental Marine Biology and Ecology*, vol. 113, no. 1, pp. 9-21.

Joyce, KE, Duce, S, Leahy, SM, Leon, J and Maier, SW 2018, 'Principles and practice of acquiring drone-based image data in marine environments', *Marine and Freshwater Research,* vol. 70, no. 7, pp. 952-63.

Kennedy, DM, Ierodiaconou, D and Schimel, A 2014, 'Granitic coastal geomorphology: applying integrated terrestrial and bathymetric LiDAR with multibeam sonar to examine coastal landscape evolution', *Earth Surface Processes and Landforms*, vol. 39, no. 12, pp. 1663-74.

Koh, LP and Wich, SA 2012, 'Dawn of drone ecology: low-cost autonomous aerial vehicles for conservation', *Tropical Conservation Science*, vol. 5, no. 2, pp. 121-32.

Koss, RS, Miller, K, Wescott, G et al., 2009, 'An evaluation of Sea Search as a citizen science programme in marine protected areas', *Pacific Conservation Biology*, vol. 15, no. 2, pp. 116-27.

Kruskal, JB 1964, 'Nonmetric multidimensional scaling: a numerical method', *Psychometrika*, vol. 29, no. 2, pp. 115-29.

Kuffner, IB, Brock, JC, Grober-Dunsmore, R, Bonito, VE, Hickey, TD and Wright, CW 2007, 'Relationships between reef fish communities and remotely sensed rugosity measurements in Biscayne National Park, Florida, USA', *Environmental Biology of Fishes*, vol. 78, no. 1, pp. 71-82.

Kuhn, M 2008, 'Building predictive models in R using the caret package', *Journal of Statistical Software*, vol. 28, no. 5, pp. 1-26.

Langlois, T, Williams, J, Monk, J et al. 2018, 'Marine sampling field manual for benthic stereo BRUVS (baited remote underwater videos)', in R Przeslawski and S Foster (eds), *Field manuals for marine sampling to monitor Australian waters*, National Environmental Science Programme (NESP), pp. 82-104.

Liaw, A and Wiener, M 2002, 'Classification and regression by randomForest', *R News*, vol. 2, no. 3, pp. 18-22.

Lilley, SA and Schiel, DR 2006, 'Community effects following the deletion of a habitat-forming alga from rocky marine shores', *Oecologia*, vol. 148, no. 4, pp. 672-81.

Linnane, A, McGarvey, R, Gardner, C, Walker, TI, Matthews, J, Green, B and Punt, AE 2014, 'Large-scale patterns in puerulus settlement and links to fishery recruitment in the southern rock lobster (*Jasus edwardsii*), across south-eastern Australia', *ICES Journal of Marine Science*, vol. 71, no. 3, pp. 528-36.

Longtin, CM, Scrosati, RA, Whalen, GB and Garbary, DJ 2009, 'Distribution of algal epiphytes across environmental gradients at different scales: intertidal elevation, host canopies, and host fronds', *Journal of Phycology*, vol. 45, no. 4, pp. 820-7.

Loya, Y, Eyal, G, Treibitz, T, Lesser, MP and Appeldoorn, R 2016, Theme section on mesophotic coral ecosystems: advances in knowledge and future perspectives, *Coral Reefs*, vol. 35, no. 1, pp. 1-9.

Lyons, MB, Keith, DA, Phinn, SR, Mason, TJ and Elith, J 2018, 'A comparison of resampling methods for remote sensing classification and accuracy assessment', *Remote Sensing of Environment*, vol. 208, pp. 145-53.

MacDiarmid, AB, Hickey, B and Maller, RA 1991, 'Daily movement patterns of the spiny lobster *Jasus edwardsii* (Hutton) on a shallow reef in northern New Zealand', *Journal of Experimental Marine Biology and Ecology*, vol. 147, no. 2, pp. 185-205.

Miller, RJ 1990, 'Effectiveness of crab and lobster traps', *Canadian Journal of Fisheries and Aquatic Sciences*, vol. 47, no. 6, pp. 1228-51.

Miskiewicz, AG, Neira, FJ and Tait, SE 1999, 'Development and ecology of larvae of the monotypic Australian fish family Dinolestidae', *Australian Journal of Zoology*, vol. 47, no. 1, pp. 37-45.

Monk, J, Barrett, N, Bridge, T et al. 2018, 'Marine sampling field manual for AUVs (autonomous underwater vehicles)', in R Przeslawski and S Foster (eds), *Field manuals for marine sampling to monitor Australian waters*, National Environmental Science Programme (NESP), pp. 65-81.

Moore, CH, Harvey, ES and Van Niel, K 2010, 'The application of predicted habitat models to investigate the spatial ecology of demersal fish assemblages', *Marine Biology*, vol. 157, no. 12, pp. 2717-29.

Morgan, EM, Green, BS, Murphy, NP and Strugnell, JM 2013, 'Investigation of genetic structure between deep and shallow populations of the southern rock lobster, *Jasus edwardsii* in Tasmania, Australia', *PLOS ONE*, vol. 8, no. 10, e77978.

Murfitt, SL, Allan, BM, Bellgrove, A, Rattray, A, Young, MA and Ierodiaconou, D 2017, 'Applications of unmanned aerial vehicles in intertidal reef monitoring', *Scientific Reports*, vol. 7, 10259.

Palomer, A, Ridao, P, Ribas, D, Mallios, A and Vallicrosa, G 2013, 'A comparison of G^2o graph SLAM and EKF pose based SLAM with bathymetry grids', *IFAC Proceedings Volumes*, vol. 46, no. 33, pp. 286-91.

Pérez-Ortiz, M, Peña, JM, Gutiérrez, PA, Torres-Sánchez, J, Hervás-Martínez, C and López-Granados, F 2015, 'A semi-supervised system for weed mapping in sunflower crops using unmanned aerial vehicles and a crop row detection method', *Applied Soft Computing*, vol. 37, pp. 533-44.

Platell, ME, Sarre, GA and Potter, IC 1997, 'The diets of two co-occurring marine teleosts, *Parequula melbournensis* and *Pseudocaranx wrighti*, and their relationships to body size and mouth morphology, and the season and location of capture', *Environmental Biology of Fishes*, vol. 49, no. 3, pp. 361-76.

Pocklington, JB, Keough, MJ, O'Hara, TD and Bellgrove, A 2019, 'The influence of canopy cover on the ecological function of a key autogenic ecosystem engineer', *Diversity*, vol. 11, no. 5, 79. https://doi.org/10.3390/d11050079

Power, B and Boxshall, A 2007, *Marine national park and sanctuary monitoring plan 2007-2012*, Parks Victoria Technical Series No 54, Parks Victoria.

Punt, AE 2003, 'The performance of a size-structured stock assessment method in the face of spatial heterogeneity in growth', *Fisheries Research*, vol. 65, no. 1-3, pp. 391-409.

R Core Team 2013, 'R: A language and environment for statistical computing'.

Raoult, V, David, PA, Dupont, SF, Mathewson, CP, O'Neill, SJ, Powell, NN and Williamson, JE 2016, 'GoPros™ as an underwater photogrammetry tool for citizen science', *PeerJ*, vol. 4, e1960.

Rattray, A, Ierodiaconou, D, Laurenson, L, Burq, S and Reston, M 2009, 'Hydro-acoustic remote sensing of benthic biological communities on the shallow South East Australian continental shelf', *Estuarine, Coastal and Shelf Science*, vol. 84, no. 2, pp. 237-45.

Roberts, CM and Ormond, RFG 1987, 'Habitat complexity and coral reef fish diversity and abundance on Red Sea fringing reefs', *Marine Ecology Progress Series*, vol. 41, pp. 1-8.

Royall, R 1997, *Statistical evidence: a likelihood paradigm*, Chapman and Hall, New York.

Russell, BC 1988, 'Revision of the labrid genus *Pseudolabrus* and allied genera', *Records of the Australian Museum, Supplement*, vol. 9, pp. 1-72.

Sappington, JM, Longshore, KM and Thompson, DB 2007, 'Quantifying landscape ruggedness for animal habitat analysis: a case study using bighorn sheep in the Mojave Desert', *The Journal of Wildlife Management,* vol. 71, no. 5, pp. 1419-26.

Sarre, GA, Hyndes, GA and Potter, IC 1997, 'Habitat, reproductive biology and size composition of Parequula melbournensis, a gerreid with a temperate distribution', *Journal of Fish Biology*, vol. 50, no. 2, pp. 341-57.

Schimel, A and Ierodiaconou, D 2015 *Hydroacoustic mapping of Wilsons Promontory Marine National Park*. Parks Victoria Technical Series No. 111, Parks Victoria.

Sequeira, AMM, Mellin, C, Lozano-Montes, HM, Vanderklift, MA, Babcock, RC, Haywood, MD, Meeuwig, JJ and Caley, MJ 2016, 'Transferability of predictive models of coral reef fish species richness', *Journal of Applied Ecology*, vol. 53, no. 1, pp. 64-72.

Shepherd, SA and Cannon, J 1988, 'Studies on southern Australian abalone (genus *Haliotis*) X. Food and feeding of juveniles', *Journal of the Malacological Society of Australia*, vol. 9, no. 1, pp. 21-6.

Shepherd, SA and Clarkson, PS 2001, 'Diet, feeding behaviour, activity and predation of the temperate blue-throated wrasse, *Notolabrus tetricus*', *Marine and Freshwater Research*, vol. 52, no. 3, pp. 311-22.

Thomas, CW, Crear, BJ and Hart, PR 2000, 'The effect of temperature on survival, growth, feeding and metabolic activity of the southern rock lobster, *Jasus edwardsii*', *Aquaculture*, vol. 185, no. 1-2, pp. 73-84.

Thompson, WL and Lee, DC 2000, 'Modeling relationships between landscape-level attributes and snorkel counts of chinook salmon and steelhead parr in Idaho', *Canadian Journal of Fisheries and Aquatic Sciences*, vol. 57, no. 9, pp. 1834-42.

Trebilco, R, Dulvy, NK, Stewart, H and Salomon, AK 2015, 'The role of habitat complexity in shaping the size structure of a temperate reef fish community', *Marine Ecology Progress Series*, vol. 532, pp. 197-211.

Turner, IL, Harley, MD and Drummond, CD 2016, 'UAVs for coastal surveying', *Coastal Engineering*, vol. 114, pp. 19-24.

Tuya, F, Wernberg, T and Thomsen, MS 2009, 'Habitat structure affect abundances of labrid fishes across temperate reefs in south-western Australia', *Environmental Biology of Fishes*, vol. 86, no. 2, pp. 311-9.

Underwood, AJ 2000, 'Experimental ecology of rocky intertidal habitats: what are we learning?', *Journal of Experimental Marine Biology and Ecology*, vol. 250, no. 1, pp. 51-76.

Valavanis, VD, Pierce, GJ, Zuur, AF, Palialexis, A, Saveliev, A, Katara, I and Wang, J 2008, 'Modelling of essential fish habitat based on remote sensing, spatial analysis and GIS', *Hydrobiologia*, vol. *612*, no. 1, pp. 5-20.

Vega, FA, Ramírez, FC, Saiz, MP and Rosúa, FO 2015, 'Multi-temporal imaging using an unmanned aerial vehicle for monitoring a sunflower crop', *Biosystems Engineering*, vol. 132, pp. 19-27.

Victorian Environmental Assessment Council 2014, *Marine investigation – final report*. Victorian Environmental Assessment Council.

Walbridge, S, Slocum, N, Pobuda, M and Wright, DJ 2018, 'Unified geomorphological analysis workflows with Benthic Terrain Modeler', *Geosciences*, vol. 8, no. 3, p. 94.

Walker, TI 2007, 'Spatial and temporal variation in the reproductive biology of gummy shark *Mustelus antarcticus* (Chondrichthyes: Triakidae) harvested off southern Australia', *Marine and Freshwater Research*, vol. 58, no. 1, pp. 67-97.

Warwick, RM and Clarke, KR 1991, 'A comparison of some methods for analysing changes in benthic community structure', *Journal of the Marine Biological Association of the United Kingdom*, vol. 71, no. 1, pp. 225-44.

Watt, CA and Scrosati, RA 2013, 'Regional consistency of intertidal elevation as a mediator of seaweed canopy effects on benthic species richness, diversity, and composition', *Marine Ecology Progress Series*, vol. 491, pp. 91-9.

Williams, J, Jordan, A, Harasti, D, Davies, P and Ingleton, T 2019, 'Taking a deeper look: quantifying the differences in fish assemblages between shallow and mesophotic temperate rocky reefs', *PLOS ONE*, vol. 14, no. 3, e0206778.

Williams, SB, Pizarro, O, Steinberg, DM, Friedman, A and Bryson, M 2016, 'Reflections on a decade of autonomous underwater vehicles operations for marine survey at the Australian Centre for Field Robotics', *Annual Reviews in Control*, vol. 42, pp. 158-65.

Williams, SB, Pizarro, OR, Jakuba, MV et al. 2012, 'Monitoring of benthic reference sites: using an autonomous underwater vehicle', *IEEE Robotics and Automation Magazine*, vol. 19, no. 1, pp. 73-84.

Wood, S 2015, Package 'mgcv', R package version, vol. 1, p. 29. https://cran.r-project.org/web/packages/mgcv/

Woods, B and Edmunds, M 2013, *Victorian Subtidal Reef Monitoring Program: the reef biota at Merri Marine Sanctuary, February 2013*. Parks Victoria Technical Series No. 87, Parks Victoria.

Yee, TW and Mitchell, ND 1991, 'Generalized additive models in plant ecology', *Journal of Vegetation Science*, vol. 2, no. 5, pp. 587-602.

Young, M and Carr, MH 2015, 'Application of species distribution models to explain and predict the distribution, abundance and assemblage structure of nearshore temperate reef fishes', *Diversity and Distributions*, vol. 21, no. 12, pp. 1428-40.

Zahawi, RA, Dandois, JP, Holl, KD, Nadwodny, D, Reid, JL and Ellis, EC 2015, 'Using lightweight unmanned aerial vehicles to monitor tropical forest recovery', *Biological Conservation*, vol. 186, pp. 287-95.

Zavalas, R, Ierodiaconou, D, Ryan, D, Rattray, A and Monk, J 2014, 'Habitat classification of temperate marine macroalgal communities using bathymetric LiDAR', *Remote Sensing*, vol. 6, no. 3, pp. 2154-75.

10. Appendixes

10.1 Section A (Appendixes 1–2)

Appendix 1: Relative abundances (mean ± SE) of all fish species observed in the 2016 BRUVS survey

Family	Taxon	Common name	Relative abundance
Aplodactylidae	*Aplodactylus arctidens*	Marblefish	0.07 ± 0.03
Aracanidae	*Aracana aurita*	Shaw's Cowfish	0.02 ± 0.02
Aulopidae	*Latropiscis purpurissatus*	Sergeant Baker	0.23 ± 0.06
Carangidae	*Pseudocaranx dentex*	White Trevally	0.02 ± 0.02
Cheilodactylidae	*Nemadactylus douglasii*	Grey Morwong	0.03 ± 0.02
Cheilodactylidae	*Nemadactylus macropterus*	Jackass Morwong	1.92 ± 0.41
Cheilodactylidae	*Nemadactylus* spp.	Morwong	0.02 ± 0.02
Cheilodactylidae	*Nemadactylus valenciennesi*	Queen Snapper	0.3 ± 0.06
Cyttidae	*Cyttus australis*	Silver Dory	0.07 ± 0.03
Dasyatidae	*Bathytoshia brevicaudata*	Smooth Stingray	0.02 ± 0.02
Dinolestidae	*Dinolestes lewini*	Longfin Pike	2.42 ± 1.21
Diodontidae	*Diodon nicthemerus*	Globe Fish	0.02 ± 0.02
Enoplosidae	*Enoplosus armatus*	Old Wife	0.2 ± 0.07
Gempylidae	*Thyrsites atun*	Snoek	0.05 ± 0.03
Gerreidae	*Parequula melbournensis*	Silverbelly	2.07 ± 0.41
Heterodontidae	*Heterodontus portusjacksoni*	Port Jackson Shark	0.53 ± 0.18
Kyphosidae	*Girella zebra*	Zebra Fish	0.05 ± 0.03
Kyphosidae	*Tilodon sexfasciatus*	Moonlighter	0.03 ± 0.02
Kyphosidae	*Atypichthys strigatus*	Mado Sweep	0.02 ± 0.02
Kyphosidae	*Scorpis aequipinnis*	Sea Sweep	0.03 ± 0.03
Kyphosidae	*Scorpis lineolata*	Silver Sweep	0.32 ± 0.24
Labridae	*Achoerodus viridis*	Eastern Blue Groper	0.02 ± 0.02
Labridae	*Dotalabrus aurantiacus*	Castelnau's Wrasse	0.02 ± 0.02
Labridae	*Notolabrus fucicola*	Purple Wrasse	0.08 ± 0.05
Labridae	*Notolabrus tetricus*	Blue-Throat Wrasse	3.17 ± 0.49
Labridae	*Ophthalmolepis lineolata*	Maori Wrasse	0.27 ± 0.09
Labridae	*Pictilabrus laticlavius*	Senator Wrasse	0.28 ± 0.08
Labridae	*Pseudolabrus rubicundus*	Rosy Wrasse	3.7 ± 0.7
Latridae	*Pseudogoniistius nigripes*	Magpie Perch	0.48 ± 0.1
Latridae	*Latris lineata*	Striped Trumpeter	0.02 ± 0.02
Latridae	*Latridopsis forsteri*	Bastard Trumpeter	0.02 ± 0.02

Family	Taxon	Common name	Relative abundance
Monacanthidae	*Acanthaluteres vittiger*	Toothbrush Leatherjacket	0.17 ± 0.13
Monacanthidae	*Eubalichthys gunnii*	Gunn's Leatherjacket	0.22 ± 0.07
Monacanthidae	*Eubalichthys mosaicus*	Mosaic Leatherjacket	0.1 ± 0.04
Monacanthidae	*Meuschenia australis*	Brown-Striped Leatherjacket	0.02 ± 0.02
Monacanthidae	*Meuschenia freycineti*	Six-Spine Leatherjacket	1.02 ± 0.17
Monacanthidae	*Meuschenia scaber*	Velvet Leatherjacket	1.12 ± 0.18
Monacanthidae	*Meuschenia* spp.	Leatherjackets	0.1 ± 0.04
Monacanthidae	*Meuschenia venusta*	Stars And Stripes Leatherjacket	0.17 ± 0.05
Monacanthidae	*Monacanthidae* spp.	Leatherjackets	0.2 ± 0.07
Monacanthidae	*Thamnaconus degeni*	Degen's Leatherjacket	3.17 ± 1.02
Moridae	*Pseudophycis bachus*	Red Cod	1.35 ± 0.37
Moridae	*Pseudophycis barbata*	Bearded Cod	0.3 ± 0.06
Moridae	*Pseudophycis* spp.	Cod	0.03 ± 0.02
Mullidae	*Upeneichthys vlamingii*	Southern Goatfish	0.78 ± 0.33
Muraenidae	*Gymnothorax prasinus*	Green Moray	0.03 ± 0.02
Myliobatidae	*Myliobatis tenuicaudatus*	Eagle Ray	0.03 ± 0.02
Odacidae	*Heteroscarus acroptilus*	Rainbow Cale	0.02 ± 0.02
Odacidae	*Olisthops cyanomelas*	Herring Cale	0.03 ± 0.02
Parascylliidae	*Parascyllium ferrugineum*	Rusty Catshark	0.03 ± 0.02
Pempheridae	*Pempheris multiradiata*	Common Bullseye	0.03 ± 0.02
Pentacerotidae	*Pentaceropsis recurvirostris*	Long-Snouted Boarfish	0.05 ± 0.03
Pinguipedidae	*Parapercis* spp.	Grubfishes or sandperches	0.03 ± 0.03
Platycephalidae	*Platycephalus bassensis*	Sand Flathead	1.3 ± 0.37
Platycephalidae	*Platycephalus* spp.	Flathead	0.15 ± 0.07
Pomacentridae	*Parma microlepis*	White-Ear	0.13 ± 0.04
Pomacentridae	*Parma victoriae*	Victorian Scalyfin	0.07 ± 0.03
Pristiophoridae	*Pristiophorus nudipinnis*	Southern Sawshark	0.02 ± 0.02
Pristiophoridae	*Pristiophorus* spp.	Sawshark	0.02 ± 0.02
Rajidae	*Dentiraja lemprieri*	Thornback Skate	0.02 ± 0.02
Rajidae	*Dipturus* spp.	Skate	0.02 ± 0.02
Rajidae	*Spiniraja whitleyi*	Whitley's Skate	0.05 ± 0.03
Rhinobatidae	*Trygonorrhina dumerilii*	Southern Fiddler Ray	0.3 ± 0.07
Scorpaenidae	*Neosebastes scorpaenoides*	Common Gurnard Perch	0.7 ± 0.11
Scorpaenidae	*Neosebastes* spp.	Gurnard perch	0.02 ± 0.02
Scorpaenidae	*Scorpaena* spp.	Scorpionfish	0.03 ± 0.02
Scyliorhinidae	*Cephaloscyllium laticeps*	Draughtboard Shark	2.02 ± 0.19

Family	Taxon	Common name	Relative abundance
Sebastidae	*Helicolenus percoides*	Red Gurnard Perch	0.25 ± 0.07
Serranidae	*Caesioperca* spp.	Perch	27.02 ± 6.19
Serranidae	*Hypoplectrodes nigroruber*	Banded Seaperch	0.17 ± 0.05
Sparidae	*Chrysophrys auratus*	Snapper	0.23 ± 0.17
Syngnathidae	*Dunckerocampus dactyliophorus*	Ringed Pipefish	0.02 ± 0.02
Tetraodontidae	*Contusus brevicaudus*	Prickly Toadfish	0.05 ± 0.03
Triakidae	*Mustelus antarcticus*	Gummy Shark	0.68 ± 0.13
Triakidae	Triakidae spp.	Hound sharks	0.02 ± 0.02
Triglidae	*Chelidonichthys kumu*	Bluefin Gurnard	0.05 ± 0.03
Urolophidae	*Trygonoptera imitata*	Eastern Shovelnose Stingaree	0.02 ± 0.02
Urolophidae	*Urolophus* spp.	Stingarees	0.03 ± 0.02

Appendix 2: Smoother estimates for the environmental predictors as obtained from generalised additive models (GAMs)

Relative species richness

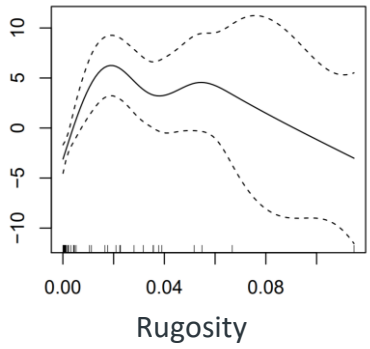

Relative family richness

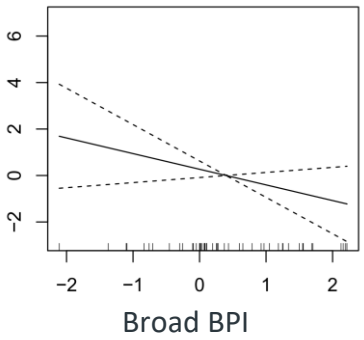

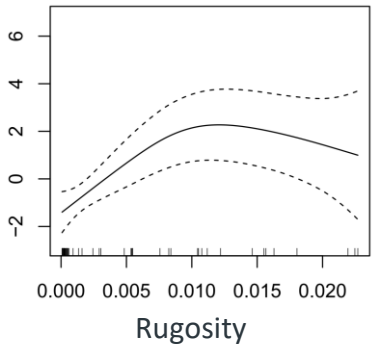

Relative family richness

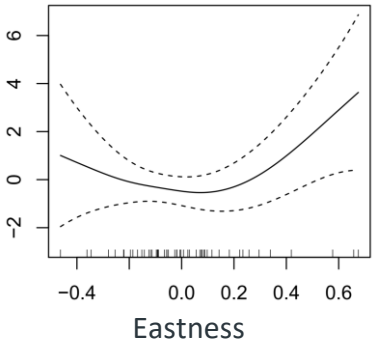

Relative abundance of *Cephaloscyllium laticeps*

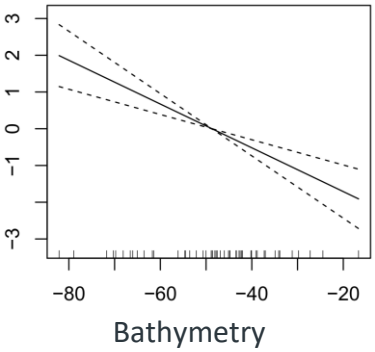

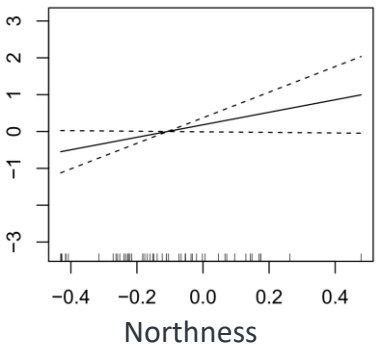

Relative abundance of
Cephaloscyllium laticeps

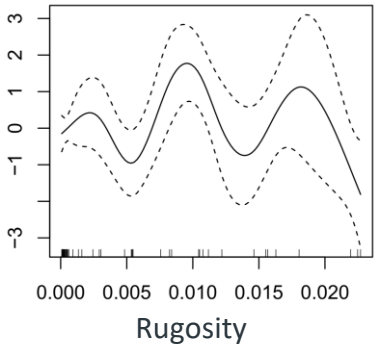

Relative abundance of
Notolabrus tetricus

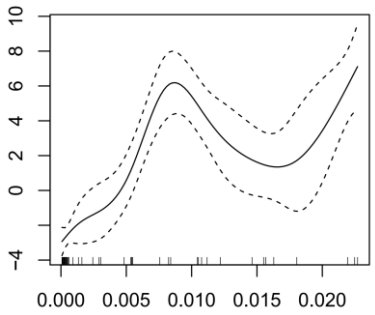

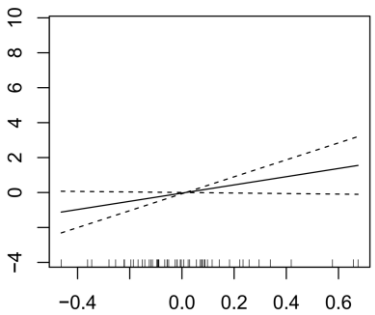

Relative abundance of
Pseudolabrus rubicundus

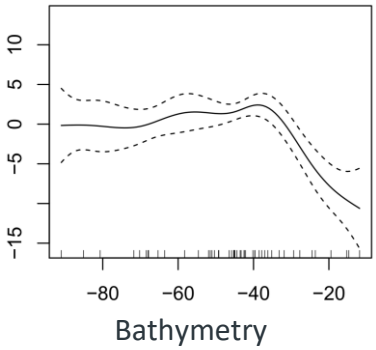

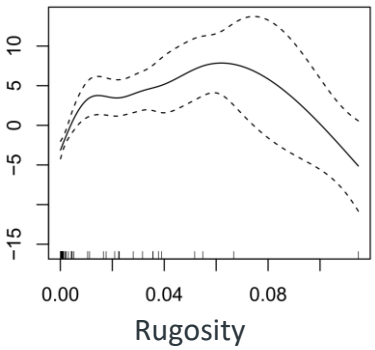

Relative abundance of
Thamnaconus degeni

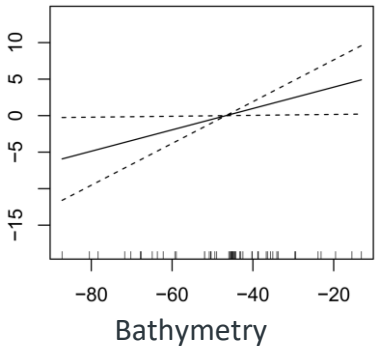

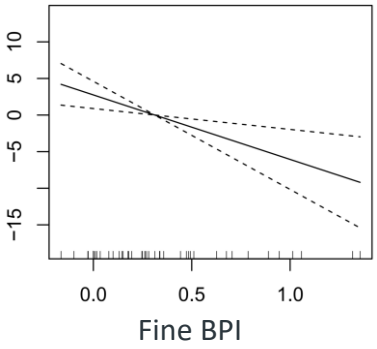

Relative abundance of
Thamnaconus degeni

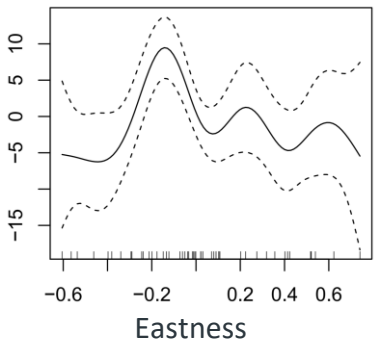

10.2 Section B (Appendixes 3–7)

Appendix 3: Time (minutes) to complete survey of all quadrats at sites

	UAV flight	UAV virtual quadrats	UAV total	On-ground quadrats
Pickering Point	8	54	62	83
Shelly Beach	7	64	71	125
Point Lonsdale	36	45	81	150
Cheviot Beach	35	39	74	136
Ricketts Point	5	71	76	142
Halfmoon Bay	3	39	42	102
Mushroom Reef	12	37	49	129
West Flinders	4	50	54	143

UAV flight = time taken to complete all flights required to capture entire survey area (active flight time at 10 m altitude).

UAV virtual quadrats = time taken to extract quadrats from orthomosaic, import into Coral Point Count (v. 4.1), and complete 50 point count of algae.

UAV total = UAV flight time and UAV virtual quadrats combined.

On-ground quadrats = time taken to complete point count of algae and abundance counts of invertebrates (active count time and walking between quadrats at site). Shaded columns show total UAV and on-ground times used in statistical comparison.

Appendix 4: PERMANOVA of square-root transformed algal group percentage cover data observed by on-ground quadrats and UAV remote sensing across all 8 sites. The Bray–Curtis dissimilarity measure was used

Source	Degrees of freedom	Mean square	Pseudo-F	$P^{1,2}$
Region	3	85,194	292.35	<0.001*
Park	1	29,063	0.99	0.436
Method	1	6,831.7	8.60	0.0102*
Region x Park	3	29,452	101.07	<0.001*
Region x Method	3	794.44	2.73	0.005*
Park x Method	1	8,041.6	55.49	<0.001*
Quadrat (Region x Park)	190	1,604.9	5.51	<0.001*
Region x Park x Method	3	144.9	0.50	0.871
Residual	190	291.41		
Total	395			

Notes: **1 Anderson et al. (2008).**
2 Statistically significant values are marked with *

.

Appendix 5: nMDS plot of percentage cover of 4 algal groups

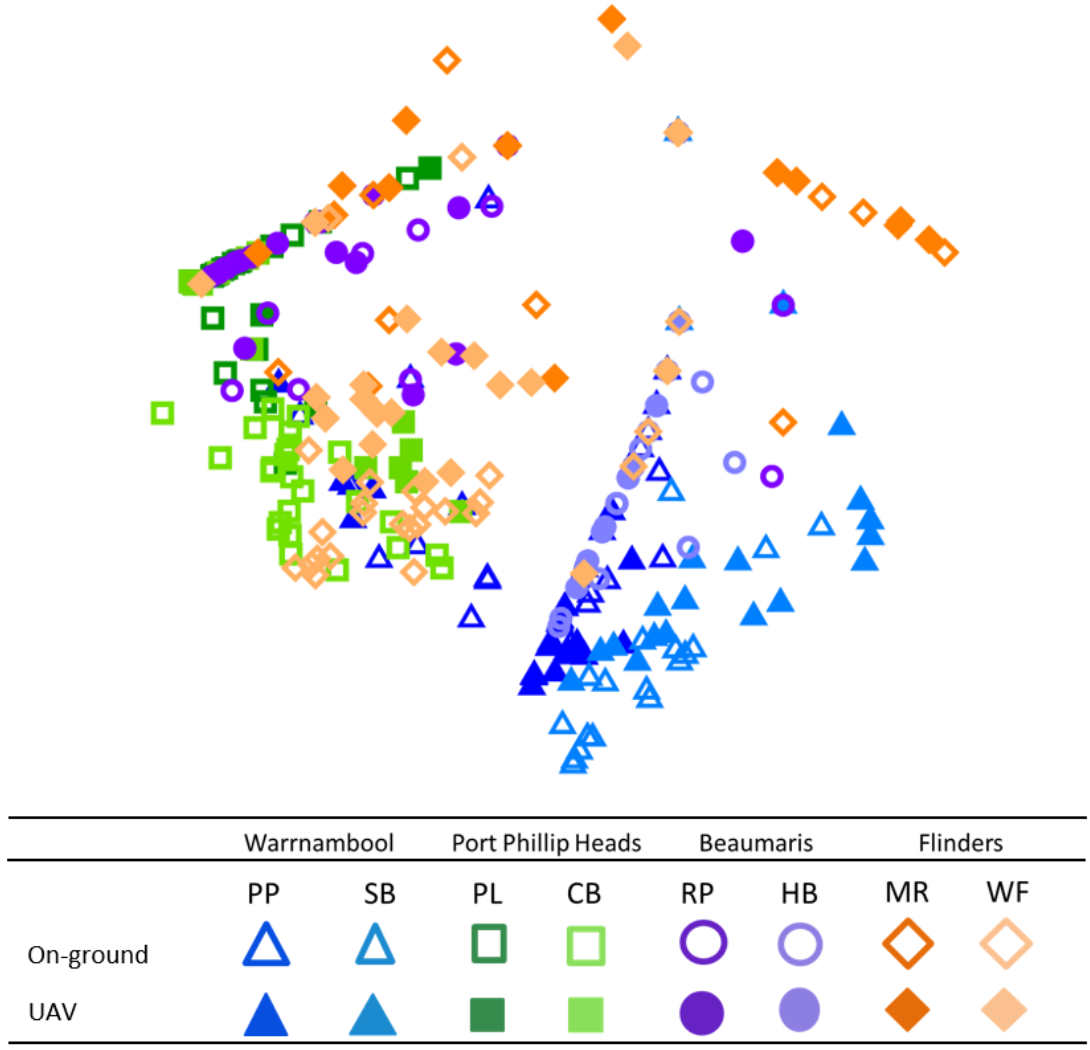

Symbols indicate: Region (triangles = Warrnambool, squares = Port Phillip Heads, circles = Beaumaris, diamonds = Flinders), Park (MPA = dark, Reference = light colour) and Method (on-ground quadrat = open, UAV = closed).

Sites: PP = Pickering Point, SB = Shelly Beach, PL = Point Lonsdale, CB = Cheviot Beach, RP = Ricketts Point, HB = Halfmoon Bay, MR = Mushroom Reef, WF = West Flinders.

Data were square-root transformed. 2D stress 0.16.

Appendix 6: Scatterplot of manual and ISO-automated estimates of percentage cover of *Hormosira banksii* in 50 quadrats at the Point Lonsdale site

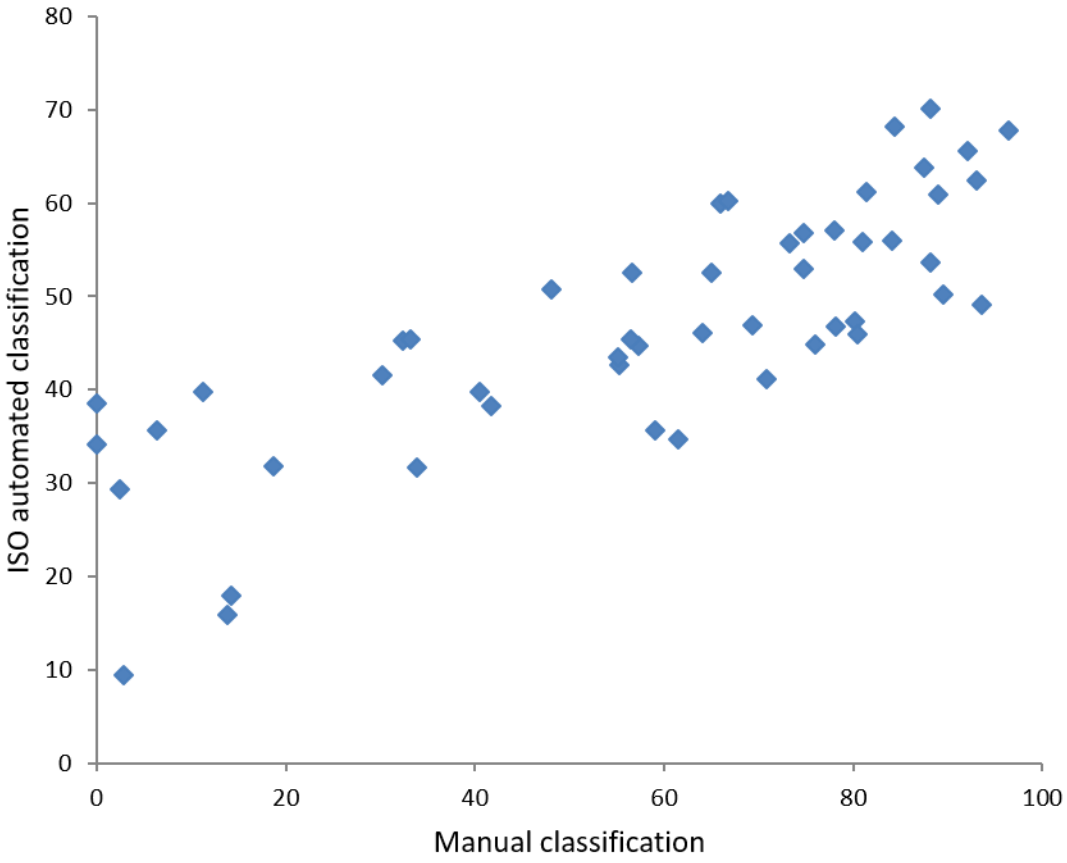

Appendix 7: Distance-based redundancy analysis (dbRDA) ordination describing the relationship between derived environmental variables and algal percentage cover from on-ground quadrat DistLM classified by site

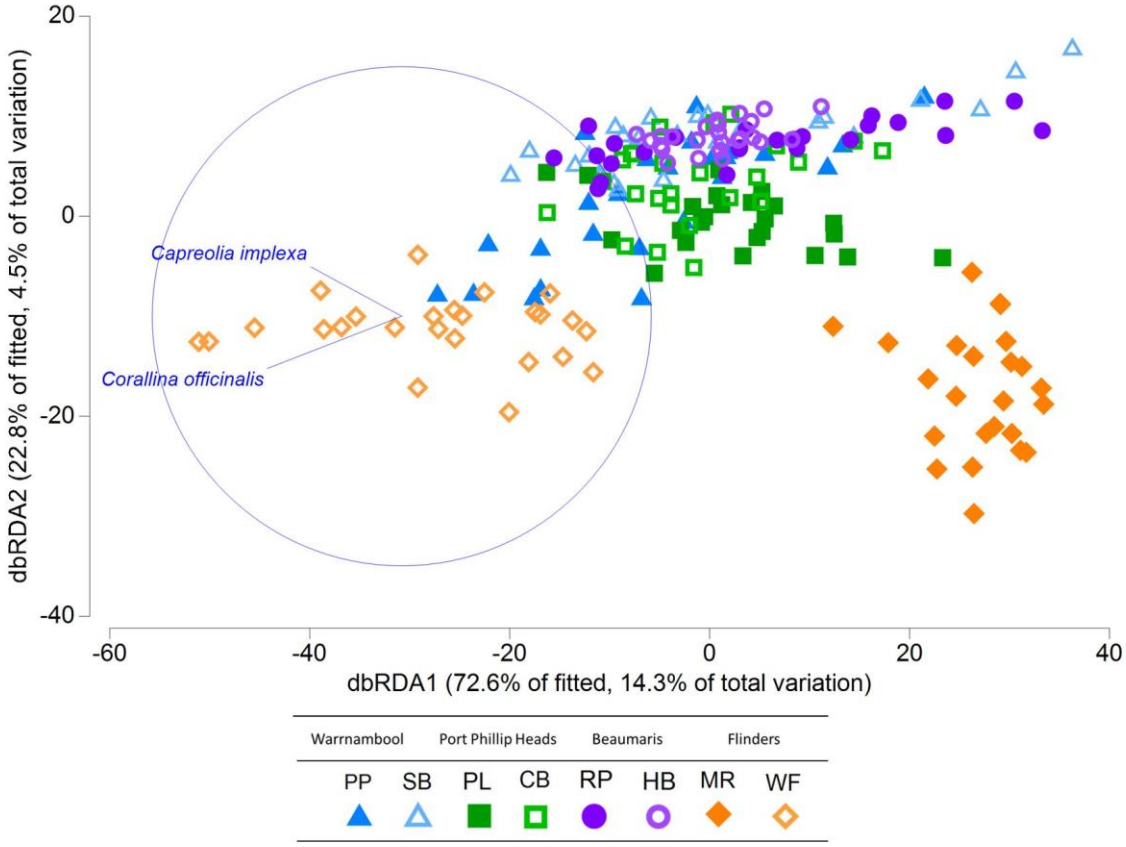

Vectors depict the effect of environmental variables influencing the presence of algal taxa with a Pearson's correlation of 0.4, with length of vector representing the strength of effect.

Axes show percentage of variation for elevation (dbRDA1) and distance to seaward reef edge (dbRDA2).

Symbols indicate: Region (triangles = Warrnambool, squares = Port Phillip Heads, circles = Beaumaris, diamonds = Flinders), Park (MPA = dark, Reference = light colour) and Method (on-ground quadrat = open, UAV = closed).

Sites: PP = Pickering Point, SB = Shelly Beach, PL = Point Lonsdale, CB = Cheviot Beach, RP = Ricketts Point, HB = Halfmoon Bay, MR = Mushroom Reef, WF = West Flinders.

Back cover: Red Velvetfish (*Gnathanacanthus goetzeei*). Photo: Parks Victoria